UCRL 3928

UNIVERSITY OF CALIFORNIA

Radiation Laboratory

TWO-WEEK LOAN COPY

This is a Library Circulating Copy
which may be borrowed for two weeks.
For a personal retention copy, call
Tech. Info. Division, Ext. 5545

BERKELEY, CALIFORNIA

DISCLAIMER

This document was prepared as an account of work sponsored by the United States Government. While this document is believed to contain correct information, neither the United States Government nor any agency thereof, nor the Regents of the University of California, nor any of their employees, makes any warranty, express or implied, or assumes any legal responsibility for the accuracy, completeness, or usefulness of any information, apparatus, product, or process disclosed, or represents that its use would not infringe privately owned rights. Reference herein to any specific commercial product, process, or service by its trade name, trademark, manufacturer, or otherwise, does not necessarily constitute or imply its endorsement, recommendation, or favoring by the United States Government or any agency thereof, or the Regents of the University of California. The views and opinions of authors expressed herein do not necessarily state or reflect those of the United States Government or any agency thereof or the Regents of the University of California.

UCRL-3928

UNIVERSITY OF CALIFORNIA

Radiation Laboratory
Berkeley, California

Contract No. W-7405-eng-48

ELECTRON-SPECTROSCOPIC STUDIES OF NEUTRON-DEFICIENT RHENIUM ISOTOPES

Charles J. Gallagher, Jr.

(Thesis)

September 1957

Printed for the U. S. Atomic Energy Commission

The Walrus and the Carpenter
  Were walking close at hand;
They wept like anything to see
  Such quantities of sand:
"If this were only cleared away,"
  They said, "it would be grand!"

"If seven maids with seven mops
  Swept it for half a year,
Do you suppose," the Walrus said,
  "That they could get it clear?"
"I doubt it," said the Carpenter,
  And shed a bitter tear.

Lewis Carroll[1]

ELECTRON-SPECTROSCOPIC STUDIES OF NEUTRON-DEFICIENT RHENIUM ISOTOPES

Contents

List of Tables - 2c

List of Illustrations- 2e

Abstract - 3

I. Introduction- 4

II. Experimental Techniques - 6

A. Energy and Intensity Measurements- - - - - - - - - - - - - 6

B. Source Preparation - 7

III. Electron-Spectroscopic Studies of Neutron-Deficient Rhenium Isotopes- 9

A. 20-Hour Re^{181}- 9

1. Mass Assignment and Half Life - - - - - - - - - - 9

2. General Resumé of Spectroscopic Results - - - - 11

3. Gamma Spectroscopy- - - - - - - - - - - - - - - - - 12

4. Electron Spectroscopy - - - - - - - - - - - - - - - 19

5. Discussion of Transitions - - - - - - - - - - - - 21

6. Decay Scheme- 22

7. Discussion of Results - - - - - - - - - - - - - - 24

B. 12.7-Hour Re^{182}- 29

1. Mass Assignment and Half Life - - - - - - - - - - 29

2. General Resumé of Spectroscopic Results - - - - 29

3. Gamma Spectroscopy - - - - - - - - - - - - - - - - 30

4. Electron Spectroscopy - - - - - - - - - - - - - - 30

5. Discussion of Results - - - - - - - - - - - - - - 34

a. Decay Scheme - - - - - - - - - - - - - - - - - - 34

b. Primary Branching and Log ft values - - - - 37

c. Conversion Coefficients and Mixing Ratios - 40

C. 60-Hour Re^{182}- 43

1. Mass Assignment and Half Life - - - - - - - - - - 43

2. General Resumé of Spectroscopic Results - - - - 43

3. Gamma Spectroscopy - - - - - - - - - - - - - - - - 44
4. Electron Spectroscopy- - - - - - - - - - - - - - - 44
5. Discussion of Results- - - - - - - - - - - - - - - 49
a. Decay Scheme - - - - - - - - - - - - - - - - - - 49
b. Discussion of New Levels in W^{182} - - - - - - - 55
c. Discussion of Transitions- - - - - - - - - - - 59
d. Spin Assignments - - - - - - - - - - - - - - - 63
e. Conversion Coefficients and Mixing Ratios- - 65
f. Primary Populations and Log ft Values- - - - 68
6. Analysis and Discussion of the New Levels Assigned to W^{182} - - - - - - - - - - - - - - - - - 69
7. Conclusion - - - - - - - - - - - - - - - - - - - 81
D. 71-Day Re^{183}- 82
1. Mass Assignment and Half Life- - - - - - - - - - 82
2. General Resumé of Spectroscopic Results- - - - - 82
3. Gamma Spectroscopy - - - - - - - - - - - - - - - 82
4. Electron Spectroscopy- - - - - - - - - - - - - - 82
5. Discussion of Results- - - - - - - - - - - - - - 84
E. 50-Day Re^{184}- 86
1. Mass Assignment and Half Life- - - - - - - - - - 86
2. General Resumé of Spectroscopic Results- - - - - 86
3. Gamma Spectroscopy - - - - - - - - - - - - - - - 86
4. Electron Spectroscopy- - - - - - - - - - - - - - 87
5. Coincidence Studies- - - - - - - - - - - - - - - 88
6. Discussion of Results- - - - - - - - - - - - - - 90
a. Discussion of Transitions- - - - - - - - - - 90
b. Decay Scheme - - - - - - - - - - - - - - - - - 92
c. Primary Population and Log ft Values - - - - 95
d. General Discussion - - - - - - - - - - - - - - 97
F. K-Auger Electrons of Tungsten - - - - - - - - - - - - - - 99

IV. An Extension of the Predictions of the Unified Model to the Determination of Electron-Capture Decay Energies - - - - 104
A. Theory - 104
B. Application to Re^{184} and 12.7-Hour Re^{182} - - - - - - 106
Acknowledgments - 109
Appendices - 110
A. Chemical Procedures - 110
B. Electron Lines Observed in the Decay of the Short-Lived Rhenium Isotopes - - - - - - - - - - - - - - - - - 114
1. Electron Lines in Order of Increasing Energy - 114
2. Electron Lines According to Transition Energy - 117
a. 60-Hour Re^{182} Lines - - - - - - - - - - - - 117
1. Electron Lines of Transitions Seen by MBMD - - - - - - - - - - - - - - - - - 117
2. Electron Lines of New Transitions - - 120
b. 20-Hour Re^{181} Lines - - - - - - - - - - - - 124
c. 71-Day Re^{183} Lines Appearing in the Short-Lived Spectrum - - - - - - - - - - - - - - - - 125
d. Electron Lines Not Definitely Assigned to an Isotope - - - - - - - - - - - - - - - - 126
C. Electron Lines Observed in the Decay of the Long-Lived Rhenium Isotopes - - - - - - - - - - - - - - - - 127
1. Electron Lines in Order of Increasing Energy - 127
2. Electron Lines According to Transition Energy - 129
a. 71-Day Re^{183} Lines - - - - - - - - - - - - 129
b. 50-Day Re^{184} Lines - - - - - - - - - - - - 132
c. Electron Lines Not Definitely Assigned to an Isotope - - - - - - - - - - - - - - - - 132
D. Electron Lines of 12.7-Hour Re^{182} Obtained from the Decay of Os^{182}, According to Transition Energy - - - 133
References - 135

LIST OF TABLES

I. Transitions in W^{181} following the decay of Re^{181}.

II. Photon peaks resolved from the 12.7-hr Re^{182} spectrum.

III. Transitions in W^{182} following the decay of 12.7-hr Re^{182}.

IV. Percentage of primary branching and log ft values for electron-capture decay of 12.7-hr Re^{182} to levels in W^{182}.

V. Comparison of theoretical and experimental conversion coefficients of transitions in W^{182}.

VI. Photon peaks resolved from the 60-hr Re^{182} spectrum.

VII. Transitions in W^{182} following the decay of 60-hr Re^{182}.

VIII. Unassigned internal-conversion electron lines of transitions of W^{182} following 60-hr Re^{182} decay.

IX. Differences supporting the proposed W^{182} level scheme.

X. Comparison of theoretical and experimental conversion coefficients of transitions in W^{182}.

a. M1-E2 mixtures

b. E1

XI. Comparison of theoretical and experimental reduced transition probabilities for de-excitation of some of the levels in W^{182}.

XII. Photon intensities of transitions in W^{183} following Re^{183} decay.

XIII. Transitions in W^{183} following the decay of Re^{183}.

XIV. Transitions in W^{184} following the decay of Re^{184}.

XV. Gamma-gamma coincidences observed in the decay of Re^{184}.

XVI. Comparison of theoretical and experimental reduced transition probabilities for E2 de-excitation of the high-energy states of W^{184}.

XVII. Inertial constants for the levels of even-even tungsten nuclei.

XVIII. Energies and intensities of KL_pL_q-Auger electrons of tungsten.

XIX. Energies and intensities of the KL_pM_q- and KL_pN_q-Auger electrons of tungsten.

LIST OF ILLUSTRATIONS

Fig. 1. Excitation function for the production of Re^{181} by alpha-particle bombardment of Ta^{181}.

Fig. 2a. Gamma-ray spectrum of Re^{181}.

Fig. 2b. Gamma-ray spectrum of Re^{182}.

Fig. 2c. Analysis of the "difference" spectrum: the gamma-ray spectrum of Re^{181} corrected for the presence of Re^{182}.

Fig. 3. A partial decay scheme proposed for Re^{181}.

Fig. 4. Nilsson diagrams for particle states in a deformed spheroidal well.
a. 82-126 odd-neutron states.
b. 50-82 odd-proton states.

Fig. 5a. Comparison of electron intensities of transitions observed in both Ta^{182} and 12.7-hr Re^{182} decay.

Fig. 5b. Transition intensities reported by MBMD for the transitions of W^{182} following Ta^{182} decay.

Fig. 6. Comparison of electron intensities of transitions observed in both Ta^{182} and 60-hr Re^{182} decay.

Fig. 7. Decay scheme of 60-hr Re^{182}.

Fig. 8a. L_I/L_{II} ratios for M1, M2, E1, and E2 multipolarities for Z = 74.

Fig. 8b. L_{III}/L_{II} ratios for M1, M2, E1, and E2 multipolarities for Z = 74.

Fig. 9. Densitometer trace of the group of electron lines between 133 and 145 kev observed in the decay of 60-hr Re^{182}.

Fig. 10. Analysis of the level spectrum of W^{182}.

Fig. 11. The level spectrum of W^{183}.

Fig. 12. Partial decay scheme of Re^{184} and some of the levels of W^{184}.

Fig. 13. Comparison of the energies of analogous states in even-even tungsten nuclei.

ELECTRON-SPECTROSCOPIC STUDIES OF NEUTRON-DEFICIENT RHENIUM ISOTOPES

Charles J. Gallagher, Jr.
Radiation Laboratory and Department of Chemistry
University of California, Berkeley, California

September 1957

ABSTRACT

The transitions arising from the electron-capture decay of the neutron-deficient isotopes of rhenium, from Re^{181} to Re^{184}, have been investigated. Five radioactive species: 20-hr Re^{181}, 12.7-hr Re^{182}, 60-hr Re^{182}, 71-day Re^{183}, and 50-day Re^{184} have been studied. Evidence confirming the mass assignment and half life of Re^{181} is reported. Twenty-one transitions are assigned to this isotope and a partial decay scheme is presented. Twelve transitions are assigned to the decay of 12.7-hr Re^{182}, and because of previous investigations on the energy levels of the daughter W^{182}, from Ta^{182} decay, it is possible to assign 15 other transitions to this isomer. A decay scheme is presented. Fifty-seven transitions have been assigned to arise from the decay of 60-hr Re^{182}, and because of previous studies on the levels of W^{182}, from Ta^{182} decay, it is possible to assign 11 other transitions to this isomer. A decay scheme is presented and the levels are analyzed in the light of the Bohr-Mottelson unified model. Evidence for five transitions in addition to those already reported for Re^{183} decay is presented, bringing the total number of transitions observed in the decay of this isotope to 25. Because of previous investigations of the levels of the daughter, W^{183}, from Ta^{183} decay, it is possible to assign at least four other transitions to this isotope. Eleven transitions arising from the decay of Re^{184} are reported, and a partial decay scheme proposed.

The K-Auger electrons observed in this study are reported, and an empirical correlation of their energies is made.

A specific prediction of the Bohr-Mottelson unified model allowing the calculation of electron-capture decay energies from primary-branching ratios is pointed out, and an application is made to the Re^{184} decay scheme.

ELECTRON-SPECTROSCOPIC STUDIES OF NEUTRON-DEFICIENT RHENIUM ISOTOPES

Charles J. Gallagher, Jr.

Radiation Laboratory and Department of Chemistry
University of California, Berkeley, California

September 1957

ABSTRACT

The transitions arising from the electron-capture decay of the neutron-deficient isotopes of rhenium, from Re^{181} to Re^{184}, have been investigated. Five radioactive species: 20-hr Re^{181}, 12.7-hr Re^{182}, 60-hr Re^{182}, 71-day Re^{183}, and 50-day Re^{184} have been studied. Evidence confirming the mass assignment and half life of Re^{181} is reported. Twenty-one transitions are assigned to this isotope and a partial decay scheme is presented. Twelve transitions are assigned to the decay of 12.7-hr Re^{182}, and because of previous investigations on the energy levels of the daughter W^{182}, from Ta^{182} decay, it is possible to assign 15 other transitions to this isomer. A decay scheme is presented. Fifty-seven transitions have been assigned to arise from the decay of 60-hr Re^{182}, and because of previous studies on the levels of W^{182}, from Ta^{182} decay, it is possible to assign 11 other transitions to this isomer. A decay scheme is presented and the levels are analyzed in the light of the Bohr-Mottelson unified model. Evidence for five transitions in addition to those already reported for Re^{183} decay is presented, bringing the total number of transitions observed in the decay of this isotope to 25. Because of previous investigations of the levels of the daughter, W^{183}, from Ta^{183} decay, it is possible to assign at least four other transitions to this isotope. Eleven transitions arising from the decay of Re^{184} are reported, and a partial decay scheme proposed.

The K-Auger electrons observed in this study are reported, and an empirical correlation of their energies is made.

A specific prediction of the Bohr-Mottelson unified model allowing the calculation of electron-capture decay energies from primary-branching ratios is pointed out, and an application is made to the Re^{184} decay scheme.

ELECTRON-SPECTROSCOPIC STUDIES OF NEUTRON-DEFICIENT RHENIUM ISOTOPES

I. INTRODUCTION

In recent years two models of nuclear structure have achieved remarkable success in explaining the physical properties and low-energy states of nuclei. The nuclear shell model, proposed independently by M. Mayer,[2] and Haxel, Jensen, and Suess,[3] has led to an understanding of the particle states of nuclei and has brought clearly into focus the relationships existing among many apparently unrelated physical phenomena. Probably its major achievement has been to establish regions in which a consistent pattern of nuclear properties can be expected. It has, in effect, provided a broad basis for thinking about the nucleus.

The unified collective- and individual-particle model of nuclear structure of Bohr and Mottelson[4,5] applies in general in the regions between the shell closures predicted by the shell model. Its principal successes have been to systematize the experimental data regarding the low-lying states of even-even nuclei,[6] and to predict what states besides the single particle states should be expected in odd-mass nuclei in these regions. The technique of Coulomb excitation, the feasibility of which was predicted by the theory, has become a magnificent tool for obtaining information on the low-lying states of stable nuclei.[6] And, very important from the viewpoint of the spectroscopist, the model makes quantitative predictions regarding the energies of states arising from collective excitations, and the transition probabilities connecting them.

The outstanding success of these theories is too well known to be discussed further here. However, in spite of the very great stimulus that they have given to the experimentalist, there is at least one aspect of the unified model that has been relatively neglected -- the study of the predicted vibrational states in even-even nuclei.

The model predicts that if the spheroidal nucleus vibrates, it can do so in one of two ways: in one way, it will preserve its symmetry about its major axis; in the other, this symmetry is lost. These modes

of vibration are called β- and γ-vibrations respectively, and are predicted to have the same parity as the ground state. Some of these states have been identified in the heavy-element and transition-element regions. A study of the rotational states based on these states is also important in order to obtain information on the moments of inertia associated with the vibrational states and, perhaps, lead to a clearer understanding of the number of particles participating in the collective motion.

Besides these states, however, other states have been observed to occur systematically in the regions where the properties predicted by the unified model begin to appear, or have already appeared. In the heavy-element region some of these states have been characterized by Stephens[7,8] as 1- states with a K quantum number of 0. These states have been attributed to the appearance of non-symmetric vibrations of octupole nature. Sheline[9] has recently pointed out that in the rare-earth and heavy transition-element region other negative-parity states occur systematically and may arise from vibrations similar in nature to the 1- vibrational states in heavy nuclei.

This study was undertaken in an effort to obtain data on the high-energy states in even-even nuclei in an effort to establish their character more exactly and perhaps through this arrive at a clearer understanding of the nucleus.

II. EXPERIMENTAL TECHNIQUES

A. Energy and Intensity Measurements

Internal conversion electron energies were measured using a "lens" type beta-ray spectrometer of 2% resolution and 2% transmission,[10] a double-focusing beta-ray spectrometer of 0.3% resolution and 0.1% transmission,[11] and 52.6-, 99-, 160-, 216-, and 350-gauss permanent-magnet spectrographs of 0.1% resolution and from about 0.01% to about 0.1% transmission.[12]

Gamma-ray energies were measured using a 1-inch by 1-1/2-inch diameter NaI (Tl) scintillation spectrometer of approximately 8% resolution. The detector was connected to 50-[13] and 100-channel[14] differential pulse-height analyzers.

Gamma-ray coincidences were studied using the apparatus described by Strominger.[15]

Internal-conversion electron line intensities were obtained wherever possible by analysis of electron spectra measured in the variable-field magnetic spectrometers. In most cases, however, the resolution of these spectrometers was insufficient to resolve the many lines present, so that the electron intensities had to be obtained from spectrograms exposed in the permanent-magnet spectrographs. Densitometer traces of these plates were made using a Dietart ARL Recording Densitometer.[16] The method of Mladjenović and Slätis[17] for relating photographic blackening to numerical intensities was used to calculate the numerical intensities listed.

Gamma-ray intensities were obtained through analysis of the various gamma spectra measured using the gamma-spectrometer and analyzers mentioned above. The correction curves of Kalkstein and Hollander[18] were used to correct the observed gamma intensities for crystal absorption and Compton effect.

B. Source Preparation

Because many types of bombardments were made to obtain the rhenium activities used in this study, several different chemical separations were utilized to isolate the rhenium activity. In order to avoid repetition, the production of the activity used in the study of each isotope will be discussed separately in the section devoted to that isotope; the chemistry used to purify the rhenium activities will in every case be described in Appendix A.

The source preparations were of two types: cathodic electrodeposition of an undetermined basic rhenium compound from $(NH_4)_2SO_4$ solution on a platinum or copper electrode; and evaporation of activities on aluminum counting plates.

The sources used in the double-focusing spectrometer and the permanent-magnet spectrographs were made by electrodeposition of the carrier-free rhenium activities on 0.010-inch diameter platinum wires in the plating cell described by Smith and Hollander.[19] The electron activity of some of these sources, measured at the surface of the wire, was as high as 30 roentgens.

Sources used in the "lens"-type beta-ray spectrometer were prepared by electrodeposition of the carrier-free rhenium activities on 0.005-inch copper foils 2 cm in diameter. The foils were first painted with finger-nail polish except for an area 2 mm in diameter in the center of the foil. This unpainted area was cleaned with insulin and dried. A drop of solution containing the radioactivity was placed on this clean area, and a platinum anode (a platinum wire with its end melted and flattened) was inserted. Electrodeposition was continued until a source of predetermined activity had been prepared. Solution must be added dropwise continually in this method owing to its high rate of evaporation from the drop. Optimum intensity for sources for this spectrometer were found to be approximately 100 mr (electron) at the surface of the source.

Electrodeposited sources used in this study were never flamed following the electrodeposition, because rhenium oxide is volatile.

The evaporation sources were prepared by evaporating a drop of carrier-free rhenium activity on aluminum counting plates. Sources were also prepared by drying Re_2S_7 slurries on aluminum counting plates. These evaporated samples were used exclusively for gamma-ray analyses and half-life measurements.

III. ELECTRON SPECTROSCOPIC STUDIES OF NEUTRON-DEFICIENT RHENIUM ISOTOPES

A. 20-Hour Re^{181}

Mass Assignment and Half Life

The 20-hr electron-capturing isotope rhenium-181 was first produced by alpha-particle bombardment of stacked tantalum foils by Sweeney,[20] who assigned it a 17-hr half life. His assignment was tentative because he only observed a 17-hr component in his decay curves when the bombarding alpha energy was greater than 40 Mev. During the present investigation of rhenium isotopes produced by 48-Mev alpha particles on tantalum, a very prominent 366-kev gamma transition was observed that decayed with an approximately 20-hr half life. On the basis of these data we assigned the 20 hr half-life to rhenium 181 and the 366-kev gamma transition as a transition in the daughter nucleus, W^{181}.

To verify this mass assignment, two experiments were done. The first consisted of two stacked-foil excitation functions performed by bombarding a stack of 0.001-inch tantalum (99.98% pure) with a very low-intensity beam of alpha particles in the Berkeley 60-inch cyclotron.

In the first experiment the foils were counted directly in a sodium iodide counter with the 50-channel differential pulse-height analyser. The intensity of the 366-kev gamma in each foil was then plotted against the mean energy of the alpha particle in each foil to give a rough excitation function. The threshold energy was approximately 33 Mev, and the curve was still rising at the full energy of the cyclotron, 48.6 Mev. This threshold and the shape of the curve clearly must correspond to a Ta^{181} $(\alpha,4n)$ Re^{181} reaction. The excitation function is illustrated in Fig. 1.

The second stacked-foil bombardment was used to determine the half-life of the isotope. Much greater activities were produced, and carrier-free chemical separation (Chemistry A, Appendix A) to obtain pure rhenium was performed on the first foil. The decay of the 366-kev transition was followed in the double-focusing beta-ray spectrometer and

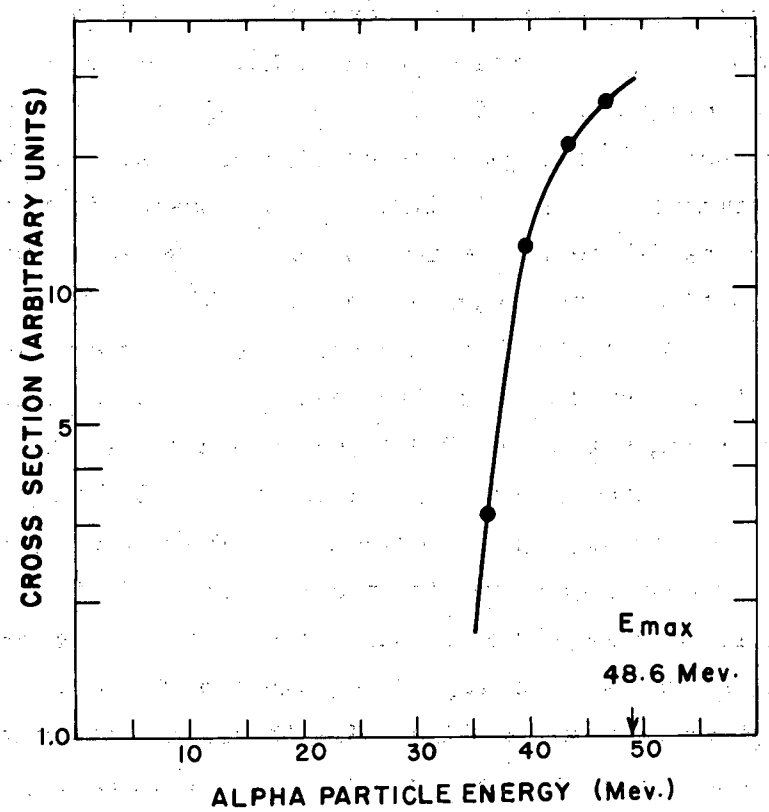

MU-13388

Fig. 1. Excitation function for the production of Re^{181} by alpha-particle bombardment of Ta^{181}. E_{max} is the maximum alpha-particle energy produced by the cyclotron.

on the 50-channel analyser. The results obtained by the two methods were in good agreement. The half life determined was 20 ± 2 hrs.

The second experiment was conducted several weeks after the second bombardment. Tungsten carrier was added to the previously separated pure rhenium activity. WO_3 was precipitated (Chemistry B, Appendix A) and the precipitate was gamma-analyzed. A single peak was observed at the energy of tantalum K x-rays. Because W^{181}, the only radioactive tungsten isotope in this region, has been observed to decay almost entirely to the ground state of Ta^{181},[21-25] and since the long-lived rhenium isotopes exhibit complex gamma spectra, we feel that this experiment further establishes the activity first observed as Re^{181}. The half life of the K x-ray peak is in agreement with the 140-day half life reported for W^{181},[26] but we have not followed it for a long enough period to verify this value.

General Resumé of Spectroscopic Results

The decay of Re^{181} is observed to populate predominantly a level 365.50 kev above the ground state of W^{181}. This level has a long ($> 10^{-6}$ sec) half life, and is observed to decay by a highly converted transition.

Besides this transition, 16 other transitions are established on the basis of conversion-electron and gamma spectroscopy. Four other transitions are reported, but their assignments are tentative.

Only a partial decay scheme is given because the data are indicative of a more complex spectrum than has been established in the present study. A total of six levels are assigned on the basis of energy sums and differences. Nine transitions are found to fit into these levels, leaving seven definitely established and the four questionable transitions unassigned.

Gamma Spectroscopy

The complexity of the radiations arising from the decay of the neutron-deficient rhenium isotopes studied made it necessary to employ a somewhat circuitous method to obtain gamma intensities for Re^{181}. Such a method was necessary because Re^{181} could not be obtained free from the rhenium isotopes of higher mass number, and because its half life is of the same magnitude as the 13-hr isomer of Re^{182}.

The following method was used to obtain the gamma spectrum of Re^{181}. A stack of 0.001-inch tantalum foils was bombarded in the 60-inch cyclotron. From excitation function curves for the Ta^{181} (α,xn) Re reactions, it was concluded that the activity in the first foil would be predominantly Re^{181}, and that in the fourth foil would be predominantly the two Re^{182} isomers, essentially free of Re^{181}.

After bombardment, chemistry C (Appendix A) was employed to prepare the samples for gamma analysis. The two gamma spectra observed from the two foils were, indeed, different. They are illustrated in Fig. 2 (a and b). Hereafter we shall refer to the sample from the first foil as the Re^{181} sample and that from the fourth foil as the Re^{182} sample.

The decay of the 1100- and 1200-kev transitions in the Re^{181} spectrum appear to be complex, with 13- and 60-hr components. The decay of the remaining peaks of the Re^{181} spectrum appeared to be complex also, but the components were approximately 20- and 60-hr. It was, therefore, concluded that transitions with energies 366-, 480-, 560-, 640-, 815-, 890-, and 980-kev were transitions arising from the decay of Re^{181}. It was not possible to decide whether there was a 20-hr component in the decay of the 1100- and 1200-kev transitions. The 1430-kev transition appeared to decay almost entirely with a 60-hr half life. However, the 1430-kev transition in the Re^{181} sample was considerably more intense relative to the 1100- and 1200-kev peaks than it was in the Re^{182} samples. Because this might possibly be due to coincident "stack-up" of some of the transitions in the sample, the assignment is tentative.

In order to obtain the intensities of the high energy gamma transitions of Re^{181} listed above, the following method was used. The 1200-kev transitions of the Re^{181} and Re^{182} spectra were used as normalization points, and the gross Re^{182} spectrum was subtracted from the

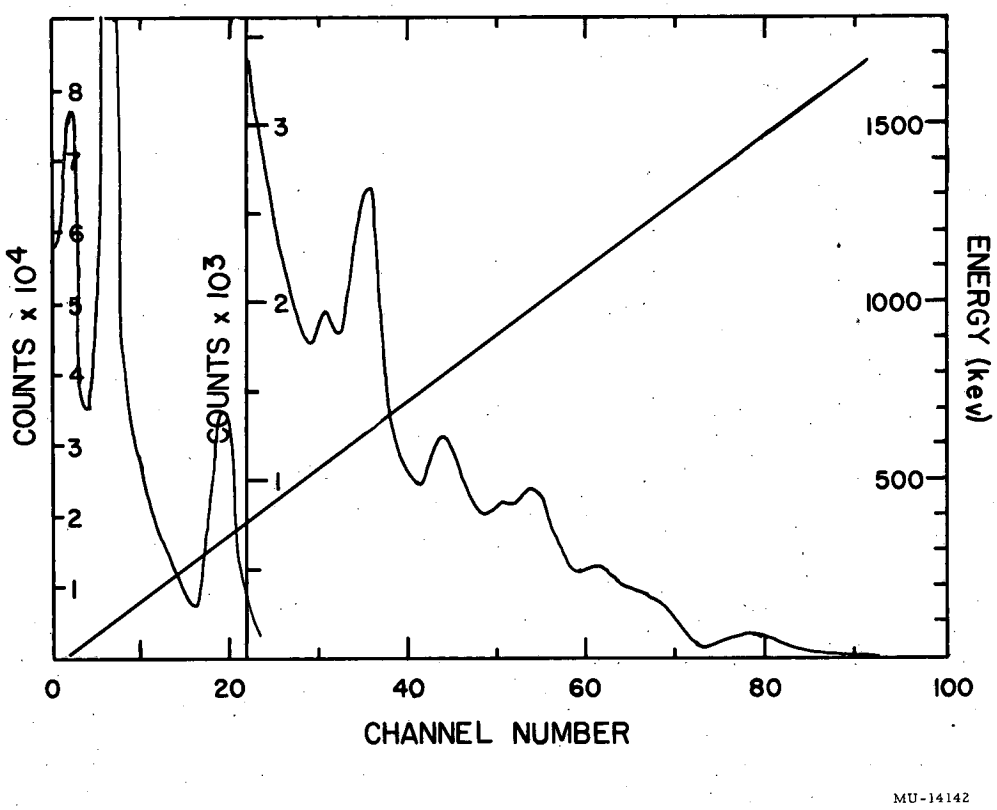

Fig. 2a. Gamma-ray spectrum of Re^{181}.

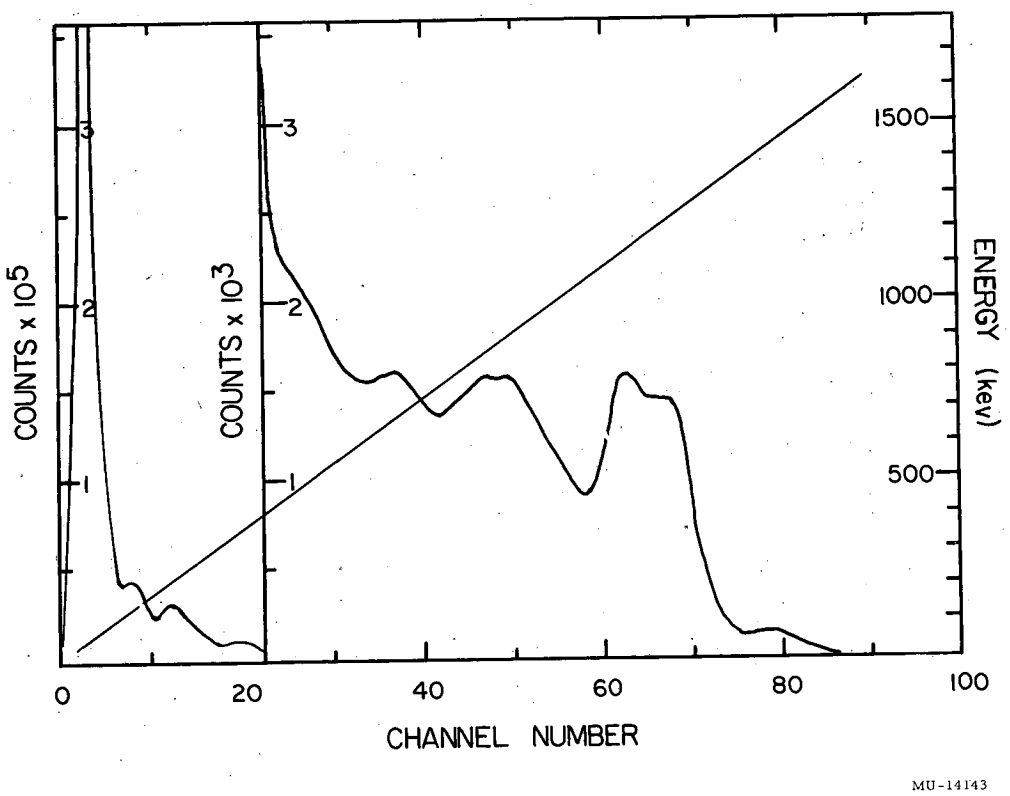

Fig. 2b. Gamma-ray spectrum of Re^{182}.

gross Re^{181} spectrum. Such a procedure is justifiable because: (1) the 1200-kev peak was used for the normalization because it had decayed as the half lives of the two Re^{182} isomers, which indicated no Re^{181} component; and (2) the transitions are all observed to decay with a composite half life, indicating a mixture of the 60-hr component.

A further consideration led us to subtract not the Re^{182} spectrum taken at the same time as the Re^{181} spectrum but rather that taken five days later when all the Re^{181} and 13-hr Re^{182} had decayed away. This was believed necessary in order to avoid subtracting any Re^{181} present in the Re^{182} sample. To insure that there would not be a serious discrepancy introduced due to possible differences in the 13-hr and 60-hr Re^{182} spectra, the Re^{182} spectrum taken immediately after bombardment was normalized against that taken five days later. The normalization showed that, at least in the region above 366-kev, the two spectra were the same to within the statistical error in the counting rate.

The difference spectrum is the envelope curve in Fig. 2 (c). The intensities of each transition have been obtained by normalizing standards to each peak, one at a time, and subtracting, starting with the highest-energy peak. This method removes the Compton contribution of this peak from the background of the lower-energy peaks, and comparison of the width of the lines permits a fair determination of the relative complexity of the peak. Bi^{207} and Cs^{137} were used as standards.[26]

When the analysis was completed, it was found that only the 980-kev peak was broader than that of the standard, indicating that there were at least two transitions with an energy difference $< 8\%$ in this peak. An 1100-kev component also appeared in the difference spectrum, indicating that there is probably a transition of this energy in the decay of Re^{181}.

The results of the intensity measurements are listed in Table I.

Dr. Donald Strominger[27] performed coincidence studies on the Re^{181}, using fast-slow coincidence pulse-analysis apparatus.[15] He observed no coincidences between the 366-kev gamma transition and K x-rays, and from this result it was concluded that the half life of the state giving rise to this gamma is greater than 10^{-6} sec. At the time of the

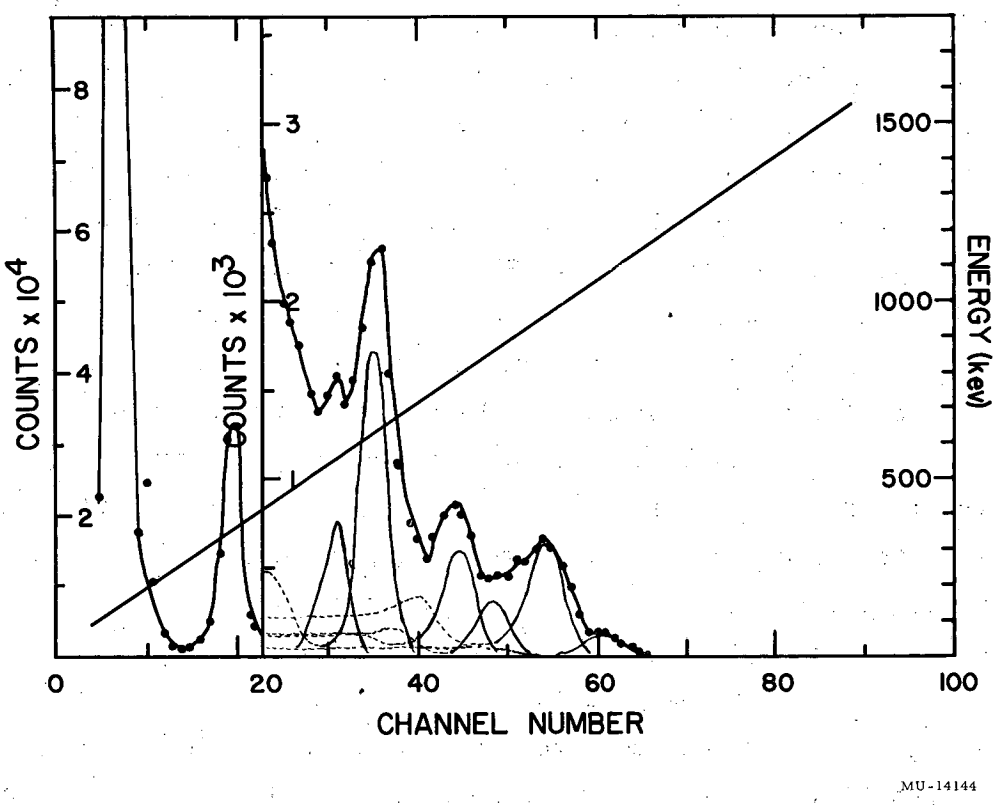

Fig. 2c. Analysis of the "difference" spectrum: the gamma-ray spectrum of Re^{181} corrected for the presence of Re^{182}.

Table I

Transitions in W^{181} following decay of Re^{181}

Initial and final energy levels	Gamma-ray energy (kev)	Gamma-ray intensity	Conversion lines observed in Re^{181} decay[a]							Multipolarity
			K	L_I	L_{II}	L_{III}	M_I	M_{II}-M_{III}	N_I	
DC	47.38±0.05[b]	c		w[b]						(M1)
EC	103.13±0.05[b]	c		ew[b,d]	ew[b]	ew[b]				(E2)
(e)	122.55±0.06[b]	c	ew[b,f]							
EB	252.3±0.2	c	vw	vvwd[g]		ew		vvwd[h]		(E2)
(e)	332.3±0.3	c	vvw	ew						
(e)	342.0±0.3	c	vvwd							
FD	360.95±0.2	c	m	vw						
BA	365.50±0.2	5.0	vs	ms	vvw	vvw	mw		vwd	M2
GD	441.9±0.4	c	vvw	ew						
(e)	469.9±0.5	c	vvw							
(e)	486.7±0.5	c	ew							
GC	489.0±0.5	c	ew							
FB	557.3±0.6	0.3	ew?							
GB	638.3±0.6	1.0	ew							
(e)	815±20	0.6	j							
(e)	894.7±0.9	0.3	ew?							
(e)	953.8±1.0	0.9	ew							
	K x-rays	8.7								
Questionable Transitions										
(e)	310.4 ± 0.3	c	vvwd[g]							
(e)	318.8 ± 0.3	c	vvwd[h]							
(e)	~1100	0.3[k]								
(e)	~1430	0.3[k]								

Notes on Table I

a. The abbreviations used for the intensities are e = extremely, d = diffuse, m = moderate, s = strong, v = very, w = weak. The intensity scale used is es, vvs, vs, s, ms, m, mw, w, vw, vvw, ew.

b. Energies and intensities obtained from a 52-gauss permanent-magnet plate. All other energies and intensities were obtained from 216- and 350-gauss magnet plates.

c. Masked by transitions of Re^{182} and Compton-electron background from the 365.50-kev transition.

d. Line possibly misassigned.

e. Unassigned in decay scheme.

f. This line might be L_I of a 65.13-kev transition.

g. K 310.4, L's 252.3 superimposed.

h. K 318.8, M's 252.3 superimposed.

j. Not observed in conversion-electron spectrum.

k. These might possibly be Re^{182} transitions which had enhanced intensities due to stack-up.

coincidence study the Re^{181} component had already decayed appreciably, and the numerous radiations from the longer-lived rhenium isotopes precluded further coincidence studies at that time.

Electron Spectroscopy

The electron lines assigned to Re^{181} have been assigned on the basis of half life alone. In spite of the fact that the rhenium spectrum is so complex, we believe that all the lines that we report are correctly assigned to Re^{181}, except possibly one group. The one exception is the group of lines assigned as the L_I, L_{II}, and L_{III} lines of the 103.13-kev transition. These lines were observed as very weak lines on only one spectrogram and might possibly be conversion electrons from an unassigned transition in 60-hr Re^{182}. All of the lines reported were sorted from among the many Re^{182} lines present in the exposures made. The major source of concern in the study of this isotope is that many lines might accidentally have the same energy as transitions in 60-hr Re^{182}, in which case they would not have been identified.

As is described in the next section, the possibility of misassignment of low-energy lines of the short-lived Re^{182} isomer to transitions in Re^{181} was greatly reduced by the preparation of sources of the 13-hr Re^{182} isomer from the decay of Os^{182}. As a further check, tantalum was bombarded below the threshold for Re^{181} production and the electron spectrum searched for the Re^{181} lines. These lines were not observed in any of the plates studied.

The decays of the high-energy transitions corresponding to the electron lines observed were followed in the gamma spectrometer. All the high-energy transitions assigned to Re^{181} were observed to decay with a 20-hr half life.

Although we have attempted to prepare electron-spectrometer sources of Re^{181} in the same manner as the Re^{181} gamma-ray sources were prepared, we have, up to the present, been unsuccessful. Our lack of success in this aspect of the work results from the fact that the

preparation of high-activity rhenium sources needed for electron studies requires intense cyclotron-beam currents and thick targets, neither of which can be used in the thin-foil techniques used to produce the predominantly Re^{181} activities.

In Table I we list the energies of the transitions in Re^{181} decay deduced from internal-conversion-electron lines. The low-energy transitions are quoted to 0.05% resolution, the higher-energy lines to 0.1%. The limits of error on the low-energy lines are based on the very accurate internal-field calibration at these energies provided by the presence of many conversion electrons of transitions that were measured by Murray et al. (hereafter referred to as MBMD),[28] using a bent-crystal gamma spectrometer. The limits of error on the high-energy lines are larger because the magnetic fields in the high-field spectrographs have not been calibrated as accurately, owing to the scarcity of precise energy standards in this region.

Of the high-energy gamma transitions observed and listed in Table I, only the 815-, 1100-, and 1430-kev transitions were not verified by at least a K-conversion line in the electron spectrum. The energy of the ~980-kev transition is calculated from its K-conversion line to be 953.8-kev, which is lower than the energy observed in the gamma spectrum by about 30-kev. It thus appears that this peak is indeed complex, as was suggested in the interpretation of the gamma spectrum. The exact energy of the other component or components has not been determined.

Visual intensities are listed in Table I because the electron lines observed were either too weak to be measured from a densitometer trace or else the background on the plate precluded determination of numerical intensities.

The energies of the conversion lines and the complex spectrum from which they were obtained are tabulated in Appendix B, part 1. In part 2 (b) of Appendix B the Re^{181} conversion lines are tabulated according to transition energy.

Discussion of Transitions

Because the 366-kev transition is more intense than the sum of the other transitions observed in Re^{181} decay, it seems likely that the state that gives rise to it is populated directly and decays directly to ground. Therefore, we shall begin our discussion by considering what is known about this transition from other experiments.

Recent studies[29,30] of short-lived isomers produced by betatron excitation of natural tungsten have revealed a 366-kev transition with a half-life of 14.4×10^{-6} sec. (We will discuss this half life in relation to the state assignment in more detail later.) The transition was reported to have a K-conversion coefficient of 0.30 ± .03. These workers assigned the transition to W^{181}. Our work confirms this assignment, because the isomer is formed in the decay of Re^{181}. Bureau and Hammer[30] (hereafter called BH) suggest that the multipolarity of the 366-kev transition, as determined by their absolute conversion coefficient, agrees with either a 28% E1 -- 72% M2 or 65% M2 -- 35% E3 mixture. From the very low intensity of the L_{II} and L_{III} conversion electrons relative to the L_I, we can rule out the M2--E3 mixture. Their mixing ratio was calculated using Rose's[31] theoretical conversion coefficients which are now generally considered to be too high because of the neglect of a finite-nuclear-size correction. Using Sliv's[32] K-shell internal-conversion coefficients, we re-calculate the mixture to be 14% E1 -- 86% M2. Furthermore, the experimental limits of error given by BH do not eliminate a pure M2 assignment. It is this latter assignment that we prefer.

The other transitions in Re^{181} decay can be discussed briefly. The 47.38-kev transition appears to be M1 on the basis that only the L_I line is seen and all other multipolarities are predicted theoretically to have relatively strong L_{II} and L_{III} conversion at this energy. Furthermore, if these lines were present in intensity comparable to the L_I (as required for M2, E1, E2, etc., multipolarities) they would have been observed. The 103.13-kev transition has already been discussed. K, L_I, L_{II}, L_{III}, M_{II}, and M_{III} conversion lines of the 252.3-kev transitions were observed. Because these were only observed on the high-field

permanent magnets, their energies are only quoted to 0.1%. It must be pointed out that it is possible to assign the L and M lines of this transition as the K lines of transitions of 310.4- and 318.8-kev. Such assignments appear to be supported by the observation of weak lines at the calculated energies of the L lines of these transitions. Because these latter were observed in the plate exposed to the strongest source we were able to prepare and the plate turned out to be damaged, we could not be confident that the lines observed were really the L lines. All three transitions are listed in Table I.

Although we have both gamma and electron intensities for the transitions above 557-kev, we do not believe that the data merit the calculation of absolute conversion coefficients, principally because of the weakness of the lines and the poor quality of the plate. However, we can estimate the relative conversion coefficients for close-lying lines. In this way it can be concluded that the conversion coefficients of the 557.3- and 638.3-kev transitions are about equal, the conversion coefficient of the 894.7 is about twice that of the 954.8, and these latter two both are more highly converted than the 815. Because the numbers calculated are so approximate we do not include them here. The essential aspects of the data leading to these conclusions can be seen from Table 1.

Decay Scheme

The partial decay scheme we assign to Re^{181} is presented in Fig. 3. Experimentally, level B is the only level which is well established, and this level is assigned to decay into the ground state on intensity arguments alone (see discussion).

The proposed ordering of levels C, D, E, F, and G is based on transition-energy sums and differences. The position of this group of levels within the decay scheme is not experimentally established. This group has several possible alternative arrangements, as can be seen from topological considerations.[33] The reasons for placing levels above rather than below B are discussed below.

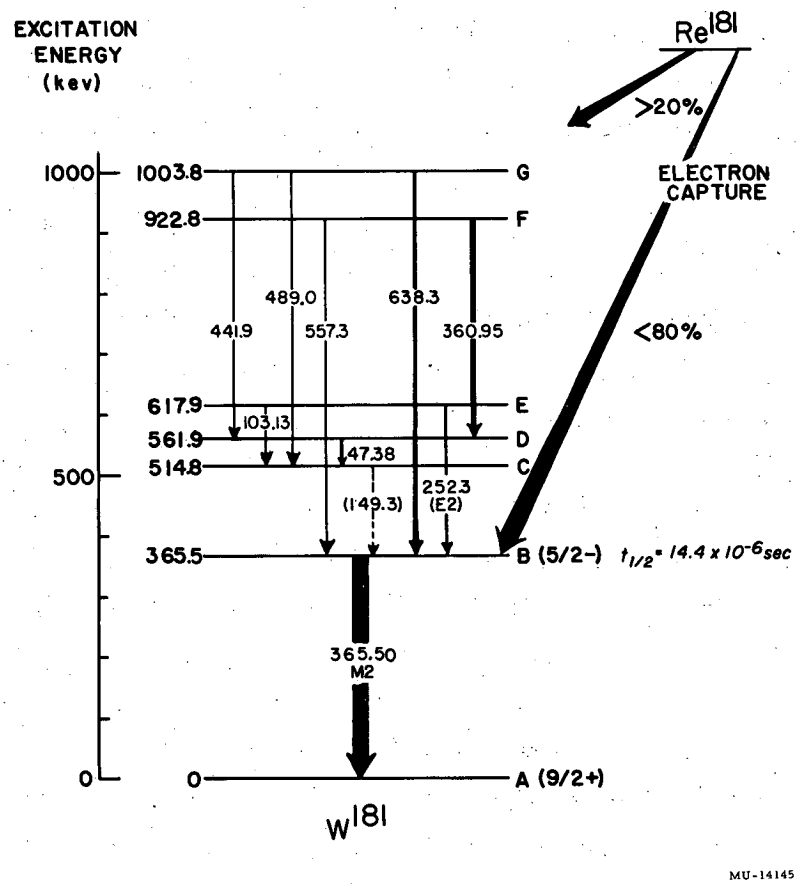

Fig. 3. A partial decay scheme proposed for Re^{181}. The transition dotted in the decay scheme would be masked by the 149.39-kev transition following 60-hr Re^{182} decay. The half life of state B was measured by Bureau and Hammer.[30]

The internal-conversion-electron lines of the transition, which is dotted in the decay scheme, would be masked by conversion lines in the electron spectra of Re^{182} and Re^{183}.

Discussion of Results

The states to which primary electron-capture decay of Re^{181} occurs are, at present, uncertain. However, from the intensity of the 365.5-kev transition in both the electron and gamma spectra, it appears that the level which gives rise to this transition is probably populated by direct electron capture. We can calculate the branching ratio in order to check this assumption, if we first assume that all the intensity of the 365.5-kev transition is due to primary capture. We obtain the corrected 365.5-kev transition intensity by correcting the gamma intensity for internal conversion using the experimentally determined conversion coefficient of 0.36 (BH's value of $\alpha_K = 0.30$ corrected for L- and M-shell conversion using our experimentally determined K/L/M ratio of 5.7/1/0.2). The total decay intensity is calculated by subtracting the total intensity of K vacancies due to the conversion of the 365.5-kev gamma from the observed K vacancies (K x-rays corrected by Auger coefficient) and correcting the remainder for K/L branching. An L/K-branching ratio of 0.16 (corresponding to a decay energy of 0.7 Mev to the 365.5-kev state) was obtained from the curves of Brysk and Rose.[34] A value of 0.045 for the Auger coefficient was obtained from a plot of Fluorescence Yield vs Atomic Number given by Gray.[35] The value of the branching ratio to this state thus calculated is 80%. The maximum limits of error which can be set from the K x-ray intensity are ± 15%. The presence of highly K-converted transitions which have not been observed will act to increase the value.

To calculate a log ft value for electron capture to this state, we estimated a total decay energy of 1 Mev from the Coryell beta systematics.[36] When we used the branching ratio above, a log ft of 5.8 was calculated.

We must now discuss our original assumption that no secondary decay occurs to this level. As is manifest from the proposed decay scheme, secondary decay does occur to the level. However, the direct result of this will be to raise the log ft value. If we now calculate what the log ft would be, assuming 50% of the decay occurs by secondary decay, we calculate a log ft of 6.1. We can, therefore, conclude that unless the unresolved and unobserved transitions in Re^{181} decay which cascade into level B are present in intensity up to almost twice that of all the other transitions that have been resolved (in which case all of the decay to level B is secondary), the log ft value for electron-capture decay to it will be about 6. It is likely, therefore, that level B is populated directly.

An explanation of the half life of level B in terms of nucleon states in a spheroidal well as calculated by Nilsson[37] has been advanced by BH. They suggest that the transition observed corresponds to a transition between two Nilsson[37] odd-neutron states, 7/2- $\longrightarrow$ 9/2+, the predominant M2 character resulting from a high degree of cancellation of E1-transition matrix elements for the Nilsson[37] states in question. Although retardation from single-particle formula[38] rates occurs generally for low-energy E1 transitions, the retardation (granting E1 admixture of 14% here) of about 10^{10} would be exceptionally large for E1 transitions not K-forbidden, retardations of 10^4 to 10^5 being the general rule.[39] These life-time considerations strengthen our alternative assignment of pure M2 character to the isomeric transition. The M2 transition is retarded by about a factor of 700.

It has been suggested by Derbrunner, Heer, Kundig, and Ruetschi[25] that the W^{181} ground state is 7/2-, as determined from the decay scheme of W^{181}. Such an assignment would not appear to be consistent with the data we have obtained. It is, furthermore, quite possible to explain the W^{181}-decay data using a 9/2+ assignment for the ground state of W^{181}. We, therefore, prefer the 9/2+ assignment.

Consideration of the Nilsson[37] diagram for odd-neutron states (Fig. 4a) shows a nearby 5/2- state that would give rise to a pure M2 transition to the 9/2+ ground state of W^{181}, and we favor this state assignment for the isomer.

Another test of the assignment of the isomeric state can perhaps be applied using our experimental value for the log ft for electron capture to the isomeric state. This test is a consequence of the asymptotic-quantum-number beta-selectron rules proposed by Alaga.[40] If we postulate that the 5/2+ odd-proton state (with asymptotic quantum numbers N, n_z, Λ = 4, 0, 2) proposed for the ground state of Re^{183},[41] Re^{185},[42] and Re^{187},[42] is also the ground state of Re^{181}, then decay to the 7/2- state (N, n_z, Λ = 5, 1, 4) proposed by BH should theoretically exhibit a larger log ft value than decay to the 5/2- state. This increased hindrance for electron capture to these states is caused by the fact that the 5/2+ $\longrightarrow$ 7/2- beta transition is first-forbidden, hindered, while the 5/2+ $\longrightarrow$ 5/2- transition is first-forbidden, unhindered. On the basis of our log ft value, the 5/2- state is favored; in fact, it appears to be almost too favored for a first-forbidden transition. Perhaps this result indicates that a large percentage of the primary-electron capture does indeed go to the higher-energy states.

The ordering of levels C, D, E, F, and G such that they populate level B, rather than A, is based on two logical extensions of the reasoning followed in assigning the spin and parity 5/2- to the isomeric state. The first is based on the 5/2+ assignment to the ground state of Re^{181}. If this assignment is correct, then Re^{181} can be expected to decay to states (assuming no second-forbidden or first-forbidden, unique, beta decay) with spins and parities 3/2±, 5/2±, and 7/2±. The second is that such states are known to be nearby from experiment and are predicted to be nearby from the Nilsson[37] diagram. They are the 3/2- state, and the rotational states of the 1/2- state observed in the W^{183} nucleus,[28,42] and the 7/2- state assigned as the ground state in Hf^{177}.[42] The 7/2- state is the state suggested for the isomeric state in W^{181} by BH. From the Nilsson[37] diagram, however, this state is expected to be below the 5/2- state in energy.

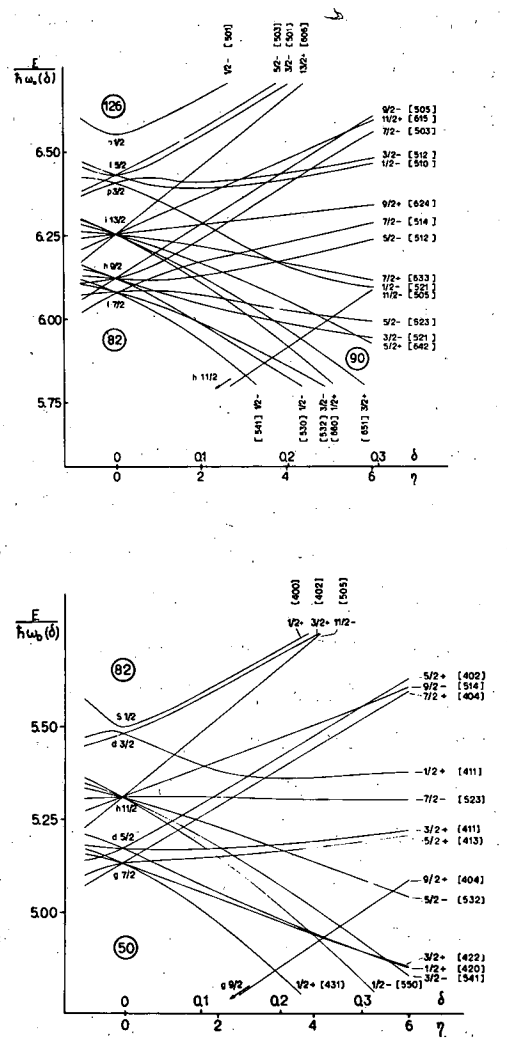

MU-14146

Fig. 4. Nilsson diagrams for particle states in a deformed spheroidal well. (a) 82-126 odd-neutron states. (b) 50-82 odd-proton states.

To carry the comparison further, we might expect to observe a decay pattern for Re^{181} similar to that observed for Re^{183} if the same odd-neutron states are available in W^{181}. Such a comparison would predict that the major part of the primary electron-capture decay would go to the 3/2- state and the spin-5/2 member of its rotational band. Only a very small fraction, or perhaps none at all, would be expected to populate the rotational states of the K = 1/2 band. Furthermore, because the 5/2- state assigned as the isomeric state has the same asymptotic quantum numbers, (5,1,2) (N, n_z, and Λ, notation) as the 3/2- state in W^{183} (i.e., they are spin orbit partners differing only in Σ), we might expect a large amount of primary depopulation to this state also. As already noted, primary decay to the 7/2- state would be hindered.

The next consideration is whether or not the other levels would lie higher or lower in energy than the isomeric state. If they were lower in energy they might be expected to receive the depopulation of the 5/2- state and also direct electron capture. On the other hand, if they were higher in energy they might be expected to decay into the isomeric state, while direct population to them would be lowered by decay-energy considerations. Therefore, in constructing the decay scheme, we favored the arrangement of levels that placed levels above, rather than below, the isomeric state.

The absence of any sums equal to the 365.50-kev transition raised a question about the position of the 7/2- state predicted in the Nilsson[37] diagram. Because many of the transitions that could make such a sum are masked, however, it is not at present possible to answer it.

It is clear from the number of unassigned transitions in W^{181} that the complete level scheme must be extremely complex. We could not fit the unassigned transitions into the decay scheme through any sum or difference within experimental error, and we believe our estimated limits of error are accurate. A possibility, which we believe we have eliminated, is that the field of the high-field magnets is slightly different from the field used in the calculations. This would change the absolute energies of the transitions but should not affect the

differences. Such energy changes might produce new sums that would fit into the decay scheme. The maximum energy change that would be caused by such a field uncertainty we believe to be about 2 kev and would apply only to those transitions whose conversion lines lie above the conversion lines of the 365.50-kev transition. The calibration used to determine the lower-energy lines has already been described.

It is clear from the proposed W^{181} spectrum that further studies must be made. These will have to be made with sources containing large percentages of Re^{181} and very little of the short-lived isotopes, especially the 60-hr Re^{182}. We hope that the present study will serve as a useful guide in such work, but until more data are obtained on the transitions of W^{181}, especially coincidence data, we believe the interpretation we give must be considered tentative.

B. 12.7-Hr Re^{182}

Mass Assignment and Half-Life

12.7-hr Re^{182} was first reported by Wilkinson and Hicks,[43] who characterized it as an electron-capturing isomer of Re^{182}. They were not able to distinguish the higher-energy state of the isomeric pair. The results of the half-life determination and mass assignment obtained in the present study are in excellent agreement with the earlier results.

General Resumé of Spectroscopic Results

The decay of the 12.7-hr Re^{182} (hereafter referred to as Re^{182}) is observed to proceed entirely to high-energy levels of W^{182} previously reported by MBMD. Only 10 of the 27 transitions reported by MBMD have been seen definitely, but they establish that 8 of the 11 levels in W^{182} reported by MBMD are populated, either directly or by cascade transitions. Two transitions that would establish the population of two of the remaining levels are masked. We have obtained no experimental verification of the MBMD level E from Re^{182} decay.

Gamma-Ray Spectroscopy

The sample used in the analysis of the Re^{182} gamma spectrum was the sample discussed in Section III-A, "Gamma Spectroscopy" and called "the Re^{182} sample". The method of preparation is described in that section.

Because of the complexity of the gamma spectrum arising from the decay of the Re^{182} isomers, the gamma spectrum could only be used as a gross check on the decay scheme. The only prominent peaks were the K x-ray and composite 1100- to 1200-kev peaks. The Re^{182} gamma spectrum is illustrated in Fig. 2 (b).

The decay of the sample was followed in the gamma spectrometer until essentially all of the 60-hr isomer had decayed away and it was no longer possible to obtain a statistically significant counting rate for the 1100- to 1200-kev peak. The 60-hr component was then subtracted from the peaks and the activities of the 13-hr components of the peaks at time zero (the time at which the sample had been taken out of the cyclotron) were calculated. These results are listed in Table II. The limits of error on the intensities are estimated to be ~ 30%.

Electron Spectroscopy

The determination of the Re^{182} conversion-electron spectrum required the preparation of sources free from the 60-hr Re^{182} activity. Such a step was necessary because it was expected that the two isomers decayed through some of the same states of W^{182} and, therefore, the short-lived component of these transitions would probably be overlooked in the very complex 60-hr Re^{182} spectrum.

To prepare these sources, a radioactive parent of Re^{182}, Os^{182}, was produced by bombardment of naturally occurring tungsten with 48.6-Mev alpha particles. It had been shown in preliminary experiments[44] that Os^{182} decayed only into the 12.7-hr Re^{182} isomer. Carrier-free-osmium chemistry[45] was performed by V. S. Shirley, and the sources were prepared by cathodic deposition of the osmium activity from $(NH_4)_2SO_4$ plating

Table II

Photon peaks resolved from the 12.7-hour Re^{182} spectrum

Gamma-ray	Intensity
K x-ray	83
1122 to 1222	40

solution at pH ~ 2 onto 0.010-inch diameter platinum wires. In the study of Re^{182}, the most important data were obtained from permanent-magnet spectrograms of the electron spectrum of a mixture of rhenium and osmium activities, prepared by J. O. Newton and V. S. Shirley.[44]

The analysis of the very complex spectrum resulting from the simultaneous presence of five radioactive isotopes, each with very many transitions, was difficult. The problem was solved by subtracting every line observed in the already carefully analyzed rhenium spectrum from the osmium-rhenium spectrum. The rhenium spectrum that was obtained was then divided into Re^{183} and Re^{182} spectra. The Re^{183} spectrum was then checked against the already-determined spectrum of this isotope[41] to insure consistency of the results. The Re^{182} spectrum was compared to the spectrum of the 60-hr Re^{182} and found to be consistent with it. To further insure correct assignment, a series of exposures was made[44] which verified the growth and decay patterns to be expected for the electron lines of osmium daughters. (Exposures from a series of bombardments at different energies[44] were compared) to insure that no new lines were actually rhenium lines. The intensities of the new lines were then checked against the estimated isotopic abundances of the osmium isotopes to which they had been assigned. The results were in agreement with the assignments that had been made. The analysis of the internal conversion-electron lines of Re^{182} by transition energy is tabulated in Appendix D. All of these lines were obtained from the osmium-rhenium electron spectrum.

The transitions observed in Re^{182} decay were surprisingly easy to analyze, because all of the transitions observed have already been seen in Ta^{182} decay and thoroughly analyzed by MBMD. We have listed in Table III all the transitions reported by MBMD and the intensities that we have observed for the conversion-electron lines of those transitions.

Table III

Transitions in W^{182} following the decay of 12.7-hr Re^{182}

Initial and final energy states	Gamma-Ray energy (kev) from MBMD	Conversion-electron intensities[a] obtained from exposure of a 13-hr Re^{182} source in a 99-gauss permanent-magnet spectrograph							Multi-polarity
		K	L_I	L_{II}	L_{III}	M_I	M_{II}	M_{III}	N_I	
ED	33.36		Not observed in Re^{182} decay							
HG	42.71		Not observed in Re^{182} decay							
KJ	65.71		10	0.9	[b]	1.4				M1 + E2
FD	67.74		32	14	16	9.1	3.4	2.1	2.5	E1
HF	84.67	[c]	26	11	7.4	7.0		3.0	5.6[d,e]	M1 + E2
BA	100.09	[c]	24[e]	104	92		<49[f]	<36[f]	<16[g]	E2
JH	113.66	15								M1 + E2
KI	116.40	<0.1[h]								(M1 + E2)
HD	152.41	5.2[j]	3.1[j]							E1
JG	156.37		Not observed in Re^{182} decay							
KH	179.36		Not observed in Re^{182} decay							
JF	198.31		Not observed in Re^{182} decay							
KG	222.05		Not observed in Re^{182} decay							
CB	229.27	[k]								E2
KF	264.09		Not observed in Re^{182} decay							
EC	927		Not observed in Re^{182} decay							
FC	960		Not observed in Re^{182} decay							
GC	1003		Not observed in Re^{182} decay							
DB	1122	ew[ℓ]								M1 + E2
EB	1155		Not observed in Re^{182} decay							
FB	1189	ew[ℓ]								E1 + M2
DA	1222	ew[ℓ]								E2
GB	1231	ew[ℓ]								M1 + E2
FA	1289		Not observed in Re^{182} decay							
HA	1375		Not observed in Re^{182} decay							
IA	1437		Not observed in Re^{182} decay							
KB	1454		Not observed in Re^{182} decay							

Notes on Table III

a. Numerical intensity units are arbitrary. Visual intensity units have the same meaning as in Table I.

b. L_{III} 65.71, L_I 67.74 superimposed.

c. Line is in region where intensity corrections are excessively large.

d. Probably N_I, N_{II}, and N_{III}.

e. On intense background.

f. Resolution of these partially superimposed lines is difficult and leads to too high intensities.

g. N_{II}-N_{III} intensities.

h. KL_IL_{III} (W), KL_IL_{II} (Re), and K 116.40 superimposed.

j. This very anomalous K/L_I intensity has been observed from two sources.

k. K 229.27, M_I 162.33 (W^{183}) superimposed.

ℓ. Lines observed on the 350-gauss permanent magnet.

Discussion of Results

Decay scheme. Because only levels observed in Ta^{182} decay are populated in Re^{182} decay, we can use these data as a check on the high-energy states in the W^{182} level scheme proposed by MBMD. We compared our electron data with theirs, and our results are in complete agreement with their level scheme for W^{182}.

The relative direct beta-decay to the various excited states in W^{182} from Ta^{182} and Re^{182} decay was determined by comparing the ratio of MBMD's electron intensities to ours. Their electron intensities were obtained by multiplying their gamma intensities by their absolute conversion coefficients. This method allows us to compare transition intensities directly, without employing assumptions about our gamma intensities. In Fig. 5 (a), we illustrate a schematic drawing of the W^{182} levels proposed by MBMD and analyzed by Alaga et al., (hereafter referred to as AABM).[46] The numbers on the transitions are the ratios of the transition intensities from Re^{182} decay to those from Ta^{182} decay. All of the transitions observed in Re^{182} decay are illustrated. The ratio for each transition is the average of the ratios of the individual conversion lines observed for that transition. The ratios have been normalized so that the intensity of transition HF is 1.0.

In Fig. 5 (b), we illustrate the same type of schematic drawing of the energy levels of W^{182} as in Fig. 5 (a). In the former case, however, the numbers on the transitions are the absolute intensities determined by MBMD to depopulate the levels after Ta^{182} decay. These numbers are adjusted so that a total intensity of 100 populates the ground state. A comparison of Figs. 5 (a) and 5 (b) allows a rapid estimation of the primary population to these states by Re^{182} decay.

It can be seen from a comparison of Figs. 5 (a) and (b) that the W^{182} states predominantly populated in Re^{182} decay are the 2- state (F) and the spin-3 member of its rotational band (H). It can also be seen that a much smaller amount of decay occurs to the two 4- levels (J and K) in Re^{182} decay than in Ta^{182} decay. Because no low-energy transitions depopulate the high-energy positive-parity states (D, G), it is not possible to determine directly the intensity of decay to these states.

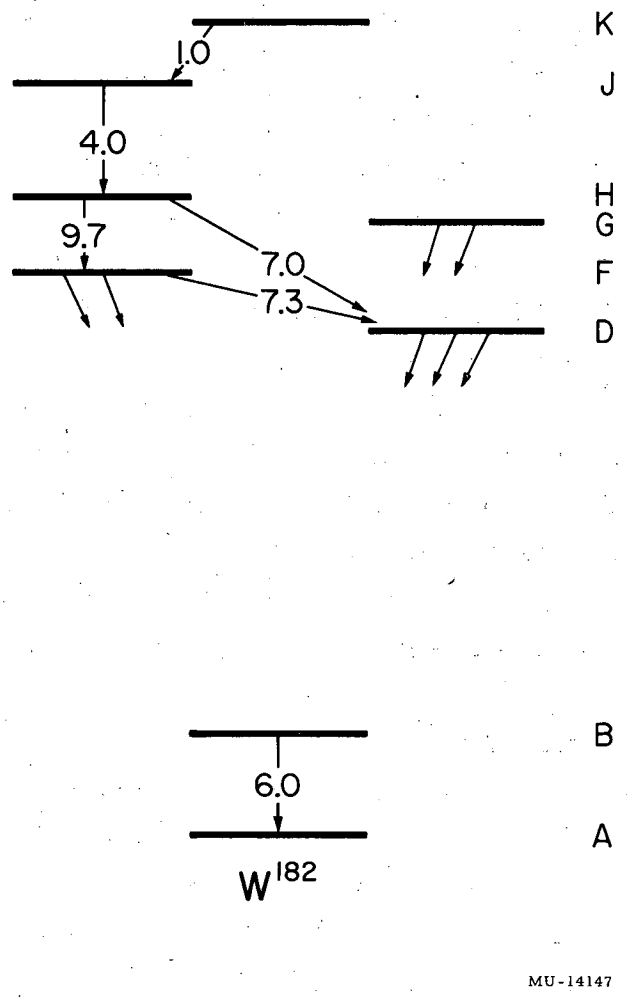

Fig. 5a. Comparison of electron intensities of transitions observed in both Ta^{182} and 12.7-hr Re^{182} decay. The ratios indicated on the transitions are normalized so that the ratio of the electron intensity of the L_I 65.71-kev transition observed following Re^{182} decay to that observed following Ta^{182} decay is 1.

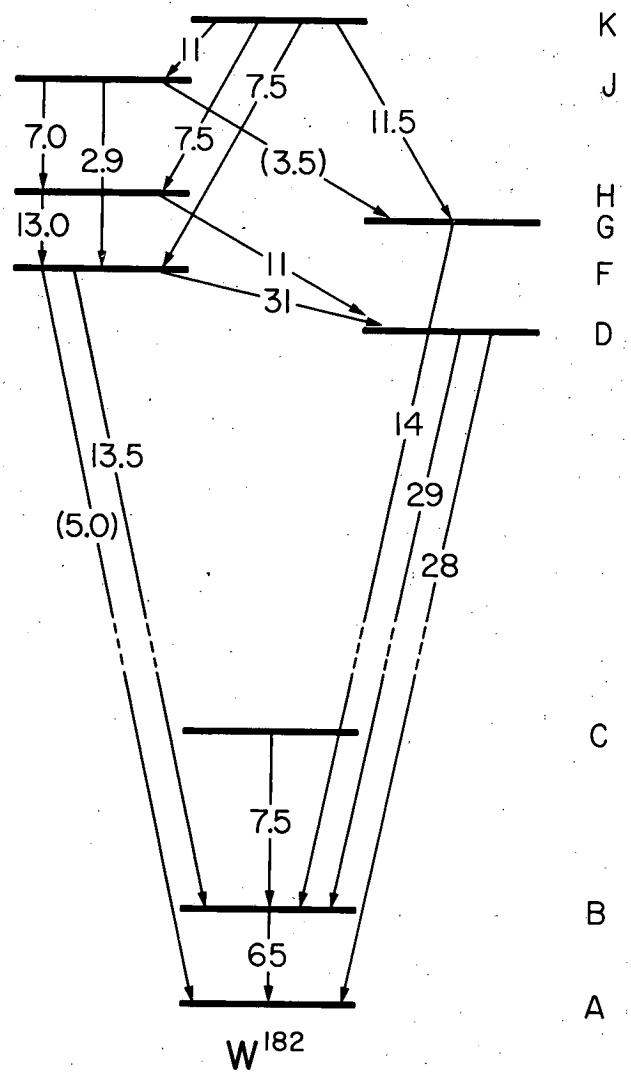

MU-14148

Fig 5b. Transition intensities reported by MBMD for the transitions of W^{182} following Ta^{182} decay. The intensities are normalized so that a total of 100 populates the ground state.

From the observed decay to states of spin 2, 3, and 4, it is most probable that the spin of Re^{182} is 3, although as discussed below, spins of 2 and 4 are possible. For decay to proceed predominantly to the negative parity states when there are states of similar spin and positive parity nearby strongly suggests that the 13-hr Re^{182} state has negative parity. Because decay occurs to the 4- states, a spin-2 assignment seems implausible since 2- ——> 4- transitions would be second-forbidden. Similar arguments from the intensity of population to the 2- state rule against the spin-4 assignment. The data thus strongly suggest the 3- state assignment.

It is interesting to consider the Nilsson[37] diagrams for odd-neutron and odd-proton states in this region, to determine what states should be available to make up a 3- state. These diagrams are illustrated in Figs. 4 (a) and (b). If we first assume that the 5/2+ odd-proton state, with the asymptotic quantum numbers (4,0,2, in the N,n_z,Λ notation) assigned the ground state of Re^{181} (Section A), Re^{183}, [41] Re^{185}, [42] and Re^{187}, [42] is the odd-proton state available in Re^{182}, we can make up a 3- state with either a 1/2- state (parallel coupling) or an 11/2- state (antiparallel coupling). An 11/2- state can be present in this region, although it has not been observed experimentally. The odd-neutron state assignment that we prefer, however, is the 1/2- state, observed as the ground state of W^{183}, and is probably the Nilsson[37] state with asymptotic quantum numbers (5, 1, 0).

<u>Primary branching and log ft values</u>. From the gamma-ray intensities quoted in Table II it is clear that these data alone are insufficient to provide more than a limit on the primary electron-capture branching of Re^{182}.

On the other hand, the branching can be determined from the electron data because the W^{182} levels, the transition multipolarities and conversion coefficients, and the branching from these levels have been established independently.

We can calculate the primary decay intensities to the high-energy negative-parity states using our electron intensities and the MBMD absolute-conversion coefficients and branching ratios. Furthermore, we can calculate the contribution to the total intensity of transition BA from the negative

parity states. If the intensity of BA is greater than the calculated intensity of the feeding transitions, we can assume either that the ground-state band is being populated directly or else decay is occurring to the high-energy positive-parity states. After having made these calculations, we found that the percentage excess of BA over the feeding intensity was about 20%. We assumed that this decay went to the high-energy states for reasons that will be discussed later. We thus obtained the total decay intensity and the primary branching to the various states. The probable errors of the primary populations listed are about 30%, the statistical error[47] in the sum or difference of the uncertainties of the intensities of the individual lines, about 20%.

The percentage primary branching to the high-energy states is shown in Table IV. We have also calculated log ft values for electron capture to these states assuming total decay energies of 1630 and 1850 kev. These values are shown in Table IV. We have used these values of the decay energy because the lower value, 1630-kev, is a limit on the K-capture energy, set by the observed population of state K, at 1554-kev. We have assumed K-capture is necessary to cause the observed ~6% population of state K. The upper energy value is arbitrary, and was chosen to represent what is believed to be an upper limit of the decay energy, because the 1554-kev decay energy limit is already ~ 300 kev greater than the decay energy estimated from the Coryell[36] beta systematics.

From the population of a level at 1554 kev, we know that the total electron-capture decay energy is above the threshold for positron production. We have attempted to determine whether or not any positrons are observed in Re^{182} decay. From failure to observe an annihilation peak in the gamma spectrum, we can rule out the possibility that the major fraction of Re^{182} nuclei decays by positron emission. However, because of interfering activities in the samples studied, we cannot rule out the possibility that a small fraction of Re^{182} nuclei decay in this way.

The failure to observe direct decay of Ta^{182} to the W^{182} ground-state rotational band strongly suggests that these transitions are K-forbidden. Such an explanation has already been proposed by AABM for Ta^{182} decay. Because the observed data are consistent with a spin of 3

Table IV

Percentage of primary branching and log *ft* values for electron-capture decay of 12.7-hr Re^{182} to levels in W^{182}. No decay has been assumed to populate the states of the ground-state rotational band.

State populated	Percentage population	Log *ft* (calculated using Q_{EC}=1850 kev)	Log *ft* (calculated using Q_{EC}=1630 kev)
D,E,G	25	6.1	5.6
F	35	5.9	5.3
H	29	5.8	5.1
J	5	6.3	5.1
K	6	6.1	3.9

for Re^{182}, we suggest that the electron-capture decay of Re^{182} to W^{182} is also K-forbidden. The possible K-forbiddenness has led us to assign the 20% excess population to state B over that owing to the depopulation of the negative-parity states as arising from direct population of the other high-energy states in W^{182}.

Conversion coefficients and mixing ratios. To calculate the primary branching, it was necessary to use conversion coefficients. We used the conversion coefficients experimentally determined by MBMD throughout, after we had reduced them by 20%. This correction was made because MBMD normalized their experimental conversion coefficients to Rose's value for the α_K of an M1 transition. From the work of Sliv and Band, which accounts for the finite nuclear-size effect neglected by Rose, Rose's conversion coefficients are estimated to be about 20% too high. However, because of recent studies on conversion coefficients by a number of workers (see for example, the paper of Wapstra and Nijgh,[48] which summarizes much of the data) there is reason to believe that even Sliv's calculations may not be exact, owing to the affect of nuclear contributions (see, for example, the papers of Church and Weneser,[49] and Nilsson[50]) which have previously been neglected. If Sliv's calculations are not exact, the mixing ratios that we have determined will have to be changed by that factor by which the α_K of the M1 of 246.05-kev used by MBMD for normalization is changed. However, it is a little too early in these investigations to be able to forecast the outcome, so that we shall not attempt further corrections here. We used MBMD's conversion coefficients in preference to the theoretical values of Sliv and Rose because we found that, although our experimental intensities were, in general, in excellent agreement (in terms of ratios) with those of MBMD, the agreement with the theoretical values for some of the transitions was not good, even after accounting for mixing. This is especially true for the M1 and M1-E2 mixtures.

It should be noted that although both the MBMD and our $L_I/L_{II}/L_{III}$ ratio (and our $M_I/M_{II}/M_{III}$ ratio) for the 67.74-kev transition are in good agreement with the ratio of the theoretical values for a pure E1

transition, the absolute values measured by MBMD are twice the theoretical values. The general trend of these conversion coefficients is in the direction of M2 mixing, but M2 mixing would enhance the L_I conversion rather than increase all three of the conversion coefficients. The difference might possibly arise owing to the experimental uncertainty in MBMD's 67.74-kev gamma intensity, although it is outside their quoted limits of error.

An anomalous value of the K/L_I ratio of the 152.41-kev E1 gamma intensity has been observed in this study. Because a similar anomaly in this ratio was observed in the study of the 60-hr Re^{182} decay, it seems possible that this effect is real. The values obtained are 1.6 ($\pm \sim 3$) and 3.4 ($\pm \sim 2$) for the 13-hr and 60-hr isomers, respectively. The limits of error are estimated; because the K-intensities are taken from a photographic plate in a region where the background is intense and the lines poorly defined, it was impossible to estimate them more accurately. In spite of the large experimental limits of error, however, the theoretical ratio of 8.3 appears to be considerably larger than that observed.

In Table V a comparison is made of the corrected absolute conversion coefficients of MBMD, theoretical values from the tables of Sliv and Rosé, and our experimental values for all the transitions of which we have seen more than one conversion line. Our values are normalized to one of the theoretical values (normalization indicated by parentheses). The L_I and L_{II} conversion coefficients were reduced by the ratio of Sliv's to Rose's K-conversion coefficients. This correction was made because we believe that the finite nuclear-size effect should be the same on both the K-, L_I-, and L_{II}-shell conversion for an M1 transition, but in view of the recent studies of Wapstra and Nijgh[49] this correction may not be sufficiently large. It is interesting to note that because we have always used the L-conversion lines for normalization the conclusions of these workers (that the reduction of the K-conversion coefficients of M1 transitions from Rose's values is greater than 20%) seem substantiated by our data.

The mixing ratios which were calculated wherever possible from the observed L-subshell conversion ratios, are listed in Table V.

Table V

Conversion coefficients of transitions in W^{182}. The conversion coefficients listed are the corrected absolute experimental values of MBMD, the theoretical values from the tables of Sliv and Rose, and our normalized conversion coefficients. These latter are obtained by normalization of an electron-line intensity to the theoretical value for that conversion-electron line for each transition. Normalization values are indicated by parentheses.

Gamma-ray energy (kev)	Source of conversion coefficient	Conversion coefficients								Mixing ratio
		K	L_I	L_{II}	L_{III}	M_I	M_{II}	M_{III}	N_I	
65.71	MBMD		2.2	0.32	0.18	0.64				99% to 1%
	Theoretical		2.3	0.21	0.04					M1 to E2
	Our normalized values		2.2	(0.21)		0.31				
67.74	MBMD		0.14	0.056	0.056	0.048			0.01	E1
	Theoretical		0.083	0.032	0.037					
	Our normalized values		0.073	(0.032)	0.037	0.021	0.008	0.005	0.006	
84.70	MBMD		1.44	0.48	0.40	0.52			0.12	84% to 16%
	Theoretical	5.0	0.78	0.50	0.36					M1 to E2
	Our normalized values		1.2	(0.50)	0.34	0.32			0.25	
100.09	MBMD	1.2	0.10	1.16	1.08		0.56		0.16	E2
	Theoretical	0.83	0.10	1.20	1.05					
	Our normalized values		<0.27	(1.2)	1.06		<0.56	<0.41	0.2[a]	
113.66	MBMD	1.4	0.32	0.056						~100% M1
	Theoretical	2.6	0.39	0.063						
	Our normalized values	(2.6)								
152.41	MBMD	0.056								E1
	Theoretical	0.11	0.013							
	Our normalized values	(0.11)	0.07							

a. This is the intensity of the N_{II}-N_{III} conversion lines.

C. 60-Hr Re^{182}

Mass Assignment and Half Life

The 60-hr electron-capturing isomer of Re^{182} was first identified by Wilkinson and Hicks.[43] The half life they reported was 64 hr, but in the present study a better value was found to be 60 ± 4 hr. We redetermined the half life by following the decay of the 1122 to 1222 peak in the NaI (Tl) gamma spectrometer, with both 50- and 100-channel gamma analyzers. We believe that this method is less susceptible to uncertainties than the absorption method used by Wilkinson and Hicks.[43] The mass assignment was verified in the stacked-foil excitation study used to determine the mass assignment of Re^{181}.

Since the initial studies of Re^{182} by Wilkinson and Hicks,[43] no further studies on the decay scheme of 60-hr Re^{182} (which will hereafter be referred to as Re^{182}) have been reported. As seen from the previous section, however, the energy levels of the daughter nucleus, W^{182}, have been extensively studies from the decay of Ta^{182}. The last and most definitive work in this study is the analysis of MBMD.

General Resumé of Spectroscopic Results

The decay of Re^{182} populates by cascade-transitions all the levels of W^{182} observed in Ta^{182} decay, with the possible exception of MBMD level E. Thirteen of the 15 low-energy transitions observed in Ta^{182} decay were seen. Besides these, a total of 40 new transitions have been identified by observation of internal-conversion-electron lines and assigned to Re^{182}. Thirty-eight of these transitions establish 10 levels based upon the high-energy states found by MBMD. We found it necessary to reassign MBMD level I. A transition was observed which has been assigned as the 6+ ⟶ 4+ transition of the ground-state rotational band, thus establishing the energy of the 6+ level. One transition is unassigned.

Gamma Spectroscopy

The sample used in the analysis of Re^{182} was the same 13-hr sample described in Section III B, "Gamma Spectroscopy". As was the case for that isomer, the only useful information which could be obtained from the gamma-ray spectrum was the ratio of the 1122 to 1222 peak to the K x-ray peak. The 60-hr contribution to these peaks was obtained by extrapolating the observed 60-hr component to time zero (time at which the target was removed from the cyclotron). These results are shown in Table VI. The limits of error on the intensities are estimated to be 20%. The activities were extrapolated to time zero in order to compare the ratio of 13 to 60-hr activities in the sample. To insure that our extrapolation was accurate, we checked the ratio of the K x-ray to 1122 to 1222 peaks in Table VI by comparison with the same ratio from data taken after essentially all of the 13-hr component had decayed.

Electron Spectroscopy

The rhenium samples used in the electron-spectroscopic studies of Re^{182} were all prepared by helium-ion bombardment of tantalum foils (Ta^{181}). The most intense sources were prepared from targets of 0.012-inch tantalum foils bombarded with 48.6-Mev helium ions, using both the internal and external beams of the cyclotron. The permanent-magnet spectrographs were employed almost exclusively because of the extreme complexity of the conversion-electron spectrum. For the low-energy spectrum, the most important results were obtained using the 99-gauss permanent-magnet spectrograph. The results on the high-energy spectrum were obtained almost entirely from the 350-gauss spectrograph. In the latter stages of the study, when a tentative decay scheme had been constructed, the multipolarities of many intermediate-energy (200 to 400 kev) transitions predicted to be E2 transitions by the decay scheme were verified by exposures on the 160-gauss spectrograph. Because its transmission is higher than that of the 99-gauss magnet, this instrument resolved the L lines, thus verifying the assignments.

Table VI

Photon peaks resolved from the 60-hr Re^{182} spectrum

Gamma-ray	Intensity
K x-rays	64[a,b]
1122-1222	28[a]

a. Corrected for crystal efficiency[18] (d = 7.8).

b. Corrected for Auger coefficient[35] = 0.045.

The conversion-electron spectrum was also studied using the double-focusing beta-ray spectrometer at a resolution of 0.3%. However, this resolution was insufficient to resolve many of the groups of lines, so that the data thus obtained were used mainly for supplementary intensity checks.

In electron-spectroscopic studies of a mixture of radioactive isotopes, a sequence of steps is usually followed, namely, the assignment of electron lines to isotopes, the assignment of electron lines to transitions (and, if possible, the assignment of multipolarities to transitions from the relative intensities of the subshell conversion), and finally the determination of the decay scheme.

In the study of Re^{182} we were able to identify most of the lines fairly readily by a series of exposures on the permanent magnets. The series allowed us to distinguish the 60-hr Re^{182} lines from those of 13-hr Re^{182}, 20-hr Re^{181}, 50-day Re^{184} and 71-day Re^{183}. The assignment of the electron lines to transitions was much more difficult because of the possibility, especially at low energies, of misassigning lines, and the ever present possibility of the accidental superposition of lines. The resolution of the spectrum, however, allowed us to assign many multipolarities, because the activity levels used in most of the experiments were sufficiently high to enable us to see the L- and higher-shell conversion lines of almost every transition. These transitions, the electron lines observed, and the intensity of these lines are listed in Table VII. In Appendix B, Part 1, the energies and visual intensities of all lines observed in the studies of the short-lived ($\leq$ 60-hr) isotopes are listed; in Part 2a the electron lines are listed by transition energy.

The numerical intensities given in Table VII were determined from photographic films by the method of Mladjenović and Slätis,[17] and have estimated uncertainties of 20%. The intensities of the stronger lines were compared to intensities for the same lines obtained from the double-focusing spectrometer and were found to be in agreement within experimental error. The intensities from the magnetic spectrometer were not used throughout because 0.3% resolution was not sufficient to resolve some of the groups of lines. We estimate the probable error of the energies as

Table VII. Transitions in W^{182} following the decay of 60-hr Re^{182}. Electron intensities are on an arbitrary scale.

Initial and final states	Transition energy (kev)	Electron intensities K	L_I	L_{II}	L_{III}	M_I	$M_{II}M_{III}$	N_I	$N_{II}N_{III}$	Total electron intensity	Multipolarity assignments First confidence	Second confidence
RQ	19.86±0.05					a----	a----	a----	a----	-----		(E1+M2)
ED	33.36±0.01[b,c]									-----	E1	
NM	39.10±0.05		13							13	(M1)	
HG	42.71±0.01[b,c]									-----	(E1)	
KJ'	52.96±0.05		a----			a----				-----		(M2)
RP	60.51±0.05		4							4	(M1)	
KJ	65.71±0.01[b]		97	15	34[d]	24				140	M1+E2	
FD	67.74±0.01[b]		34[d]	11	12	17	a---- a----	1.2		68	E1	
MK	68.10±0.08			a,e--						-----		(E2)
IG	74.41±0.05		a----	f----	g---					-----		(E1)
HF	84.67±0.02[b]	250	49	17	13	26	a------a--	a----	a---	360	M1+E2	
BA	100.09±0.02[b]	130		~1080			~260		h----	1470	E2	
NK	107.13±0.05	29	5.9	8.8	6.0					50	(M1+E2)	
PN	108.57±0.05	19	4.4			0.8		<0.6		24	(M1)	
JH	113.65±0.02[b]	170	34	5.8	58[j]	12	3.4	a----		220	M1+E2	
IF	116.40±0.02[b]	7.2[k]	λ----	m-----						-----		(M1+E2)
MJ'	120.94±0.06	a----	n----							-----		(E1)
J'H	126.40±0.06	o----										
SR	130.76±0.07	220	40	15	7.3	12		6.0		290	(M1+E2)	
TR	131.30±0.07	a,p--								-----		-----
MJ	133.78±0.07	80[g]	100[q]			5.3				98	(M1)	
PM	147.68±0.07	15	5.6	3.7	<7.5[r]					27	(M1+E2)	
PL	148.81±0.07	46	9.2	<7.5[r]	15[s]					<78		(E1+M2)
QN	149.39±0.07	16	<7.5[r]	≤2.6[t]	u----					<26		(E1)
TQ	151.19±0.08	a----								-----		-----
HD	152.41±0.03[b]	>12[v]	3.6							>16	E1	
JG	156.37±0.04[b]	>4.0[v]	4.9	13[w]	3.5[x]					>8.9	E1	
NJ'	160.09±0.08	>6[v]	3.4							>9.4		(E1)
RN	169.18±0.08	256[h]	43	3.5	y----	13		1.3		315	(M1)	
NJ	172.78±0.09	58[j]	10			2.5				71	(M1)	
KH	179.36±0.05[b]	31	7.2	3.3	1.2	1.2				44	M1+E2	
OK	181.63±0.09	3.2								3.2		(M1)
QL	189.48±0.10	6.2								6.2		(M1)
SP	191.31±0.10	100[q]	16							<116	(M1)	
JF	198.31±0.06[b]	19		85[z]	6.1		aa			34	E2	

Table VII (cont.)

Initial and final states	Transition energy (kev)	Electron Intensities K	L_I	L_{II}	L_{III}	M_I	$M_{II}M_{III}$	N_I	$N_{II}N_{III}$	Total electron intensity	Multipolarity assignment First confidence	Second confidence
RM	208.18±0.10	15[s]	<3			bb				<18	(M1)	
RL	209.33±0.10	5.5								5.5		(E1)
LI	214.41±0.11	13[w]	bb			bb				<13		-----
PK	215.69±0.11	3.5[x]		bb	bb					3.5	(E2)	
(cc)	221.60±0.11	9.5								9.5		-----
KG	222.05±0.07[b]	7.9	bb							7.9	E1	
TO	226.10±0.11	30	6.9			bb				37		-----
CB	229.27±0.08[b]	96		bb	bb					96	E2	
MH	247.43±0.12	19	bb	bb	bb					19	(E2)	
QK	256.37±0.13	85[z]	13			bb				<98	(M1 or M2)	
KF	264.09±0.10[b]	12	a	a	a					12	E2	
RK	275.30±0.14	15	bb	bb	bb					15	(E2)	
PJ	281.42±0.14	8.6	bb	bb	bb					8.6	(E2)	
NH	286.52±0.14	37	bb	bb	bb					37	(E2)	
SN	299.88±0.15	2.5	dd ee	bb	bb					2.5	(E2)	
TN	300.49±0.15	3.0	dd ee							3.0		-----
SM	338.98±0.17	(4.8)	ff bb	bb	bb					4.8	(E2)	
C'C	351.02±0.18	(2)	ffbb	bb	bb					2	(E2)	
EC	927 ±1[b]	c									(E3)	
FC	960 ±1[b]	c									(E3)	
GC	1003 ±1[b]	c									(M1+E2)	
IC	1076.7 ±0.6	bb										(E1+M2)
DB	1121.6 ±0.2[gg]	bb	bb								M1+E2	
EB	1155 ±1[b]	c									E1+M2	
JC	1158 ±0.6	bb										(E1+M2)
FB	1189.3 ±0.2[gg]	bb									E1+M2	
DA	1221.8 ±0.2[gg]	bb									E2	
GB	1231.3 ±0.5	bb									M1+E2	
EA	1254[gg]	hh										(E1)
HB	1273[gg]	hh										(E1+M2)
FA	1289 ±1[b]	c									(M2)	
HA	1375 ±2[b]	c									(E3)	
?	1437 ±4[b]	ii										
KB	1454 ±4[b]	c									(M2+E3)	

Table VII (cont.)

Notes on Table VII.

a. Intensity too weak to be obtained from densitometer trace.

b. Limits of error assigned by MBMD.

c. Not seen in 60-hr Re^{182} decay.

d. L_I 67.74, L_{II} 65.71 superimposed.

e. The assignment of this line is questionable.

f. L_{II} 74.41, M_I 65.71 superimposed.

g. L_{III} 74.41, K 133.78 superimposed.

h. K 169.18, $N_{II}N_{III}$ 100.09 superimposed.

j. K 172.78, L_{III} 113.66 superimposed.

k. K 116.40, KL_IL_{III} superimposed.

λ. L_I 116.40, M_I 107.13 superimposed.

m. L_{II} 116.40, M_{III} 107.13 superimposed.

n. Seems too intense to be L_I 120.94, but because K is on a dark background, it is difficult to be sure.

o. KL_IN_I-N_{III} would be superimposed on K 126.40.

p. This line observed only weakly on one plate. It may belong to Re^{181}

q. K 191.31, L_I 133.78 superimposed.

r. L_I 149.39, L_{II} 148.81, L_{III} 147.68 superimposed.

s. K 208.18, L_{III} 148.81 superimposed.

t. This line visible only on densitometer trace as a low-energy tail of K 208.81 (Re^{183}) line.

u. K 208.81, L_{III} 149.39 superimposed. A comparison of intensities of Re^{183} transitions in sample with the intensities of the Re^{183} lines in a pure Re^{183} sample indicates a very low intensity for the L_{III} 149.39.

v. On very dark background.

w. K 214.41, L_{II} 156.37 superimposed.

x. K 215.69, L_{III} 156.37 superimposed.

y. K 229.27, L_{III} 169.18 superimposed.

z. K 256.37, L_{II} 198.31 superimposed.

aa. L_I 208.81 (Re^{183}), $M_{II}M_{III}$ 198.31 superimposed.

bb. Weak line observed on higher-field, less-accurately-calibrated magnets.

cc. Transition not assigned in decay scheme. K 221.60, L_{III} 162.33 (Re^{183}) superimposed.

dd. The sum of the intensities of the lines was observed as equal to 5.6 on the exposure used to calculate intensities, but the lines were not resolved. The intensity ratio was estimated visually from another exposure.

ee. This line was diffuse and difficult to read.

ff. These intensities were estimated from a second plate.

gg. Limits of error assigned by Bäckstrom.

hh. Lines reported by Backstrom and not by MBMD in the decay of Ta^{182}. Not observed in Re^{182} decay.

ii. This transition was assigned as IA by MBMD. Because we have reassigned level I, it not longer fits into the decay scheme. It should be noticed that the K 1437 and L_I 1375 would be superimposed.

0.05% which we feel is an accurate evaluation. It is only possible because of the excellent field calibration provided by the presence of a large number of conversion lines of transitions whose energies were very accurately measured by MBMD with a bent-crystal gamma spectrometer.

Discussion of Results

Decay scheme. The high-energy resolution and probable multipolarity assignments for the more intense transitions enabled us to build on the existing level scheme of W^{182} proposed by MBMD. Many transitions, assigned on the basis of a number of their conversion lines were found to fit into this scheme. The scheme also predicted weak transitions, whose K- or L-conversion lines were observed but were unassigned. Only 8 electron lines assigned to Re^{182} are not assigned definitely to transitions in the decay scheme. These eight, their probable assignments, and their intensities relative to other lines on the same plate are listed in Table VIII.

Because much of our interpretation assumes the correctness of the decay scheme of MBMD, we shall review other experiments (Coulomb excitation of W^{182} and studies of the decay scheme of Ta^{182}) which support it.

Coulomb excitation[51-55] of W^{182} has verified level B. Mihelich[56] has performed gamma-gamma coincidences that indicate that DB (1122) and BA (100.09) are in coincidence, while DA (1222) and BA are not. Williams and Roulston[57] have recently performed gamma-gamma angular correlation experiments on the cascades F-D-A, H-D-A, and F-D-B, and their results agree with spin assignments to these levels of 2-2-0, 3-2-0, and 2-2-2, respectively.[57] Bäckstrom[58] has carried out high-resolution electron spectroscopy on the transitions DB, FB, and DA and has determined the energies 1121.6 ± 0.2 kev, 1189.3 ± 0.2 kev, and 1221.8 ± 0.2 kev, respectively.[58] He has also observed, for the first time, conversion lines that correspond to transitions EA (1254) and HB (1273). Because of the high-resolution gamma spectroscopy employed by MBMD to study the low-energy transitions in Ta^{182} decay, the energies and arrangement of levels D through K (excepting I) seem excellent. The careful studies mentioned above gave confidence for building upon this level scheme for interpretation of the highly complex decay of 60-hr Re^{182}.

Table VIII

Unassigned internal-conversion electron lines of transitions of W^{182} following Re^{182} decay

Energy	Intensity	Possible assignment
54.99	ew?	KL_IM Auger electrons
56.64	ew	L_{II} 68.10-kev
58.86	ew?	$KL_{III}N$ Auger electrons
66.28	ew	KMN Auger electrons
74.86	ew	L_{II} 86.40-kev
76.16	ew?	L_{III} 86.36-kev
108.99	ew	L_I 120.94-kev
187.44	ew	Probably film imperfection (PM IV, plate 397)

In order to determine whether the levels of W^{182} populated by Ta^{182} decay were also populated by Re^{182} decay we first determined whether we saw all of the low-energy transitions (< 300 kev) reported by MBMD. We found that all except the 33.36- and 41.72-kev transitions were seen. Because these two are very weak in Ta^{182} decay, their absence in no way affects the levels proposed by MBMD.

Because of the low transmission of our high-resolution instruments, we were able to see the electron lines of only six high-energy transitions. Two of these, the 1158- and 1076.6-kev transitions, have not been reported previously. The 1158 was found to fit the energy difference JC very well and has been so assigned; the 1076.6 has been assigned as transition IC.

Another useful item of information, adding confidence to the MBMD scheme, was obtained by comparing the relative intensities of transitions common to both decay schemes. We did this by comparing our electron intensities with the electron intensities of MBMD calculated by multiplying their gamma intensities by the experimental conversion coefficients they report. The ratios of our electron intensities to MBMD's for these transitions are illustrated in Fig. 6 which is a schematic diagram of the MBMD decay scheme. The numbers on each transition are the ratio of the electron intensities of the conversion lines of the transition in the Re^{182} spectrum to those in the Ta^{182} spectrum. The ratio for each transition is the average of the ratios for all the conversion lines seen in both spectra. All ratios are normalized by assuming that the ratio for the L_I of the 65.71-kev transition is 1.

A positive check on the MBMD level scheme is provided by these ratios. If their scheme is correct, the ratios that we calculate for the transitions depopulating one of their levels will be equal, within experimental error, whereas this would probably not be so if they have misassigned some of the transitions. From the ratios shown in Figs. 5 (a) and 6, it can be seen that our results are consistent with the MBMD level scheme, because the deviation in the ratios is within the probable error of the electron intensities. From a comparison of Fig. 6 and Fig. 5 (b), we can readily draw some conclusions about differences in level populations between Ta^{182} and Re^{182} decay. It is clear from the comparison that a large

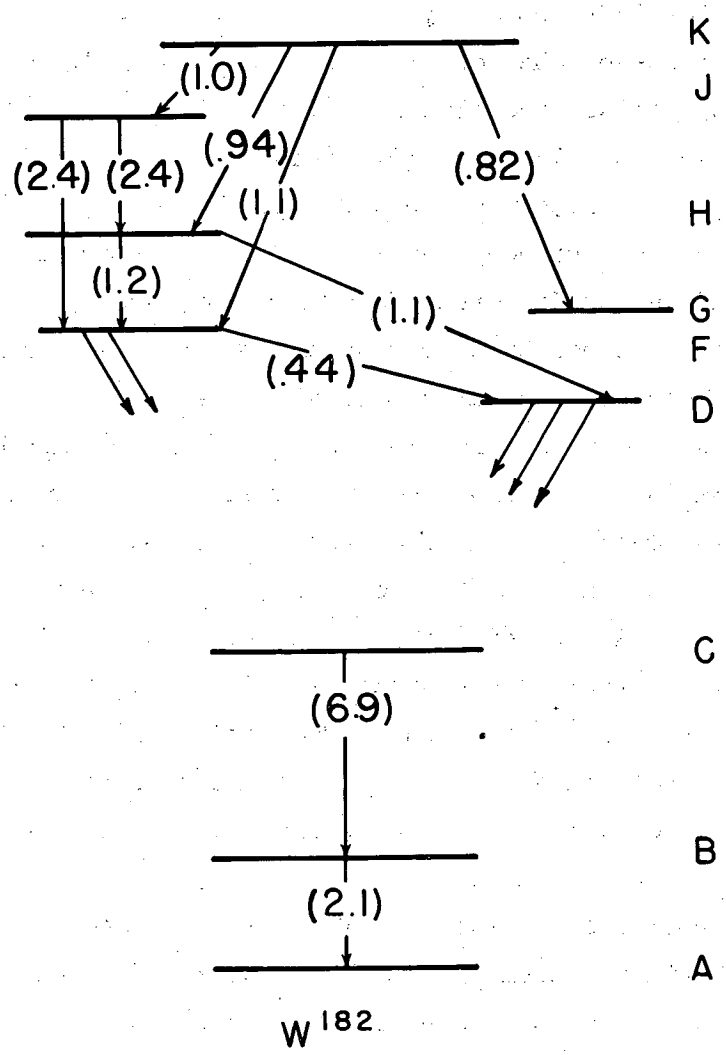

Fig. 6. Comparison of electron intensities of transitions observed in both Ta^{182} and 60-hr Re^{182} decay. The ratios indicated on the transitions are normalized so that the ratio of the electron intensity of the L_I 65.71-kev transition observed following Re^{182} decay to that observed following Ta^{182} decay is 1.

percentage of depopulation in Re^{182} decay cascades through states J and K, whereas in Ta^{182} decay a large part of the primary beta decay goes directly to level F and H. It also indicates a much larger population of level C than in the former case, thus indicating that states of higher spin must receive more direct population in Re^{182} decay.

Figure 7 illustrates our proposed decay scheme for Re^{182}. It includes all the transitions reported by MBMD (including those unobserved by us) and the new transitions reported by Bäckstrom[58] (also unobserved by us). This level scheme is based primarily on agreement of energy sums of pairs of transitions being equal to the energy of a third transition. Because of the complexity of this decay there are many accidental energy sums; thus there are several alternative decay-scheme possibilities if the energies alone are considered. Fortunately, the intensities and multipolarities of the observed transitions often guided the choice of alternative level schemes. The new parts of the scheme of Fig. 7 are based solely on conversion-electron-spectroscopic results. High-resolution gamma-ray spectroscopy and coincidence studies would be of the greatest value toward confirming or revising our proposed scheme. We will discuss the sums that constitute the basis of the decay scheme later. We feel in particular that the high-energy electron spectrum deserves much further study, because the new decay scheme predicts many weak high-energy transitions that our low transmission prevents us from seeing.

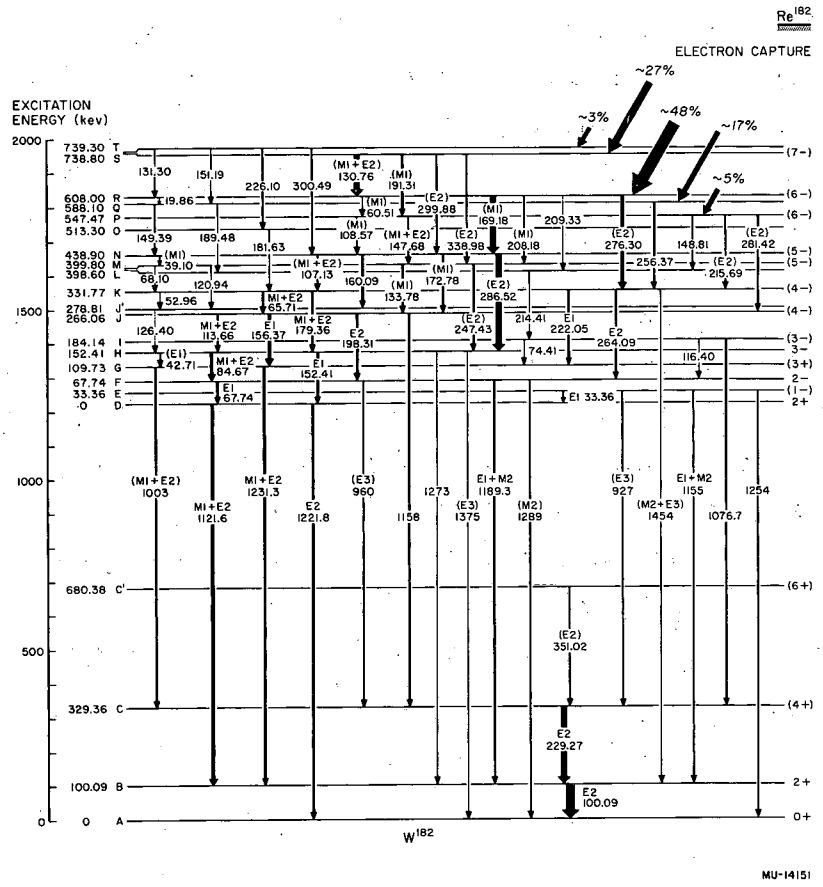

Fig. 7. Decay scheme of 60-hr Re^{182}.

Discussion of the new levels in W^{182}. As previously stated, the energies of the levels were based primarily upon sums and differences. The levels may be considered to fall into three "confidence" groups. The first is those levels that were placed from differences equal to differences between levels established by MBMD. The second is those placed by differences corresponding to differences between states established by MBMD and our "primary" states, and the third arises from differences not involving any levels of MBMD. Levels I, M, and N, are in the first group; J', P, Q, and R are in the second group; and L, O, S, and T in the third. The agreement of the sums for the various groups is shown in Table IX. We do not include all possible differences in Table IX, but rather only those that directly support each state. Level C' is so placed because C'C is E2, and its energy fits the theoretically predicted rotational spacing for the 6+ state of the ground rotational band of W^{182}. Because all of the levels except C' and O have at least three transitions tying them into the decay scheme (and some have as many as seven), we feel that the statistical significance of the scheme is quite large. Before discussing the level spin assignments we shall digress first to discuss the method of determining multipolarities and then the transitions for which multipolarities are not very well established. This will then allow us to discuss the level spin assignments.

In Fig. 8 (a) and (b), we illustrate the L_I/L_{II} and L_{III}/L_{II} ratios for M1, M2, E1, and E2 transitions that were calculated using Rose's theoretical L-subshell conversion coefficients. We have not considered higher multipole orders for the low-energy transitions because their much longer half lives were expected to prevent their competing favorably with the dipole and quadrupole transitions. From Fig. 8 (a) it is clear that at low energies the presence of L_{II} conversion comparable to L_I is usually indicative of electric radiation. L_{III} conversion stronger than L_{II} conversion is usually indicative of E1 or M2 radiation at the energies of interest.

The L_{II} and L_{III} conversion is greatest for the electric quadrupole, for which the L_I conversion only becomes equal to the L_{II} at about 350 kev. In the E1, however, the L_I/L_{II} ratio is unity at about 25 kev, three at

Table IX

Differences supporting the proposed W^{182} level scheme

Transition 1	Transition 2	Difference	Transition 3	Energy of state above D	State designation
Group I					
1076.7	74.41	1002.3	1003	184.14	I
1076.7	116.40	960.3	960	184.14	I
247.43	133.78	113.65	113.66	399.84	M
172.78	107.13	65.65	65.71	438.84	N
286.52	172.78	113.74	113.66	438.93	N
Group II					
160.09	120.94	39.15	39.10	278.81	J'
160.09	52.96	107.13	107.13	278.81	J'
281.42	215.69	65.73	65.71	547.48	P
281.42	147.68	133.74	133.78	547.48	P
281.42	108.57	172.85	172.78	547.48	P
256.37	149.39	106.98	107.13	588.14	Q
276.30	169.18	107.12	107.13	608.07	R
208.18	169.18	39.00	39.10	607.98	R
Group III					
215.69	148.81	66.88	66.83[a]	398.60	L
209.33	189.48	19.85	19.86	398.67	L
209.33	148.81	60.52	60.51	398.67	L
338.98	299.88	39.10	39.10	738.78	S
338.98	191.31	147.67	147.68	738.78	S
338.98	130.76	208.22	208.18	738.78	S
191.30	130.76	60.54	60.51	738.78	S
151.19	131.30	19.89	19.86	739.28	T
300.49	169.18	131.31	131.30	739.34	T

a. The line supporting this transition can also be assigned as the L_{II} 68.10.

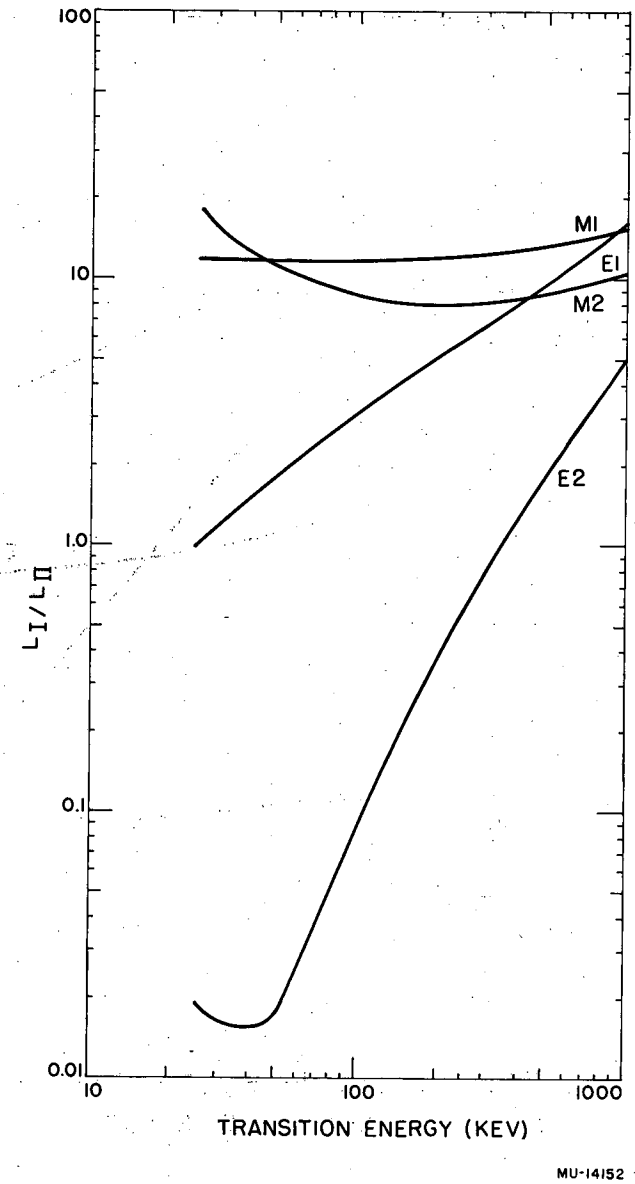

Fig. 8a. L_I/L_{II} ratios for M1, M2, E1, and E2 multipolarities for Z = 74.

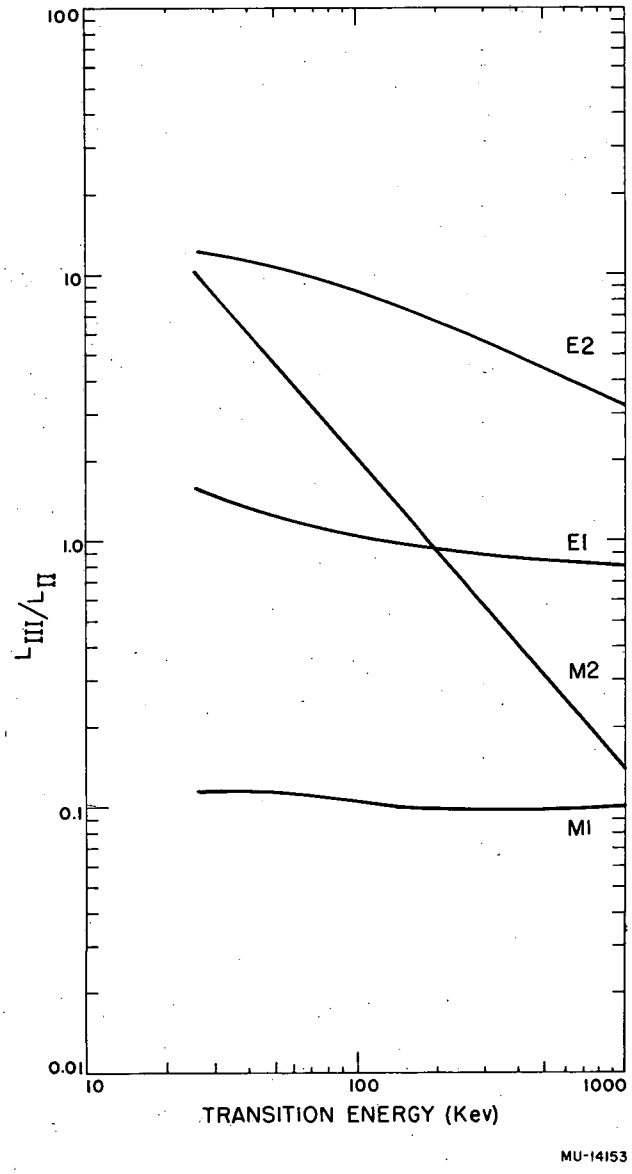

Fig. 8b. L_{III}/L_{II} ratios for M1, M2, E1, and E2 multipolarities for Z = 74.

100 kev, and about seven and a half at 350 kev. In both cases the L_{III}/L_{II} ratio decreases slowly. From these considerations it is clear that for transitions between 250 and 350 kev the presence of L_{II}-L_{III} conversion in intensity greater than that of the L_I is indicative of E2 character. New transitions which were assigned E2 character on this basis are PK, MH, RK, PJ, NH, SN, SM, and C'C. We assigned these transitions pure E2 character, although M1-E2 mixing is possible. The amount of M1 admixture is very small if present; the L_I/L_{II} ratio, wherever it was possible to observe it, was in good agreement with (if not somewhat smaller than) the theoretical L_I/L_{II} ratio for E2.

In the case of the three new transitions assigned as M1-E2 mixtures, transitions NK, SR, and PM, the $L_I/L_{II}/L_{III}$ ratios ruled out E1. The remaining transitions in Table VII with M1-E2 mixing were so assigned on the basis of MBMD's results. In Table VII we list M1-E2 mixing ratios. The basis of these ratios will be discussed later.

Above 100 kev it really becomes difficult, on the basis of electron spectroscopic results alone, to distinguish between M1, M2, and E1 transitions. Sometimes, however, it is possible to differentiate between them by remembering that the total conversion of magnetic transitions is much higher than that of electric transitions. Therefore, if we know that a certain transition in this energy range is a pure E1 of total intensity comparable to strong M1 and E2 transitions in the sample, we can use its electron-conversion lines to serve as a sort of internal intensity standard. We can do this if we say that all transitions with electron lines three or more times more intense than those of the standard cannot be E1 because then the total intensity of this transition would be too large to be consistent with the decay scheme. In W^{182} there are three transitions, JF, HD, and KF, whose multipolarities were established by MBMD, which we used in this way. The decay scheme was used where possible to differentiate between M1 and M2.

We have not found it possible to differentiate between weak M1 or M2 and strong E1 transitions on the basis of subshell conversion alone.

From subshell-conversion ratios alone it has not been necessary to assign to any electric transition a multipole order higher than E2. In

three or four cases there appeared to be M2 character in the transitions. In at least one of these cases this may be E1-M2 mixing. We will discuss these cases later.

Although in many cases our multipolarity assignments seemed clear cut, the very complexity of the spectrum engendered some ambiguity. We will now discuss the cases where such ambiguity exists.

Discussion of transitions. The 19.86-kev transition (RQ) was assigned on the basis of two M- and two N-conversion lines. The electron energies were established using the calibration afforded by the K lines of transitions HF and BA. Because the second line was diffuse and very difficult to read, it was not possible to decide definitely whether the spacing between it and the first line corresponded better to an M_I-M_{II} or an M_I-M_{III} spacing. Because this also introduced an uncertainty in deciding whether the lowest-energy line was an M_I or M_{II} line we felt it was necessary to try to establish the energy of the transition using the decay scheme. When this was done it was found that the line exactly fitted the energy of the M_I line of a transition of energy equal to RQ. If this transition energy is correct, then the presence of two lines, one of which is the M_I line, favors E1 or M2 assignment for RQ.

Weak L_I- and M_I-conversion lines of the 52.96-kev transition (KJ') were observed, indicating that the multipolarity of this transition is probably either M1, M2, or E1. However, this transition was not observed by MBMD in their gamma spectrum; although it probably should have been if the transition is M1 or E1. The absence of this transition from the gamma spectrum might indicate that it is M2. We feel that M2 or E1-M2 is the most likely assignment.

The evidence for the 68.10-kev transition (MK) consisted solely of a weak L_{II} line, therefore, the transition must be considered highly tentative. The line was so assigned only because the L_{II}-line is consistent with an M1-E2 or E2 assignment for MK, which might be expected from the decay scheme. The L_{III} was not observed although it is not masked, but because the L_{II} is extremely weak, we do not believe this is a serious discrepancy.

Only the L_I line of the 74.41-kev transition (IG) was seen. A multipolarity assignment was difficult to make because the L_{II} and L_{III} lines are masked by the M_I line of transition KJ, and the K line of transition MJ, respectively. The presence of the L_I line rules out pure E2 multipolarity for this transition.

The 116.40-kev transition (IF) was reported by MBMD, but they were unable to assign a multipolarity to it, although their data essentially exclude all multipolarities except M1, E1, or E2. We are also unable to assign it a multipolarity. By accident, the K line is masked by the K L_I L_{III} Auger line, the L_I line by the M_I line of transition NK, and the L_{II} line by the M_{II} M_{III} lines of NK. The L_{III} line might be in the diffuse low-energy tail of the N lines of NK, but it appears to be missing. However, we can calculate what fraction of the intensity of the peak containing the K line is due to it because we have data from Re^{183} on the relative intensities of the KL_p L_q Auger lines. Knowing the K-line intensity, we can calculate that the L_{III} line of a pure E2 transition would be seen were it there. This, therefore, further restricts the multipolarity to M1, E1, or an M1-E2 mixture that is predominantly M1.

The K and L_I lines of the 120.94-kev transition (MJ') were both observed, but the L_I intensity appears too large. Because the K line is on a dark background (which makes intensity calculation difficult) and no other assignment could be found for the L_I, we retained this assignment.

The K line of the 126.40-kev transition (J'H) is masked by the K L_I N_I-N_{III} Auger electrons. Because the line is diffuse, and has about the same intensity relative to the K L_p L_q Auger lines as that observed in an exposure of a sample containing only Re^{183} and Re^{184}, the latter assignment is probably correct, and J'H, if present, is not detectable.

Only the K line of the 131.30-kev transition (TR) was observed. However, because none of the other transitions would have a line at this energy the assignment is probably correct.

The most complex group of transitions is that containing the L lines of the 147.68-, 148.81-, and 149.39-kev transitions (PM, PL, and QN).

We have had to assign these transitions as M1-E2, E1-M2, and E1, respectively, to obtain consistency between the observed intensities and the decay scheme. Because these three transitions have nine possible L lines and since there are also two K lines and the L lines of two other transitions in this same energy region (approximately 10 kev), the resolution of the group was difficult. Although we believe our analysis is correct, it is definitely not unique. For this reason we illustrate a densitometer trace of this group of lines in Fig. 9, with our analysis indicated.

The energy of the 151.19-kev transition (TQ) was ascertained from only one conversion line. However, since this line was visible on on every plate, there seems to be little question of its validity.

MBMD were unable to observe the K- and L_I-conversion lines of the 156.37-kev transition (JG). In Re^{182} decay this transition is much stronger, and we saw both the K and L_I lines. Besides these, however, we have also observed lines that correspond to the calculated energies of the L_{II} and L_{III} lines of this transition. On the basis of the MBMD gamma spectroscopy, we have, however, assigned these latter two lines as the K lines of transitions LI and PK. Because we have observed the L lines of these transitions we believe the assignments are valid.

The K and L_I lines of the 160.09-kev transitions were observed, indicating that it is probably E1, M1, or M2. Only the K lines of the 181.63- (OK), 189.48- (QL), 209.33- (RL), and 221.60-kev transitions were observed. Consequently, we are unable to assign multipolarities to these transitions.

The K- and L_I-lines of the 214.41- (LI), and 226.10-kev (TO) transitions were observed, indicating that they are probably E1, M1, or M2.

Only the K-line of the 300.49-kev transition (TN) was observed definitely. The L_I line appears to be present, but is masked by the L lines of the 299.88-kev E2 transition (SN).

All of the remaining transitions have been assigned M1, M1-E2, or E2 multipolarities. The basis of the M1 assignments, where given, is that these transitions connect states whose parity is established by

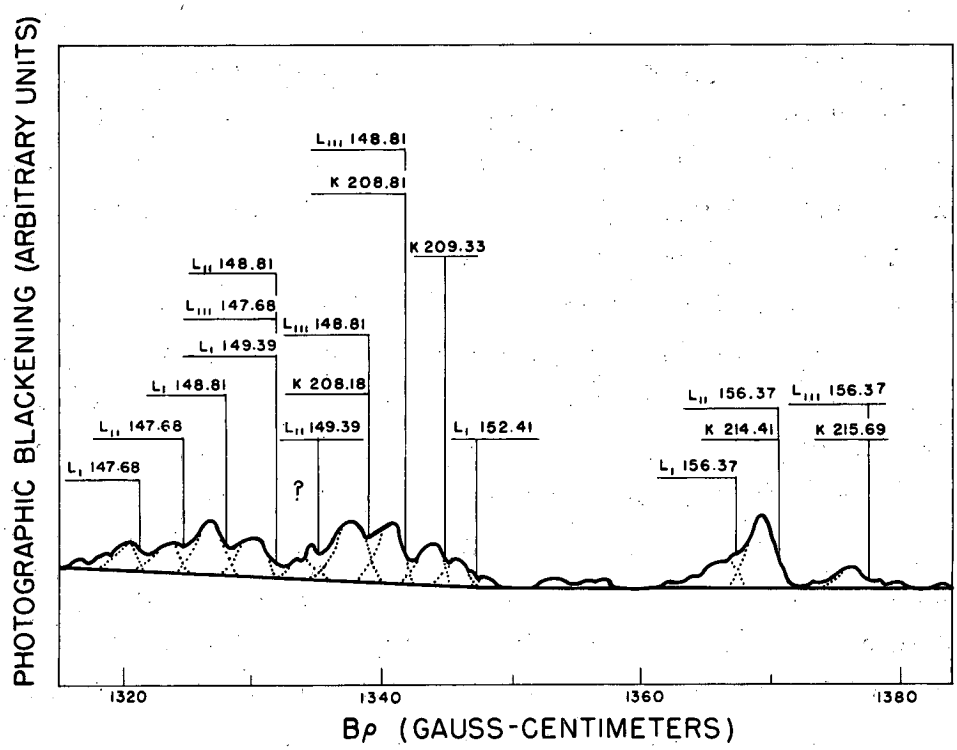

MU-14150

Fig. 9. Densitometer trace of the group of electron lines between 133 and 145 kev observed in the decay of 60-hr Re^{182}. The analysis is indicated. In cases where alternative assignments are possible the assignment preferred is (accidentally) the higher (highest) of the transition energies indicated.

interconnecting E2 transitions. For this reason we will not discuss them individually. The multipolarities of these three groups are listed in the "First Confidence" multipolarity column of Table VII. The multipolarities that we believe are the best assignments for the transitions that were discussed individually are listed in the "Second Confidence" multipolarity column of Table VII.

Spin assignments. The spin assignments of five of the new levels in W^{182} were based upon the E2 transitions. Negative parity was established for these five states since the E2 transitions populate the negative parity states assigned by MBMD. The levels so fixed are M, N, P, R, and S. The spin assignments are illustrated in Fig. 7. Most of these levels are also connected by transitions consistent with M1 and M1-E2 assignments, serving as a further check on the spins. We assume that the E2 transitions connect states with $\Delta I = 2$ in order to assign the spins shown in Fig. 8, although it is possible that a predominantly E2 transition may connect states with $\Delta I = 0$ or 1.

Besides these five levels, we place six other levels in the decay scheme. These are levels C', I, J', L, O, and T. We shall discuss the evidence relating to the spin and parity of each of these states separately, because they are not as well established as the first five.

The spin and parity assignment of 6+ to level C' has been discussed previously.

Level I in our decay scheme is not the MBMD level I. In their decay scheme they suggested that the 116.40-kev transition depopulated level K and populated a level at 215.37 kev above the 2+ state. Because their data were not definitive they regarded their assignment as tentative. The two other transitions that now establish our level I make it appear that the assignment of the 116.40-kev transition as IF is better justified than its previous assignment as KI. The data do not allow us to decide between positive or negative parity for the level. A spin of 3 is consistent with the data. A spin of 2 appears to be ruled out because LI is probably E1, M1, or M2. A spin of 4 or 5 is ruled out if IF is M1, M1-E2, or E1, as the data suggest.

Level J' can be assigned either positive or negative parity. If negative, the possible spin assignments are 4 or 5. This must be so because all three gammas populating this level convert in the K and L_I shells, which in this case would mean the transitions would have to be M1. If positive, spins of 3, 4, or 5 are possible, because the K- or L_I-shell conversion is also characteristic of E1 and M2 transitions.

Level L can have a spin of 4 or 5, positive parity, or a spin of 5 or 6, negative parity. A total of four transitions populate and depopulate this level. Two of these, RL and QL, are very weak and are observed to convert in the K shell only. PL is strongly converted in the L_I shell and may also convert in the L_{II} and L_{III} shells, although this is not likely (see Discussion). Hence, this transition is probably magnetic, but can be either M1 or M2. LI is observed to convert in the K and L_I shells and may be M1, E1, or M2. These restrictions on the transitions' multipolarities place the restrictions on the level's spin and parity.

Level O is the most poorly established level in the decay scheme. It is based solely upon the fact that the sum of TO and OK is equal to the difference between levels T and K, although a transition of energy equal to TK is not observed. For this reason the transitions could be reversed so that O would lie 557.87 kev above state D. The level is so placed because TO is stronger than OK. TO converts in the K and L_I shells, indicating magnetic radiation. (On the basis that the M_I line was seen, we tentatively rule out E1). The radiation can be either M1 or M2. Only the K-conversion line of OK was seen, so that we cannot determine its multipolarity. From consideration of the spin and parity assignments of levels T and K, we believe that the state probably has a spin of 4 or 5, negative parity.

Level Q is populated by two transitions (besides probable direct population) and depopulates by three. The feeding transition RQ is probably an M1-E2 mixture, E1, or M2. This restricts the level spin to either 5, 6, or 7. Transition QK is so highly converted that it must be predominantly magnetic radiation. This eliminates spin 7 and restricts the spin to 5 for negative parity and 5 or 6 for positive parity.

Transitions QL and QN are consistent with either of these assignments but do not definitely decide between them.

Level T was established by four depopulating transitions. Only transition TO was observed to convert in other than the K shell, and level O is so poorly established as to be of little value in assigning a spin and parity to level T. The fact that T is directly populated suggests, however, that its spin is 6 or 7 (from consideration of the spins of the directly populated negative-parity states). The data are consistent with either spin, and with positive or negative parity.

In Fig. 7 we only indicate possible spins and parities for the states connected by E2 radiation. In cases where the multipolarity of a transition is in doubt it is not indicated on the transition in Fig. 7. As stated previously, proposed assignments for these transitions are given in the "Second Confidence" multipolarity column of Table VII. We defer until later our analysis of the decay scheme, which we consider to be the most reasonable interpretation of the data. It is from this analysis, however, that the "Second Confidence" multipolarities of the weaker transitions were deduced.

Conversion coefficients and mixing ratios. The presentation of the conversion coefficients in Table X is identical to that of Table V. In addition, the observation of several more L-electron lines of some of the transitions reported by MBMD has allowed us to extend the Table.

It can be seen from Table X that we have used two methods to normalize our electron intensities to the theoretical values. This is because two normalization points are needed to obtain normalized conversion coefficients for mixed transitions: the first, to obtain the mixing ratio; the second, the normalization constant. In the cases in Table X in which only one normalization point is indicated, we have used the mixing ratio calculated from the 12.7-hr Re^{182} data; the other cases are those reported for the first time in Table X, hence two normalization points are needed. Normalization points are indicated by parentheses in Table X. In order to obtain L conversion coefficients corrected for

Table X

Comparison of theoretical and experimental conversion coefficients of transitions in W^{182}

Gamma-ray energy (kev)	Source	Conversion coefficients K	L_I	L_{II}	L_{III}	M_I	Multi-polarity and mixing ratio M1-E2
A. M1-E2 Mixtures							
65.71	MBMD		2.2	0.32	--[a]	0.64	99% to 1%
	Theoretical[b]		2.3	0.21	0.04		
	This work[c]		1.4	(0.21)	--[a]	0.33	
84.67	MBMD		1.44	0.48	0.4	0.52	84% to 16%
	Theoretical	5.0	0.78	0.50	0.36		
	This work[c]		1.44	(0.50)	0.38	0.77	
113.66	MBMD	1.4	0.32	0.056			95% to 5%
	Theoretical	2.5	0.38	0.062	0.026	0.12	
	This work	1.9	(0.38)	(0.065)	0.025	0.14	
179.36	MBMD	0.33	0.12		0.005		62% to 38%
	Theoretical	0.55	0.074	0.034	0.025	0.032	
	This work	0.32	(0.074)	(0.034)	0.012	0.012	
107.13	Theoretical	2.0	0.31	0.46	0.38		50% to 50%
	This work	1.5	(0.31)	(0.46)	0.30		
130.76	Theoretical	1.4	0.20	0.077	0.05	0.066	84% to 16%
	This work	1.1	(0.20)	(0.077)	0.04	0.06	
147.68	Theoretical	0.96	0.13	0.086	0.061		63% to 37%
	This work	0.82	(0.13)	(0.086)			
B. E1 Transitions							
67.74	MBMD		0.14[a]	0.056	0.056	0.048	
	Theoretical		0.083	0.032	0.037		
	This work		--[a]	(0.032)	0.035	0.050	
152.41	MBMD	0.056					
	Theoretical	0.11	0.013				
	This work	~0.04[d]	(0.013)				
156.37	MBMD						
	Theoretical	0.11	0.013				
	This work	~0.01[d]	(0.013)				
160.09	Theoretical	0.09	0.011				
	This work	~0.02[d]	(0.011)				

Notes on Table X

a. L_{III} 65.71, L_I 67.74 superimposed.

b. Theoretical conversion coefficients were obtained in the following way:

$$\alpha_K = \alpha_K\,(\text{Sliv});\ \alpha_{L_I} = \alpha_{L_I}\,(\text{Rose}) \cdot \frac{\alpha_K(\text{Sliv})}{\alpha_K(\text{Rose})};$$

$$\alpha_{L_{II}} = \alpha_{L_{II}}(\text{Rose}) \cdot \frac{\alpha_K(\text{Sliv})}{\alpha_K(\text{Rose})};\quad \alpha_{L_{III}} = \alpha_{L_{III}}(\text{Rose});$$

$$\alpha_{M_I} = \alpha_{M_I}(\text{Rose})\ (\text{unscreened}).$$

c. Only one line was used for normalization of these transitions because the mixing ratio was determined from the decay of 12.7-hr Re^{182}.

d. These intensities may be too small by a factor of 2 or 3, because the lines are on a very intense background. Unless something completely unexpected is affecting the photographic blackening of the plate here, however, the K/L_I ratio is much too small.

finite nuclear size, we reduced Rose's L_I- and L_{II}-conversion coefficients by the ratio α_K Sliv/α_K Rose. This correction essentially assumes that Rose's L_I/K ratios are correct, a point that is not clear at present.

It is apparent from Table X a, that in every case where M1-E2 mixing occurs our experimental results indicate that the K conversion of these transitions is low. We at first suspected a systematic error in our intensities; however, after completing the comparison of our normalized coefficients with the corrected absolute experimental conversion coefficients of MBMD shown in Tables V and X, it became apparent that the experimental results are consistent and both are at variance with the theoretical values, even when the latter have been corrected for finite nuclear-aize effects. The general direction of the experimental results indicates that the theoretical K conversion coefficients are still too high. Such a conclusion has also been reached by Wapstra and Nijgh.[48]

In part b of Table X, we show the results for transitions that we believe to be E1. The 67.74-, 152.41-, and 156.37-kev transitions have been definitely assigned E1 multipolarity by MBMD. The 160.09 is assigned E1 multipolarity from the decay scheme. It is apparent from Table X that, at least for the transitions around 150 kev, the L_I/K-conversion ratio seems high. Although this discrepancy may reflect the large experimental difficulty involved in obtaining the K intensities of this group of transitions because they lie on a very intense background, the fact that a similar result was obtained for the 152.41-kev transition in 13-hr Re^{182}, where the conditions are more favorable, tends to support these conclusions. The high L_I/K ratios suggest a possible systematic error perhaps owing to the neglect of some geometry factor in calculating the intensities. In fact, the direction of the results is the same as for the M1-E2 transitions, but such an error seems unlikely because of the similar results obtained by MBMD for the M1-E2 mixtures.

Another transition, the 120.94-kev, which was assigned an E1 multipolarity from the decay scheme, appears to have too large an L_I/K ratio. In this case the intensities of both lines were too weak to be calculated from the densitometer trace, but because both were visible

the K/L_I ratio must be about the same as those of the transitions listed, if the line assignments are correct. This might be the first observation in this region of the periodic table of anomalous E1 conversion coefficients similar to those which have been observed in the heavy-element region by Asaro.[59] However, because of the large uncertainties in our electron intensities and the absence of gamma data, we do not believe that further discussion of this aspect of the problem is warrented here.

Primary population and log *ft* values. Although the complexity of the decay scheme prevented accurate determination of primary electron-capture branching from electron data alone, we attempted to estimate primary branching by assuming that the total decay proceeds through states Q, P, R, S, and T. This assumption is probably not strictly correct, but the intensities populating and depopulating the lower energy states are consistent with it. Furthermore, because we have no high-resolution gamma-intensity data, the percentage primary populations we calculated are multipolarity-dependent. Using the electron intensities and assigned multipolarities shown in Table VII, we calculated that the percentage primary populations to states Q, P, R, S, and T, are, respectively, 17%, 5%, 27%, 48%, and 3%.

An estimate of the decay energy was made, but as is almost always true for electron-capturing isotopes, it has large uncertainties. We know that the total decay energy must be greater than the energy of the highest state populated, so that the total decay energy must be greater than 1960 kev. Because an appreciable fraction of decay goes to state S, we estimated that the decay energy is probably 200 kev greater than the excitation energy of S. Using this estimated decay energy, the primary-branching percentages discussed above, and the L_I/K-capture ratios from the curves of Brysk and Rose,[34] we calculated log *ft* values for K capture of 6.4, 6.9, 6.1, 5.5, and 6.7 to the states Q, P, R, S, and T, respectively.

Because most of the observed decay of Re^{182} is to levels assigned spin 6 and 7, although levels assigned spin 5 are present, it seemed reasonable to assign a spin 7 to Re^{182}. Since the major fraction of decay goes to the states which definitely appear to have negative parity, and because the log ft for decay to S may be as low as 5.5 these electron-capture transitions are probably allowed and hence Re^{182} probably has negative parity.

Because of the unusually high spin of the isomer we looked for odd-proton and odd-neutron states observed in neighboring nuclei which could couple to produce a 7- isomer. There are only two such states observed. The odd-proton state is the 7/2+ state observed as the ground state in Ta^{181};[42] the odd-neutron state is the 7/2- state assigned as the ground state of Hf^{177}.[42] (There is also a 7/2- excited state observed in W^{183}; it is not known whether the two states are the same although they probably are not). From the Nilsson diagrams for odd-neutron and odd-proton states[37] (Fig 3, (a) and (b)) we determined that only the two states above and a second 7/2- odd-neutron state are expected to be present on theoretical grounds. Thus if it is assumed that the state is composed of only two particle states, these states seem the most probable.

Analysis and Discussion of the Levels of W^{182}

The presence of large numbers of low-energy magnetic-dipole and electric-quadrupole transitions between states of over 1 Mev of excitation energy is rather remarkable and cannot be understood in terms of single-particle transitions. However, the marked similarity of such patterns to those observed for low-energy states in strongly deformed nuclei indicates that these states may have a collective character. AABM have previously analyzed the levels of W^{182} populated by Ta^{182} in such a way. They grouped all but three of the states into rotational bands.

In Fig. 10 we present a possible analysis into rotational states for the levels in W^{182} above 1 Mev. This interpretation assigns the eighteen levels into four rotational bands and six extra levels. It must be pointed out that this interpretation is consistent with the experimental data now known but is not completely proved by them.

Because the explanation of our analysis requires some discussion in addition to that already given, we shall begin by discussing the experimental evidence supporting the assignment of the base states of the four bands.

Level D is assigned K = 2, + because of the agreement of the observed branching ratio from this state to levels B and A (and C) by E2 radiation with that predicted theoretically. The assignment of K = 2 to this level was originally proposed by AABM, who calculated the experimental value

$$\frac{B\ (E_2;\ 2,2 \longrightarrow 2,0)}{B\ (E_2;\ 2,2 \longrightarrow 0,0)} = 1.61$$

from the data of MBMD, assuming transition DB was pure E2. Using the 10% to 90% E2-M1 mixing ratio determined by Williams and Roulston from angular-correlation studies involving transition DB,[57] we recalculate this value to be 1.42, in excellent agreement with the theoretical value for $K_i = 2$, of 1.43. The theoretical ratio for $K_i = 0$ is the same, but the choice $K_i = 2$ is clearly made in view of the weakness of the transition to level C.

No evidence supporting level E was obtained in this study, but the data of MBMD and Bäckstrom[58] support this level quite conclusively. The 1- assignment was made by MBMD. In order to determine which of the two possible K-quantum numbers (0 or 1) is the most likely for level E, we again compared the experimental branching ratio from this state to states B and A with the theoretical branching ratio for E1 transitions. Because we did not observe the transitions supporting this level, we had to use the data of MBMD and Bäckstrom[58] which fortunately were sufficient. The theoretical reduced transition probabilities for depopulation of states with K = 0 and K = 1 are, respectively,

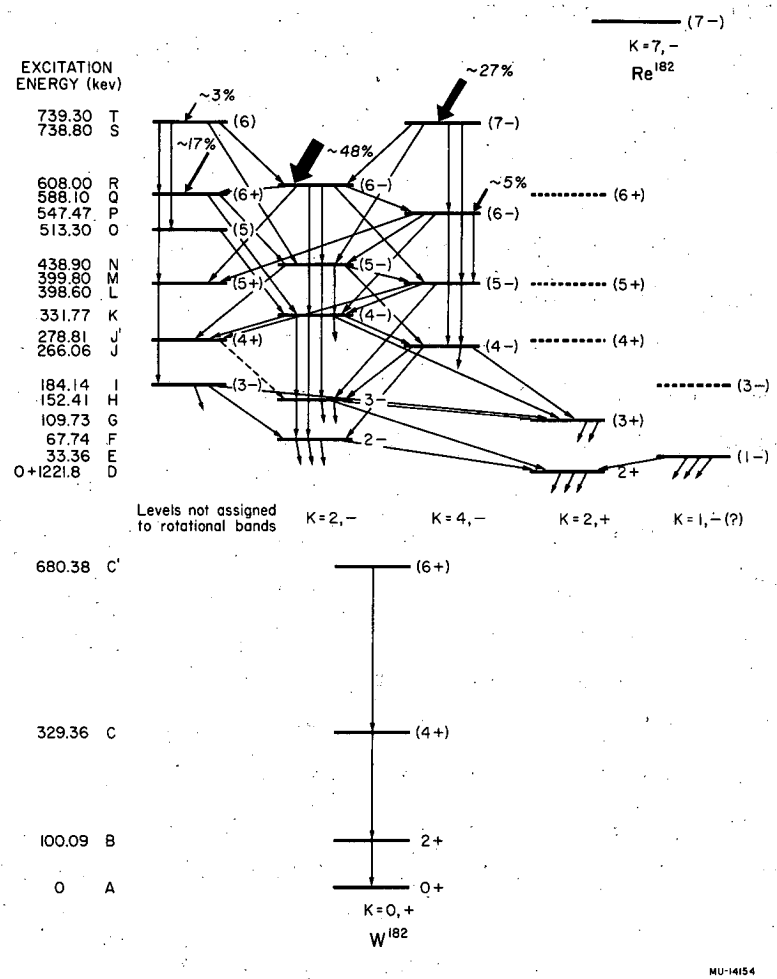

Fig. 10. Analysis of the level spectrum of W^{182}.

$$\frac{B\ (E1;\ 1,1 \longrightarrow 2,0)}{B\ (E1;\ 1,1 \longrightarrow 0,0)} = 0.50$$

and

$$\frac{B\ (E1;\ 1,0 \longrightarrow 2,0)}{B\ (E1;\ 1,0 \longrightarrow 0,0)} = 2.0$$

We have used the algebraic tables of Clebsch-Gordan coefficients prepared by Sears and Radtke,[60] to calculate the Clebsch-Gordan coefficients throughout this paper. Transition EB was seen by MBMD and assigned M2 multipolarity. However, because their conversion coefficients are at least 20% too high (see discussion under "Conversion coefficients" in Section III B) we reduced their α_K for this transition by 20%. Their corrected α_K is consistent with an 83% E1 - 17% M2 mixture. We used Sliv's conversion coefficients of 0.0012 (E1) and 0.013 (M2) to calculate the mixing ratio. Using MBMD's gamma intensity of 6.5 for this transition, we found that the total amount of E1 radiation is, on the same scale, 5.4. An estimate of the gamma intensity of the 1254 photon is somewhat more uncertain, because it was not observed by MBMD although it was observed by Bäckstrom.[58] Fortunately, Bäckstrom has published the electron spectrum containing the K line of the 1255-kev (EA) and the L_I lines of the 1189-kev (FB) and 1222-kev (DA) transitions. Using MBMD's conversion coefficient and K/L ratio for FB, and Bäckstrom's[58] K line intensity for the 1255, reduced by 22% to account for the L_I line of the 1155 which he shows as superimposed, we obtained a ratio of the intensities of the L_I lines of the 1155- and 1255-kev transitions. By assuming that the 1255 is pure E1, and α_K = 0.001 (Sliv's value), we obtained a gamma intensity of 10.5 for the 1255, on the same scale as above. From these data, we calculated the experimental reduced transition probability ratio

$$\frac{B\ (E1);\ (1155)}{B\ (E1);\ (1255)} = \left(\frac{5.4}{10.5}\right)\left(\frac{1255}{1155}\right)^3 = 0.79$$

which, in spite of the number of factors involved, is in much better agreement with the theoretical value for K = 1 than for K = 0. Its intensity indicates that previously it has probably been included in

the 1231 peak, which would account for the fact that it has not been reported by MBMD. State E is assigned K = 1 rather than K = 0 on this basis.

The assignment of K = 1 to state E suggests the possibility that level F, which was assigned by AABM as the base state of a K = 2,- band might actually be the second member of the K = 1,- rotational band. Using the results of MBMD and Bäckstrom,[58] in order to obtain experimental data to compare with the theoretical predictions, we were able to show that AABM's assignment is correct. Because F has spin 2,[57] it will be expected to decay to levels A and B by M2 radiation. The ratio of reduced transition probabilities for M2 radiation from state F to states B and A is, for K = 1

$$\frac{B\ (M2;\ 2,1 \longrightarrow 2,0)}{B\ (M2;\ 2,1 \longrightarrow 0,0)} = 0.345,$$

and for K = 2

$$\frac{B\ (M2;\ 2,2 \longrightarrow 2,0)}{B\ (M2;\ 2,2 \longrightarrow 0,0)} = 1.43.$$

Although MBMD did not see the 1289-kev (FA) transition, they did measure the gamma intensity, K/L ratio, and absolute K-conversion coefficient for transition FB. They assigned the transition as an M2 − E3 mixture. However, after their value was reduced by the 20% correction previously discussed, the only possible interpretation for this transition (assuming only two components) was that it is a 69% to 31% E1-M2 mixture. Sliv's conversion coefficients α_K (M2) = 0.013 and α_K (E1) = 0.00113 were used to determine the mixture. From this mixing ratio we calculated an M2 gamma intensity of 14 on the MBMD gamma-intensity scale.

Bäckstrom[58] resolved the L lines of the 1289- (FA) and 1189- kev (FB) transitions. Without making any assumptions about the multipolarity of FB, we calculated a gamma intensity from these data, assuming an M2 multipolarity for FA. From the assignment of 2- to level F the multipolarity can only be M2. To calculate the gamma intensity of FA, we first calculated the absolute L_I-shell conversion coefficient of 0.00074 for FB

from the MBMD α_K (corrected) and the K/L_I ratio for this transition. The theoretical α_{L_I} for an M2 transition of 1289 kev is, from Rose's tables, 0.0015. We estimated a finite-nuclear-size correction for the α_{L_I} by assuming that the K and L_I shells are similarly affected. Rose's α_{L_I} was then reduced by the ratio α_K (Sliv)/α_K (Rose). By this method we obtained a value $\alpha_{L_I} = 0.00135$. The gamma intensity of FA (on the MBMD intensity scale) calculated from these data and Bäckstrom's experimental L line intensities[58] is 12.9. The experimental value of the reduced transition probability is

$$\frac{B\ (M2);(FB)}{B\ (M2);(FA)} = \left(\frac{14}{12.9}\right)\left(\frac{1289}{1189}\right)^5 = 1.61$$

which agrees quite well with the theoretical value, 1.43, for a state with K = 2. It thus appears that level F is the base state of a K = 2 band and is not the second state of a K = 1 band.

Because state F fails to satisfy the branching expected from the I = 2 member of the K = 1,- rotational band, and because we have not been able to find evidence for a state close in energy to state F that might be so assigned, we are led to question the K = 1,- assignment of state E, and suggest that a K = 0,- assignment is preferable. We shall later suggest other reasons why a K = 0,- assignment would be preferred for state E. However, because the present branching-ratio data agree with the K = 1,- assignment to level E, this assignment is illustrated in Fig. 10.

From these calculations we concluded that there are at least three rotational bands to be expected in the W^{182}- level spectrum above 1000 kev. Besides these three, a fourth with K = 4, was postulated by AABM in their analysis of the W^{182} levels observed from Ta^{182} decay. We have attempted to analyze the observed levels in terms of rotational states based upon these four states. Our analysis is shown in Fig. 10.

Before discussing our analysis, we would like to point out that, because it is based upon comparison of theoretical and experimental E2 reduced transition probabilities, there exists the possibility that other assignments can also be made which will be in agreement with other theoretical values. In order to avoid this possibility, we calculated reduced

transition probabilities for all the values of K less than 4, for all the states (but keeping the present spin assignments) and found that the best over-all fit of the data was given by the assignments illustrated.

In Fig. 10 we have assigned twelve of the eighteen levels as levels of four rotational bands. Five have been assigned to the K = 2,- band, four to the K = 4,- band, two to the K = 2,+ band, and only one, the base state, to the K = 1,- band. We have also assigned tentative spins and parities to the levels unassigned in Fig. 7. The multipolarities shown in the "Second Confidence" multipolarity column are deduced from the level scheme in Fig. 10.

It is immediately clear from Fig. 10 that our proposed assignment does not show the expected rotational-energy spacing between levels. Although we attempted at first to analyze the levels by energy relationships (which ended by assigning levels K, N, and R as states of the K = 4,- band, J, M, P, and S as members of the K = 2,- band, all other levels being unchanged) from Fig. 10 it became clear almost immediately that the energy levels of the observed states do not fall into well-developed rotational patterns. This is not excessively surprising, since the interactions acting to perturb the rotational spacing at this excitation energy must be quite large.

The analysis shown in Fig. 10 is based on the comparison of the reduced transition probabilities for E2 transitions from the rotational levels to other members of their same rotational bands, and also for the crossover radiations to rotational states in the other bands. The comparison of experimental and theoretical reduced transition probabilities is shown in Table XI. The agreement of the experimental with the theoretical values is remarkable, considering the amount of K-mixing that must be responsible for such large perturbations of the level energies. In making the analysis we have given the greatest weight to the agreement of the intraband transitions.

States J (K = 4,-) and K (K = 2,-) have been changed from the previous assignment given by AABM, on the basis of the results in Table XI, although the energy spacings favor the earlier assignment. State N (K = 2,-) was so assigned largely because the ratio of the reduced transition

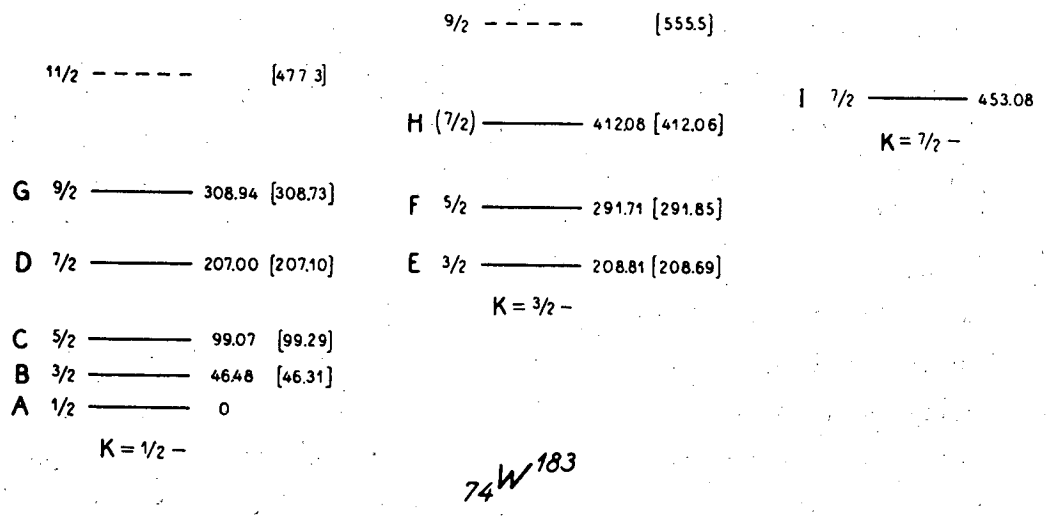

MU-14169

Fig. 11. The level spectrum of W^{183} proposed by MBMD.[28] The analysis into rotational bands is due to Kerman.[61]

Table XI

Comparison of theoretical and experimental reduced transition probabilities for de-excitation of some of the levels in W^{182}

K,π	Transitions compared	Reduced transition probability calculated	Theoretical	Experimental
1,-	EB/EA	$\frac{B(E1\ 1,1\text{--}2,0)}{B(E1\ 1,1\text{--}0,0)}$	0.50	0.80[a]
2,+	DB/DA	$\frac{B(E2\ 2,2\text{--}2,0)}{B(E2\ 2,2\text{--}0,0)}$	1.43	1.42[b]
2,-	FB/FA	$\frac{B(M2\ 2,2\text{--}2,0)}{B(M2\ 2,2\text{--}0,0)}$	1.43	1.61[a]
2,-	RN/RK	$\frac{B(E2\ 6,2\text{--}5,2)}{B(E2\ 6,2\text{--}4,2)}$	0.36	---[c]
2,-	NK/NH	$\frac{B(E2\ 5,2\text{--}4,2)}{B(E2\ 5,2\text{--}3,2)}$	1.00	2.42[d]
2,-	KH/KF	$\frac{B(E2\ 4,2\text{--}3,2)}{B(E2\ 4,2\text{--}2,2)}$	2.24	1.90[e]
2,-	RP/RM	$\frac{B(E2\ 6,2\text{--}6,4)}{B(E2\ 6,2\text{--}5,4)}$	5.9	---[c]
2,-	NM/NJ	$\frac{B(E2\ 5,2\text{--}5,4)}{B(E2\ 5,2\text{--}4,4)}$	10.	---[c]
4,-	SP/SM	$\frac{B(E2\ 7,4\text{--}6,4)}{B(E2\ 7,4\text{--}5,4)}$	2.6	---[c]
4,-	PM/PJ	$\frac{B(E2\ 6,4\text{--}5,4)}{B(E2\ 6,4\text{--}4,4)}$	5.5	4.3[f]
4,-	SR/SN	$\frac{B(E2\ 7,4\text{--}6,2)}{B(E2\ 7,4\text{--}5,2)}$	1.6	~50.[g]
4,-	PN/PK	$\frac{B(E2\ 6,4\text{--}5,2)}{B(E2\ 6,4\text{--}4,2)}$	1.35	---[c]
4,-	RK/RH	$\frac{B(E2\ 5,4\text{--}4,2)}{B(E2\ 5,4\text{--}3,2)}$	1.00	---[c]
4,-	JH/JF	$\frac{B(E2\ 4,4\text{--}3,2)}{B(E2\ 4,4\text{--}2,2)}$	0.56	0.90[h]

Notes on Table XI

a. Calculated from the data of MBMD and Bäckstrom.

b. Calculated from MBMD gamma intensities assuming a 10% to 90% M1-E2 mixture in FB(deduced by Williams and Roulston from angular-correlation data).

c. The E2 component of the transition is too small to be detected from L-subshell conversion, in agreement with the theoretical prediction.

d. Calculated from electron intensity data assuming a 50% to 50% M1-E2 mixture in SP.

e. Calculated from MBMD gamma intensities and 62% to 38% M1-E2 mixture in KH.

f. Calculated from electron intensities assuming a 63% to 37% M1-E2 mixture in PM.

g. Calculated from electron intensity data assuming an 84% to 16% M1-E2 mixture in SR. Although the uncertainty in the intensity of SR is quite large, we do not believe the intensity data are in error by an order of magnitude.

h. Calculated from MBMD gamma intensities assuming a 95% to 5% M1-E2 mixture in JH.

probabilities from N to K and H is in excellent agreement with that for K = 2 for all these levels. The E2 radiations from M are so weak that reduced transition probabilities cannot be calculated with much certainty, but the data are consistent with the assignment. M and P are assigned to the K = 4,- band because the ratio of the reduced transition probabilities from P to M and J is in excellent agreement with the theoretical value for K = 4.

The assignment of levels S and R, although not dotted in Fig. 10, must be considered somewhat tentative because the radiations populating and depopulating R and S show anomalous behavior. The evidence supporting the present assignment for R is that RN is an extremely strong M1, and the crossover E2 goes to K and not J. The E2 component of RN is also predicted to be small, which it is. On the other hand, the large primary population of R relative to that observed to state P, which has been assigned the same spin and parity would suggest (assuming that K-forbiddenness will be a factor in inhibiting primary electron capture) that R has K = 4. It might be possible to explain this if we postulate that R has a very large admixture of higher-K wave functions. However, in the present state of knowledge this is a moot point.

If level S has K = 4, it can be expected to receive a large amount of primary population, and this is observed. It is also observed to decay by strong M1 radiation to P and by strong E2 radiation to M and N, SM being much the stronger of the two, which also supports the assignment. The anomalous features are the strength of transition SR, which is about twice as strong as SP, and the ratio of reduced transition probabilities (which is much larger than that predicted theoretically) from S to R and to N, which seems well outside the experimental limits of error on the intensities.

We have not been able to assign any states definitely to a rotational band based on E. Of the unassigned states there are three that might possibly be assigned as members of this band. Of these, state I is the most likely, and we have tentatively assigned it in Fig. 10 (dotted level) to this band. We have previously discussed the reasons why we believe a spin of 3 is most probable for this level. That it has

K = 1, rather than K = 2, or 3, is supported by the observation that it is populated only weakly from Ta^{182} decay, and very weakly, it at all, from 13-hr Re^{182} decay, both isotopes probably having K =3. It also decays at least partially to ground, which suggests a low K value.

The possibility that state I is the spin-3 member of the K = 1 band, whereas no state has been observed with I = 2, K = 1, suggests that this latter is only weakly populated, if at all. Because this level must be present if the assignments of states E and I are correct, it would be very interesting to attempt more detailed studies of Ta^{182} and 12.7-hr Re^{182} to see if evidence for such a state could be found.

Only two states of the eighteen observed have definitely been assigned positive parity. These were both assigned by MBMD. We have observed three states which we have tentatively assigned (dotted levels in Fig. 10) to the K = 2,+ band. The reason for such an assignment is that the observed branching to these states occurs with the same branching pattern from the high-spin, negative-parity levels as is observed from the low-spin, negative-parity levels to the 2+ and 3+ states. Furthermore, no strong radiations are observed to depopulate levels J' and L, which is consistent with the interpretation that they would decay directly to the high-spin members of the ground-state rotational band. Such an explanation could account for the increased intensity of population of the spin-4 member of the ground-state band in Re^{182} decay over that observed in Ta^{182} decay (cf. Fig. 6). State Q is assigned to this band although the observed radiation pattern from this state differs from that of the lower states, which might possibly indicate that states with higher K are mixed in this state.

Although the experimental data are inconclusive about many aspects of the interpretation presented, it is interesting to speculate upon a possible interpretation of the very strongly perturbed rotational-band energy spacings that appear as a consequence of the assignments. It must be emphasized that what is written below is in the line of speculation and will require much additional data to prove.

If we consider the positive parity states first, including the levels only tentatively assigned, it is very interesting to observe that

the level spacings are alternately large and small. This is extremely interesting, because as discussed in the introduction, the unified model predicts the presence of β-vibrational states, whose characteristic rotational pattern is 0+, 2+, 4+, etc. If we assume that perturbation theory holds, (which is probably incorrect) it is interesting to observe that Bohr[4] has suggested a perturbation that he called U_2, which can couple states of $\Delta K \pm 2$, $\Delta \Omega = 0$. If this perturbation is applicable, states of β- and γ- vibrational modes can couple, and only even-spin states would couple because of the absence of odd-spin states in the β-vibrational band. Such an effect could produce a rotational pattern similar to that postulated.

An explanation of the negative-parity states is more difficult, because of the greater number of negative-parity states observed. It is interesting to note, however, that the effect of a Coriolis interaction, as suggested by Kerman,[61] (which could couple rotational state bands with K = 1,- and K = 2,-) would not be expected to produce the alternation in level spacing observed for the K = 2,- band. However, if state E did not have K = 1 but perhaps has K = 0, then the alternation of the energy-level spacing could be due to the same interaction postulated to couple the K = 0,+ and K = 2,+ rotational-band states, because the K = 0,- band also has an alternating spin pattern, in this case 1, 3, 5, etc. This would require, however, that the K = 2,- and K = 0,- band have the same intrinsic wave function, a suggestion that has already been proposed by Sheline.[9] It must be admitted, however, that the very large spacing KH suggests that there are additional forces at work, if state I is really the spin-3 member of a K = 0,- band.

If we try to estimate whether the levels of the K = 4,- band are perturbed, we can only conclude that level P appears to be about 13 kev lower than the energy calculated from the moment of inertia calculated from spacing MJ, whereas spacing JS is approximately that calculated. The moment of inertia calculated from spacing MJ is about 20% greater than that of the ground-state band. It seems qualitatively, however, that the states of the K = 4,- band are not as seriously perturbed as those assigned to the other bands.

Conclusion

The rather tenuous evidence for the assignment of the positive-parity states demonstrates the need for high-resolution gamma-spectroscopic studies. Such studies would definitely establish the validity of many of our assignments and the predicted strong E1 radiations should be easily observable. Further studies also need to be carried out on the high-energy spectrum, the results of which are needed to verify some of the present assignments, especially those of J' and L.

The negative-parity states we have observed appear to have good K-quantum numbers, if we base our conclusions on the reduced transition probabilities alone. From the observed energy spacings, however, K is not expected to be a good quantum number, because the energy-level perturbations appear to be large. A similar anomaly appears in the observed primary electron-capture branching, which suggests that the assigned spin-6 levels should be interchanged, although their gamma branching favors the assignment given. The levels observed appear to account for the expected members of the K = 2,- and K = 4,- bands, but do not account for all the expected levels of the K = 1,- band. Furthermore, we have not definitely established whether other negative parity states due to still other rotational bands are present.

In general, the data most needed are gamma intensities obtained from high-resolution gamma spectroscopy. These will serve to check our assigned multipolarities and reduced transition probabilities, and establish more accurately the primary electron-capture branching intensities.

D. 71-Day Re^{183}

Mass Assignment and Half Life

The 71-day electron-capturing isotope Re^{183} was first produced by Wilkinson and Hicks,[43] who assigned it a 120-day half life. The investigations that led to the present half-life assignment are discussed in the recent paper of Thulin, et al., (hereafter referred to as TRGSH) on Re^{183} decay.[41] The mass assignment was verified by the stacked-foil excitation function described in Section A.

General Resumé of Spectroscopic Results

The decay of Re^{183} is observed to populate only states in W^{183} that are populated by the decay of Ta^{183}.[28] Of the 29 transitions reported by MBMD for this nucleus, 20 were reported by TRGSH. Besides these 20, internal-conversion lines of five of the others were observed in the present study.

Gamma Spectroscopy

The gamma-spectroscopic studies of Re^{183} were made by Dr. Donald Strominger,[62] who obtained the gamma-ray intensities reported in Table XII. The intensity of the 160- and 208-kev transitions relative to the transitions around 300 kev supports TRGSH's assignment that primary decay occurs predominantly to the 3/2 state at 208.81 kev. The low resolution and the known complexity of this spectrum, however, make these data useful only for such a gross intensity check. We will not, therefore, attempt to analyze them further.

Electron Spectroscopy

The electron lines of Re^{183} were studied in the 99-, 216-, and 350-gauss permanent-magnet spectrographs. The sources were prepared in two ways, the first of which is described in TRGSH. The second method

Table XII

Photon intensities of transitions of W^{183} observed in Re^{183} decay

Photon	Intensity
K x-rays	100.0
108	6.3
160	12.9
210	1.4
250	~0.8

was to bombard a thick (0.12-inch) tungsten foil in the high-intensity low-energy deuteron beam of the Livermore A-48 linear accelerator.[63] The rhenium activity was produced by barrier-penetration reactions because the deuteron energies were $\leq$ 7.6 Mev, which is below the Coulomb barrier for (d,xn) reactions in tungsten. After the foil had been allowed to cool for several months, Chemistry D was employed to remove the bulk of the natural tungsten and Chemistry E was used to prepare the carrier-free rhenium activities. These were electrodeposited on a 0.010-inch-diameter platinum wire in the manner previously described.[12,19]

The second source was exposed in the 99-gauss magnet for 30 days. The Re^{183} lines observed are reported in Table XIII; only visual intensities are listed. In Appendix C, Part 1, we list all the electron lines observed in this study in order of increasing energy. In Part 2, a, the electron lines are listed by transition energy. The transition energies in Table XIII are those reported by MBMD.

Discussion of Results

The data obtained in this study are consistent with the results previously reported by TRGSH. Although we observed several transitions that they did not report, these transitions arise from levels that they showed were populated by Re^{183} decay and hence had to be present. The level spectrum of Re^{183} determined by MBMD and analyzed by Kerman[61] is reproduced in Fig. 11.

In our analysis of the electron spectrum we attempted to check the mixing ratios predicted by Kerman[61] in his analysis of the levels in W^{183}. Unfortunately, we were not able to obtain any data in addition to those already reported by TRGSH to check Kerman's[61] theoretical predictions.

Table XIII. Transitions in W^{183} following the decay of Re^{183}. The intensity symbols are: s = strong, m = moderate, w = weak, v = very, e = extremely. Ordinary type refers to an exposure in the 99-gauss magnet. Underlined intensities were observed in an exposure in the 216-gauss magnet. Doubly-underlined transitions were observed in an exposure in the 350-gauss magnet.

Initial and final states	Transition energy (kev) (from MBMD)[a]	Conversion lines observed in Re^{183} decay.								
		K	L_I	L_{II}	L_{III}	M_I	M_{II}	M_{III}	N	O
IH	40.97		ew	---[b]	ew?					
BA	46.48		vs	w	w	ms	ew	ew	w	vw
CB	52.59		ms	w	vw	wm	ew[c]	ew[c]	w	
FE	82.92		ew	ew	---[b]	ew[c]	ew[c]	ew[c]	ew[c]	ew[c]
FD	84.70	ew	≤m[d]	ew[c]	≤ew[e]	ew			ew[c]	
CA	99.07	vw	vw	ms	ms		<wm[f]	w	vw	
GD	101.94			no lines seen from Re^{183} decay						
g	102.49			no lines seen from Re^{183} decay						
HG	103.14			no lines seen from Re^{183} decay						
DC	107.93	m	wm	≤wm[f]	≤vw[h]	vw				
EC	109.73	ms	wm	≤vw[h]	≤w[j]	vw				
HF	120.38			no lines seen from Re^{183} decay						
g	142.25	≤m[d]								
IG	144.12	≤ew[e]								
DB	160.53	ew								
IF	161.36	ew								
EB	162.33	vvs	ms	w	vw	wm			vw	ew[c]
FC	192.64	ew,<u>w</u>								
HE	203.27			no lines seen from Re^{183} decay						
HD	205.06	ew[c]								
EA	208.81	m,<u>ms</u>	vw,<u>m</u>			<u>vw</u>				
GC	209.87	ew?[c]			ew[c]					
IE	244.26	ew[c]								
FB	245.3[k]	ew								
ID	246.05	w,<u>ms</u>	<u>w</u>							
FA	291.71	<u>wm</u>		<u>w</u>			<u>w</u>			
HC	313.03	<u>w</u>								
IC	354.04	<u>w</u>	<u>ew?</u>[c]							
HB	365.60	<u>ew?</u>[c]								
IB	406.58	<u>ew?</u>[c]								

a. See reference 28.

b. Masked.

c. Re^{183} lines reported for the first time.

d. L_I 84.70, K 142.25 superimposed.

e. L_{III} 84.70, K 144.12 superimposed.

f. L_{II} 107.93, M_{II} 99.07 superimposed.

g. Transitions not assigned to the decay scheme by MBMD.

h. L_{III} 107.93 and L_{II} 109.73 superimposed.

j. L_{III} 109.73 and L_{II} 111.20 (Re^{184}) superimposed.

k. Lines of transition FB were not seen by MBMD. The energy of this transition was reported by TRGSH.

E. 50-day Re^{184}

Mass Assignment and Half Life

The 50-day electron-capturing isotope Re^{184} was discovered by Fajans and Voigt.[64] Wilkinson and Hicks reported the 50-day half life.[43] The mass assignment, and the half life of 52 ± 10 days determined in this study[61] are in excellent agreement with the results of the earlier workers.

General Resumé of Spectroscopic Results

Analysis of the long-lived internal-conversion line spectrum of the neutron-deficient rhenium isotopes has made it possible to assign eight transitions to Re^{184} decay. From energy sums, six of these transitions establish four excited levels in W^{184}. Two of these levels fit the energies of the predicted 2+ and 4+ rotational levels of the ground-state rotational band. The other two states have an excitation energy of nearly 1 Mev, and have been tentatively assigned as the 2+ and 3+ members of a γ-vibrational band on the basis of their E2 branching to the ground state. (A crucial test of our assignment will be the measurement of the cross section for Coulomb excitation of this level.) Three definitely established and one questionable transition are unassigned.

Coincidence studies by Dr. Donald Strominger[65] have shown the validity of the electron-spectroscopic assignments. Coincidences were observed between some of the established transitions and weak transitions that were not seen in either the electron spectrum or the singles gamma spectrum. It has not been possible to establish uniquely the energies of the states giving rise to these transitions.

Gamma Spectroscopy

The samples used in the gamma-spectroscopic studies of Re^{184} were prepared from the carrier-free rhenium activities that were discussed in Section E under Electron Spectroscopy. All the samples contained a mixture of Re^{183} and Re^{184} activities. The gamma-spectroscopic studies were carried out largely by Mr. John Unik and Dr. Donald Strominger.[65]

The relative intensities of the photons present in mixed Re^{183} - Re^{184} samples containing various proportions of Re^{183} and Re^{184} were studied with the scintillation spectrometer previously described. From this study it was possible to deduce which photons belong to Re^{184} and to obtain rough intensities for them. Because the photon peaks are complex, they will be discussed later.

Electron Spectroscopy

The sources used in the study of Re^{184} were the same as those described in Electron Spectroscopy in Section E. The first of these was found to contain little Re^{184}; the second sources were prepared specifically to study this isotope. The studies were made using the 99- and 350-gauss permanent-magnet spectrographs.

Wilkinson and Hicks[43] examined the conversion-electron spectrum of Re^{184} with a magnetic spectrometer and reported transitions of energies 43-, 159-, 205-, and 285-kev. Wilkinson[26] also studied Re^{184} decay and found electron lines corresponding to transitions of 159-, 206-, 244-, 784-, and 890-kev. The assignment of these transitions to Re^{184} was made on the basis of the rate of decay of the electron lines.

From our studies we conclude that all of the transitions except the 784- and 890-kev transitions assigned to Re^{184} in previous studies were incorrectly assigned. The low-energy transitions reported are very similar in energy to transitions in Re^{183} (cf. Re^{183} gamma spectrum, Table XII), and we believe that they should be so assigned. The incorrect assignment could very easily be due to the incorrect 120-day half life previously reported for Re^{183}. (cf. discussion of this point in TRGSH, Ref. 41.) The 71-day half life determined by Strominger[41] can perhaps explain why these low-energy lines were previously assigned to 50-day Re^{184}. It is also interesting to note that the 120-day half life reported for Re^{183} is in excellent agreement with the reported half life of W^{181}.[21-25] It seems very likely, therefore, that Re^{181} was produced in the original studies of the rhenium isotopes by Wilkinson and Hicks[43] but was not identified.

Their assignment of a 346-kev transition to Re^{182} seems to support this conclusion. The W^{181} that was formed by Re^{181} decay would then cause the 120-day tail in the rhenium decay curves.

The transitions of Re^{184} are shown in Table XIV. These transitions were so assigned only after the internal-conversion line spectrum of the long-lived rhenium isotopes had been carefully analyzed, and the many transitions of Re^{183} accounted for. We list only visual intensities for the conversion lines in several cases where the intensities, if calculated, would be subject to excessively large corrections from either the photographic-efficiency or photographic-blackening corrections. In Appendix C, Part 1, we list the long-lived conversion-electron spectrum in order of increasing line energy; in Part 3 we list the electron lines of Re^{184} by transition energy.

Coincidence Studies

The coincidence studies that are reported here were carried out by Dr. Donald Strominger.[65] The fast-slow coincidence circuit used in the study has been described previously.[15]

In the previous section we noted that the 780- and 890-kev transitions were assigned to Re^{184} on the basis of half life. Coincidences were looked for between these two photons and other photons in the sample to help determine the decay scheme of Re^{184}. Unfortunately, the samples prepared by the previously described methods contained large admixtures of Re^{183} activities. To produce a Re^{184} source relatively free from Re^{183}, a 0.001-inch foil of natural rhenium was bombarded in the fast-neutron beam of the Berkeley 60-inch cyclotron. The neutron beam is produced by stripping ~ 15 Mev deuterons in a beryllium block. The sample was shielded on both sides with 1/4-inch cadmium absorbers, to reduce the number of thermal-neutron-induced reactions. After bombardment, the foil was allowed to cool for two months to allow the 92.8-hr Re^{186} [26] produced by the Re^{187} (n,2n) Re^{186} reaction to decay. No purifying chemistry was performed, because charged-particle reactions had been eliminated by thick shielding foils. The long cooling period, small cross sections, and

Table XIV. Transitions in W^{184} following Re^{184} decay. Conversion coefficients listed are normalized and depend on the absolute values of the coefficients in parentheses. Two values were used for normalization, because the high- and low-energy ranges were measured separately.

Initial and final states	Gamma-ray energy (kev)	Gamma-ray intensity	Conversion coefficients K	L_I	L_{II}	L_{III}	Total	Decay fraction	Multi-polarity
(a)	97.33±.05	-----		weak	weak	-----[b]	-----	-----	(M1+E2)
BA	111.20±.06	15	-----[c]	-----	(.72)[d]	.46	2.6	56	E2
(a)	210 ±20	~0.1					-----	0.1	(E1)
(a)	220 ±20	~0.4					-----	0.4	(E1)
(a)	241.1 ±0.2	~0.8	.01				-----	0.8	(E1)
CB	252.84±0.1	~0.6	.08	weak	weak	weak	.15	0.7	E2
(a)	330 ±25	~0.3					-----	0.3	----
DC	540 ±40	~0.3					-----	0.3	(E2)
EC	641.7 ±0.6	~0.5	.008				.008	0.8	M1+E2
(a)	787.7 ±0.8	-----	weak				-----	-----	-----
DB	792.1 ±0.8	41	.009	.001			.010	41	M1+E2
EB	894.5 ±0.9	15	.006				.006	15	E2
DA	903.5 ±0.9	46	(.0045)[e]	weak			.0045	46	E2
	K x-rays	100							

a. Not assigned in decay scheme.

b. L_{III} 97.33 masked by L_{II} and L_{III} 99.07 (Re^{183} decay).

c. Correction factors excessively large for this line.

d. Value used for normalization of conversion coefficients of low-energy lines. Rose's value of $\alpha_{L_{III}}$ was used.

e. Value used for normalization of conversion coefficients of high-energy lines. Sliv's value of α_K was used.

coincidence apparatus were believed to be effective discrimination against the products of any (n,xp) reactions. The sample, when studied, showed a much larger Re^{184}/Re^{183}-activity ratio than had been obtained by the other methods employed.

Table XV summarizes the results of the coincidence experiments. The photon intensities listed in Table XIV were determined from the coincidecne measurements.

Delayed coincidence studies were also made on Re^{184} decay by Dr. Donald Strominger.[65] He was able to set an upper limit of 1.1 mμsec for the half life of the state giving rise to the 903.5- and 791.2-kev transitions. He also measured a half life of 1.3 ± 0.4 mμsec for the 111.20-kev level. These results and the experimental methods used in these studies will be reported in more detail elsewhere.[68]

Discussion of Results

Discussion of transitions. The L_I and L_{II} lines of a 97.33-kev transition were observed. The expected L_{III} line is masked by the L_I and L_{II} lines of the strong 99.07-kev transition in Re^{183}. On the basis of the relative L-subshell intensities, the transition was assigned as M1-E2.

The two most intense low-energy transitions in Re^{184} are the 111.20-kev and 252.84-kev transitions. They were assigned E2 multipolarities on the basis of their observed $L_I/L_{II}/L_{III}$ ratios. Because we obtained both gamma and electron intensities for these transitions, we calculated their absolute conversion coefficients. The experimental electron-to-gamma ratios we obtained were normalized against the theoretical conversion coefficient for the L_{II} line of an E2 transition of 111.20-kev. The absolute conversion coefficients, so calculated for the conversion lines of the 111.20- and 252.84-kev transitions, agree within experimental error with the theoretical E2-conversion coefficients of Sliv and Rose. The 241.1-kev transition is assigned E1 multipolarity on the basis of its low K-shell conversion coefficient. The anomalously small value is probably due to the very great uncertainties in both the gamma and electron intensities of this transition.

Table XV

Gamma-gamma coincidences observed in the decay of Re^{184}

Transition	K x-rays	110	210	230	250	330	540	640	790	900
K x-rays	Y	Y	-	-	Y	-	-	-	Y	Y
110	-	-	-	-	Y	-	-	-	Y	Y[a]
250	-	-	-	-	-	-	Y	Y	Y[b]	Y[b]
790	-	-	Y[c]	-	Y	Y[d]	N	N	N	N
900	-	-	Y[e]	Y	Y	Y[d]	N	N	N	N

Y. Coincidence definitely observed.

N. Coincidence looked for but not observed.

a. 25% of 900-kev photons are in coincidence with 250-kev photons.

b. ~1% of 790-kev and 900-kev photons are in coincidence with 250-kev photons.

c. 210-kev, 790-kev coincidences are observed in extremely weak intensity.

d. ~0.3% of 790-kev and 900-kev photons are in coincidence with 330-kev photons.

e. ~1% of 900-kev photons are in coincidence with 230-kev photons.

The high-energy transitions for which we were able to obtain absolute conversion coefficients are EC, DB, EB, and DA. Because the electron intensities of these high-energy transitions were obtained from a different study, and consequently had a different scale factor than those of the low-energy transitions, the previous normalization could not be used. To normalize these conversion coefficients, we assumed that the K line of the 903.5-kev transition has Sliv's theoretical α_K (0.0045) for an E2 of this energy. The results shown in Table XIV indicate that the data are consistent with the assignment of E2 and M1-E2 multipolarities to these transitions. We shall discuss later why we used the 903.5-kev transition for normalization.

A very weak K line is the only evidence for the 787.7-kev transition. Because we cannot resolve the two ~790-kev photon peaks, we estimated what fraction of the 790-kev photon peak would belong to this transition if it had E1, M1, or higher multipolarity. If the transition is E1, the gamma intensity will be about a fourth of the observed peak. On the other hand, if the transition has M1, E2, or higher magnetic or electric multipolarity, its contribution to the photon peak can be neglected. In the later discussions we assume that the intensity of the 787.7-kev photon can be neglected relative to that of the 791.2.

The ~210-, ~230-, and ~330-kev photons were detected only in the coincidence studies. We believe an E1 assignment is most probably correct for the ~210- and ~230-kev photons, because we failed to observe their K-conversion electron lines although their intensities are large relative to that of the 252.84-kev photon, the conversion electrons of which were seen. The data do not permit an unambiguous multipolarity assignment to the ~330-kev transition.

Decay Scheme. The level scheme porposed for W^{184} is shown in Fig. 12. The first excited state of W^{184} was determined to have an energy of 111.25 ± 0.10 kev from Coulomb excitation experiments.[55] The energy of this transition is in excellent agreement with the 111.20 ± 0.05-kev transition observed in our study and the latter transition is therefore assigned as transition BA.

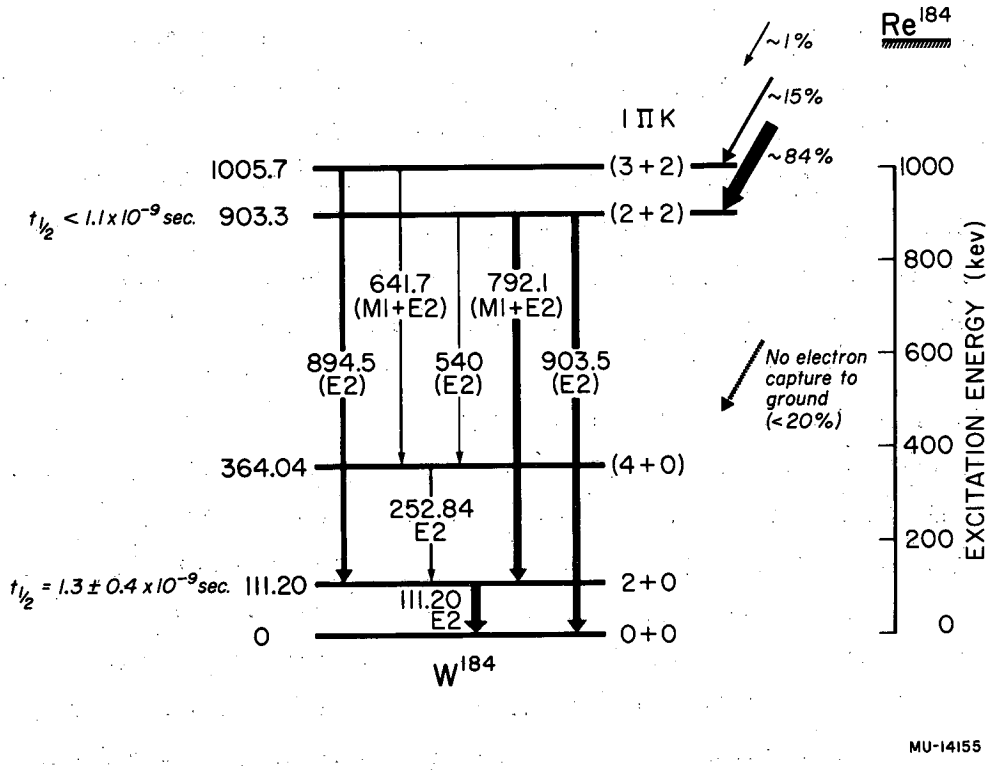

Fig. 12. Partial decay scheme of Re^{184} and some of the levels of W^{184}.

The coincidence data of Table XV show that most of the ~900-kev transitions are in coincidence with K x-rays. Therefore, the 903.5-kev transition is placed to decay into the ground level (A), establishing level D. Strong ~790- 110 coincidences were also observed, and the sum, 792.1 + 111.2 = 903.3, is equal to transition energy DA within the energy uncertainty of 0.1%, thus, further supporting level D.

The coincidence data show that about 20% of the 900-kev photons are in coincidence with 111.20-kev transitions. The strong 894.5-kev transition is therefore placed to establish level E. It can then be seen that the sum, 252.8 + 641.7 = 894.5, is equal to transition EB. Because the 252.84-kev transition is in excellent agreement with the expected 4+ ⟶ 2+ rotational spacing, the 252.84-kev transition is placed to establish level C.

Although our coincidence data indicate that the complexity of the W^{184} level scheme is considerably greater than is shown in Fig. 12, we have not been able to establish the energies of the other levels uniquely, so that we do not include them in Fig. 12.

We believe that because there is a possibility that the high-energy W^{184}-level spectrum may be as complex as that of W^{182} populated by Ta^{182} decay, the final analysis of these high-energy states must await further high-resolution studies with more intense sources.

It is interesting to note that the levels of W^{184} have also been studied from Ta^{184} decay by Butement and Poë.[66] In this study 110-, 160-, 210-, 240-, 300-, 405-, 780-, 890-, and 1180-kev photons were reported with relative intensities 3, 1, 1, 6, 3.5, 10, 1.7, 9, and 5. Because the resolution of the photon energies is insufficient to define the energies of the states with the precision that the studies of the levels of W^{182} now indicate is necessary at this excitation energy, we have deferred any attempt to analyze these data until more high-resolution spectroscopy has been performed on Ta^{184} decay.

Primary population and log ft values. The most striking feature of Re^{184} decay, as it was in 12.7-hr Re^{182} decay, is that apparently the total primary electron-capture decay occurs to a group of levels around 1 Mev. Such behavior is difficult to explain on the basis of the single-particle model because the spins are similar to spins of states much lower in energy, but can perhaps be understood in terms of the K forbiddenness predicted by the unified model.[46] In order to obtain an idea of the strength of the K forbiddennes , we calculated a lower limit of the log ft value to state A. From our absolute upper limit of 20% decay to ground, and assuming a 1300-kev decay energy and an L_I/K ratio of 0.13, we calculated a log ft value of ≥ 8.7, compared to the usually observed log ft of 7.5 for a first-forbidden transition. This indicates a hindrance of at least 20 for the decay.

The reported primary branching, 84% to level D, 15% to level E, was deduced from the ratio of the total intensity of the high-energy transitions to the observed K x-ray intensity reported in Table XIV.

Level D was assigned a spin of 2 because it decays to levels A, B, and C. Level E is assigned spin 3 because it decays to B and C, but not to A. The states have been assigned positive parity because the normalized absolute conversion coefficients discussed previously are consistent with E2 and M1-E2 multipolarities. No normalization other than that used leads to results that are consistent with all of the data.

The branching ratios from, and energies of, states E and D provided a check on the applicability the wave functions of the unified model to the high-energy states through comparison of the experimental and theoretical reduced transition probabilities. In Table XVI these data are compared. The agreement of the experimental and theoretical values for the ratios DB/DA and DC/DA supports our assignment of spin 2 to this level; while EC/EB is in reasonable agreement with the theoretical value assuming E has spin 3, and suggests that K is a good quantum number for these states. The experimental reduced transition probabilities DB/DA and EC/EB do not agree as well as DC/DA but are estimated to be within experimental error of the theoretical values. We assumed that all the

Table XVI

Comparison of experimental- and theoretical-reduced transition probabilities for E2 de-excitation of the high-energy states of W^{184}. All transitions were assumed to be pure E2.

K,π	Transitions compared	Reduced transition probability calculated	Theoretical	Experimental
2,+	DB/DA	$\frac{B(E2\ 2,2\text{--}2,0)}{B(E2\ 2,2\text{--}0,0)}$	1.43	1.72
2,+	DC/DA	$\frac{B(E2\ 2,2\text{--}4,0)}{B(E2\ 2,2\text{--}0,0)}$	0.072	0.08
2,+	EC/EB	$\frac{B(E2\ 3,2\text{--}4,0)}{B(E2\ 3,2\text{--}2,0)}$	0.40	0.28

transitions were pure E2; the absolute conversion coefficient for DB suggests it has some M1 mixing, which would tend to reduce the experimental ratio DB/DA in Table XVI. EC and EB probably also have some M1 mixing; we have not attempted to determine these mixing ratios because the uncertainties in the intensities are too large to make such a calculation meaningful.

From the observed primary decay of Re^{184} to 2+ and 3+ states and not to ground, it is possible that Re^{184} has a spin of 2 or 3. Because the log ft to state D, calculated assuming a decay energy of 600 kev to this state, is ~ 7.5, decay is probably first-forbidden, suggesting negative parity for this state. On the basis of calculations which will be discussed in Section IV, we assign a spin 3 to Re^{184}. From these latter calculations we obtain log ft values of 7.1 and 7.5 to states D and E, respectively, and a total electron-capture decay energy of 1325 kev.

General Discussion

It is interesting to note that the moment of inertia calculated from spacing DE is about 10% greater than the ground-state-band moment of inertia. This result is to be compared with the analogous moment of inertia in W^{182}, which is 10% smaller than that of the W^{182} ground state. We do not believe it is possible from data now known to determine the cause of this change, but it is possible that such an effect results from the perturbation of the even spin levels of the K = 2,+ band by the as yet unobserved states of a near-lying β-vibrational band. These states, because they have the same intrinsic nucleonic wave functions can couple through the U_2 interaction described by Bohr. (cf. Ref. 4, Ch. V, p. 35.) Only even spin states can couple because the symmetry of the wave functions prevents the appearance of odd-spin states in a beta-vibrational band.

The results of the present study on the levels of W^{182} and W^{184} can be compared with the energies of levels in W^{186}. Unfortunately, only the energy of the 2+, 0 state (I π, K notation) in W^{186} has been determined.[67,68] In Fig. 13 we compare the experimental data for the energies

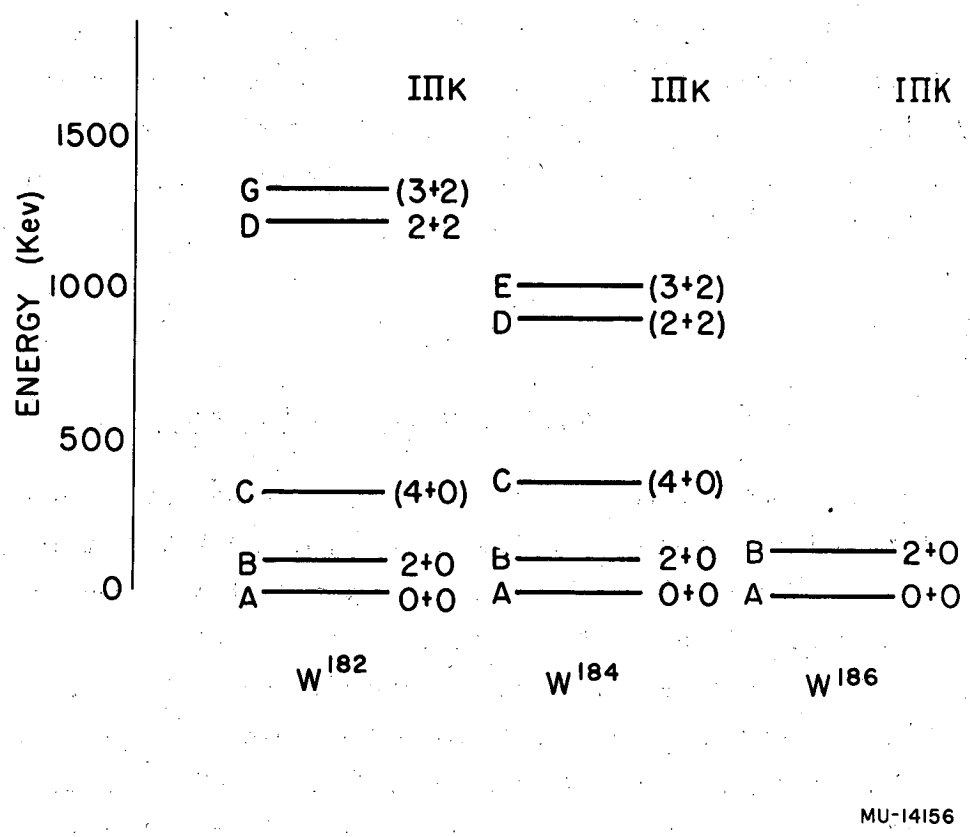

Fig. 13. Comparison of the energies of analogous states in even-even tungsten nuclei.

of analogous levels in the even-even tungsten nuclei. It can be seen immediately that a striking trend exists. In Table XVII we compare the inertial constants calculated from these data. The results show that the energies of the 2+ states manifest a marked dependence on the mass number. The increased vibration-rotation interaction also shows this dependence. Such results probably indicate an increased "softening" of the nuclear potential toward shape vibrations as the nuclei move out of the mass region of stable spheroidal deformation. Although the energy of the 2+,2 state in W^{186} is not known, the increase in energy of the 2+,0 state between W^{186} and W^{184} indicates an even larger vibration-rotation interaction in W^{186} than in W^{184} or W^{182}. Such a result indicates that the second 2+ state in W^{186} is probably lower in energy than that in W^{184}.

F. K-Auger Electrons of Tungsten

The study of the electron spectrum of the electron-capturing rhenium isotopes provided an excellent opportunity to obtain intensities and energies of many of the K-Auger electron lines of tungsten. These data are listed in Table XVIII.

The data have been used to test the conclusions of Bergström and Hill[69] regarding the calculation of energies of KL_pL_q-Auger lines. From these energies we calculated a "ΔZ" for each transition. These are in very good agreement with the ΔZ's proposed by Bergström and Hill.[69] These energy data have previously been reported by TRGSH.[41]

In Table XVIII we also list intensities for the KL_pL_q-Auger electrons, again from the two samples. The method of relating intensities to photographic blackening has been described by Mladjenović and Slätis.[17] The uncertainty in the intensities is about 20%.

In a treatment similar to that employed for the KL_pL_q-Auger lines, the energy, ΔZ, and intensity of the KL_pM_q-Auger lines observed are reported in Table XIX. Because of the smaller energy difference

Table XVII

Inertial constants[a] for the levels of even-even tungsten nuclei

Nucleus	C (kev)	C' (kev)	D (kev)
W^{182}	16.68	16.77	0.0153
W^{184}	18.53	18.68	0.0237
W^{186}	20.5		

a. The inertial constants are defined by the relationships:

1. $E_I - E_{I_o} = C\ \{I(I+1) - I_o(I_o+1)\}$
2. $E_I - E_{I_o} = C'\ \{I(I+1) - I_o(I_o+1)\} - D\ \{I^2(I+1)^2 - I_o^2(I_o+1)^2\}$ where E_I is the energy of the rotational state with spin I.

Table XVIII

Energies and intensities of KL_pL_q - Auger electrons of tungsten. The lines observed on plate 1 were mainly from Re^{183} decay; those on plate 2 from Re^{182} decay. The uncertainties in ΔZ are set by those of E_e.

Auger Electron	Relative intensities Plate 1	Plate 2	Average	Plate 1 Energy	ΔZ	Plate 2 Energy	ΔZ	Average ΔZ
KL_IL_I	1.4±0.3	1.3±0.3	1.3±0.2	45.09±0.05	0.57±0.12	45.07±0.05	0.61±0.14	0.59±0.09
KL_IL_{II}	-----	2.7±0.5	2.7±0.5	45.91±0.05[a]	-----	45.63±0.05	0.60±0.14	0.60±0.14
KL_IL_{III}	0.9±0.2	2.3±0.5[b]	0.9±0.2	46.93±0.05	0.88±0.14	46.97±0.05	0.76±0.14	0.82±0.10
$KL_{II}L_{II}$	Not seen							
$KL_{II}L_{III}$	2.3±0.5	2.6±0.5	2.5±0.4	47.50±0.05	0.82±0.14	47.51±0.05	0.79±0.14	0.80±0.10
$KL_{III}L_{III}$	1.0[c]	1.0[c]	1.0	48.86±0.05	0.76±0.14	48.85±0.05	0.79±0.14	0.78±0.10

a. KL_IL_{II}, N_I 46.48 superimposed. (Re^{183} exposure)

b. KL_IL_{III}, K 116.40 superimposed. (Re^{182} exposure)

c. Value used for normalization.

Table XIX

Energies and intensities of the KL_pM_q - and KL_pN_q -Auger electrons of tungsten. The limits of error of ΔZ correspond to the limits of error on the electron energies. The intensities are normalized relative to value of 1 for the intensity of the $KL_{III}L_{III}$ intensity in Table XVIII.

Auger electron	Intensity	Electron energy	ΔZ	E_e calculated assuming $\Delta Z=1$
KL_IM_I	0.6±0.2	54.51±0.05	0.83±0.41	54.49
KL_IM_{II}	0.5±0.2	54.74±0.05	1.09±0.45	54.75
KL_IM_{III}	0.6±0.2	55.03±0.05		55.06
$KL_{II}M_I$			1.07±0.41	55.04
$KL_{II}M_{III}$	0.3±0.1	55.53±0.05	1.89±0.55	55.61
$KL_{III}M_I$	0.5±0.2	56.37±0.05	1.08±0.41	56.38
$KL_{III}M_{II}$	0.7±0.3	56.64±0.05	0.91±0.45	56.63
$KL_{III}M_{III}$ [a]	0.9±0.3	56.96±0.05	0.89±0.55	56.95
KL_IN_I-N_{III} [a]			-----	-----
$KL_{II}N_I$-N_{III}	0.5±0.2	57.43±0.05	-----	-----
$KL_{III}N_I$-N_{III}	0.2±0.1	58.82±0.05	-----	-----
KMM-N	weak bands			
KNN	weak bands			

a. $KL_{III}M_{III}$, KL_1N's superimposed.

between the M_q shells relative to that between the L_q shells, the limits of error on ΔZ corresponding to the same energy uncertainty are much larger. We do not report a ΔZ for the KL_pN_q-Auger lines in Table XIX because the energy difference is less than the energy uncertainty. The intensity uncertainties are also larger in these cases because the lines are very close-lying, making accurate analyses difficult. Very weak bands corresponding to the KMM- and KNN-Auger lines were also observed, but the energy uncertainty was too great to permit any interpretation of the data.

It is interesting to note that the over-all trend indicates ΔZ tends to approach one as the binding energy of the third electron decreases.

IV. An Extension of the Predictions of the Unified Model to the Determination of Electron-Capture Decay Energies

Theory

In the regions of the periodic table where orbital-electron capture is an important mode of decay for beta-unstable nuclides, it has not been possible in many cases to determine the energy differences between the ground states of neutron-deficient isobars. Such information is important, however, in many calculations.

The methods of determination of electron-capture decay energies - mass measurements, "closed cycles", internal bremsstrahlung spectra, and L_I/K-capture ratios - have experimental drawbacks. Mass measurements are not sufficiently sensitive in the heavy-mass region, closed cycles can be used only where alpha-emitting isotopes exist, and internal bremsstrahlung is easily masked by high-energy transitions. L_I/K-capture ratios are difficult to measure for all but the simplest decay schemes, and because they are so extremely energy-dependent, are essentially limited in application to cases where a single energy level is populated by a very low-energy electron-capture transition.

The predictions of the Bohr-Mottelson unified model[4,5] regarding the beta-decay transition probabilities to states of a rotational band provide a fifth method for the determination of electron-capture decay energies. This method utilizes only the measurement of direct primary branching to a number of rotational states, and hence is a measurement that is usually made in spectroscopic studies. This relationship can be seen from consideration of the expression (cf. Ref. 46, Eq. 12) for the beta-transition probabilities to two rotational states of the same band from a given initial state:

$$\frac{\log \underline{ft}\ (A \longrightarrow X)}{\log \underline{ft}\ (A \longrightarrow Y)} = \frac{\left\langle I_A\ L\ K_A\ K_B\text{-}K_A \mid I_A\ L\ I_Y\ K_B \right\rangle^2}{\left\langle I_A\ L\ K_A\ K_B\text{-}K_A \mid I_A\ L\ I_X\ K_B \right\rangle^2}\ , \qquad (1)$$

where $K_X = K_Y = K_B$ is the K quantum number of the final state,

K_A is the K quantum number of the initial state,

I_n is the spin of state n (n = A, X, Y),

and

L is the vector change in angular momentum between initial and final states.

The right-hand side of the equation is seen to be dependent only on the spins and K-quantum numbers of the initial and final states, and the vector change in angular momentum between them.

The comparative lifetimes of the left-hand side of Equation (1) have an implicit energy dependence through the expressions for K-capture to state A:

$$\left(f_K \; t_K\right)_A = \frac{\pi}{2} \; g_K^2 \; q_{KA}^2 \cdot t_{KA}, \tag{2}$$

$$t_{KA} = \frac{T_{1/2}\,(\text{exp.})}{\left(\dfrac{K + L_I}{K}\right)_A \cdot \left(\begin{array}{l}\text{exp. branching}\\ \text{to state A}\end{array}\right)} \tag{3}$$

$$\left(\frac{K + L_I}{K}\right)_A = 1 + \frac{g_{L_I}^2 \; q_{L_I A}^2}{g_K^2 \; q_{KA}^2}, \tag{4}$$

where g is the value of the large component of the radial Dirac-electron wave functions evaluated at the nuclear surface,

and q_X is the neutrino energy in units of m_0c^2 for X-shell capture.

Expressions (2) and (4) have been shown to be valid for allowed and first-forbidden, non-unique electron-capture transitions by Hoff and Rasmussen.[70] The reasons for neglecting all modes of electron capture except L_I and K capture have been discussed by Brysk and Rose.[34]

It is implicit in these expressions that the beta-decay selection rules proposed by Alaga[40] are valid. Such an assumption implies that in the case of allowed and first-forbidden transitions, only the operators that change K by ± 1 contribute to the transition probability. The relaxation of these rules would introduce additional terms with cross

products in Expression (1) and the matrix elements would no longer cancel. The method would then have no use to the experimentalist because the number of parameters would be larger than the number of experimental measurements that could be made.

Since it is inherently based on the energy dependence of L_I/K-capture ratios, this method is applicable largely to cases where the decay energy to a given rotational band is small. Because of its model dependence, it can also only be applied in regions where K is a good quantum number. However, in these regions and especially for odd-odd nuclei, this method should be applicable because, as has been shown for example in this study, the electron-capture decay of odd-odd nuclei populates high-energy states in even-even nuclei, many of which appear to have the characteristics of rotational states. Because of the limited amount of high-resolution data now available on the decay of neutron-deficient isotopes to a series of rotational states, we shall only attempt to apply the method to the decay of odd-odd isotopes that we have studied.

The ideal nucleus for the testing of this method would be one which has an observed positron group. Unfortunately, the decay scheme of such a nucleus has not yet been studied with sufficient resolution to give any confidence in the results obtained. We can, however, test the method to see whether it yields results that are consistent with the experimental measurements made in this study.

Application to Re^{184} and 12.7-hr Re^{182}

Of the nuclei studied, the two Re^{182} isotopes and Re^{184} are the most carefully worked out. The 60-hr Re^{182} is not at present a good choice because of its complexity. The 12.7-hr Re^{182} and 50-day Re^{184} are simpler and seem the logical choices to use. Of these, Re^{184} is definitely the better, because the decay occurs predominantly to only two states, when then decay to the ground-state band, allowing a determination of both the primary population and permitting a check on the "goodness" of the K-quantum number of the states.

The decay of Re^{184} populates two states that (cf. Part III, Sec. E) have been assigned spins of 2 and 3. The reduced transition probabilities from these states to the lowest three members of the ground-state rotational band support the assignment of K = 2 to these bands. The spin of 50-day Re^{184} deduced from these data is 2 or 3. We calculated the theoretical values of the ratio for branching from states with I = K = 2 and I = K = 3 to states with I = 2 and 3, K = 2, which are 2.00 and 2.85, respectively. Using the curves of Brysk and Rose[34] to determine the necessary parameters, we calculated the values of the decay energy that gave best agreement between the observed data and the theoretical values for a Re^{184} spin of 2 and 3. The decay energies calculated are, respectively, 320 and 420 kev to state D. We can rule out the first possibility because a 330-kev transition is observed in coincidence with an ~900-kev transition. The values of log ft calculated for decay to states D and E are 7.1 and 7.5, respectively. It thus seems that the experimental data are in best agreement with a 3- state assignment and a total electron-capture decay energy of 1325 kev for Re^{184}.

It should be pointed out that in the calculations of log ft values, only a vector-like beta-decay operator corresponding to an angular momentum of 1 unit has been considered, whereas a tensor term that has 2 units of angular momentum should also be included. However, because these latter operators are known to result ($\Delta I = 2$, yes, beta decay) in log ft values of ~ 8.5, and because the log ft to state D is about 7.1, we believe that we are just on the borderline of the region where we can neglect the tensor term.

The 12.7-hr Re^{182} would provide a better test than Re^{184} if the transition intensities were more accurately established than from electron data alone. This test is a consequence of the fact that Re^{182} populates three rotational states with I = 2, 3, and 4 of a K = 2,- rotational band with the absolute branching percentages of 35%, 29%, and 6%, respectively. The theoretical ratios (compared to the I = 2 state) are 1:2.85:20. It is immediately clear from the branching percentages that even at infinite decay energies the observed primary

branching will not match the theoretical values, but will attain the ratio 1:1.2:5.8, whereas for smaller decay energies the ratio will change so as to lower the ratios to the I = 2 and I = 3 states. The disagreement between theory and experiment suggests that more precise studies should be made on the primary branching of 12.7-hr Re^{182}.

Although the present data are inconclusive regarding the general applicability of the method, the consistency of the data in the case of Re^{184} suggests that the method is applicable. It is hoped that the rapid increase in the number of experimental studies on nuclear energy levels and the increased refinement of the techniques and data will soon provide further tests of the method.

ACKNOWLEDGMENTS

I wish to express my sincere pleasure in having had the opportunity to work with Prof. J. O. Rasmussen, Jr., whose continual encouragement and invigorating outlook have been a major factor in helping me to complete this study.

The continued interest of Profs. Glenn T. Seaborg and Isadore Perlman is gratefully acknowledged.

I appreciate the assistance of Dr. J. M. Hollander in many aspects of the permanent-magnet studies.

I would like to acknowledge helpful discussions with Drs. Donald Strominger, Frank Stephens, and Frank Asaro regarding many nuclear spectroscopic techniques.

The assistance of Dr. Sigvard Thulin, Mrs. V. S. Shirley, and Mr. John Unik in the preparation of some of the sources used in these studies is greatly appreciated.

The crew of the Berkeley 60-inch cyclotron has been most helpful and able in carrying out the bombardments in which the sources were prepared.

The Health Chemistry group, especially Mrs. Roberta Delke, were a very great help in minimizing the radioactive hazard that my very "hot" targets and sources presented.

And, with a few less misconceptions than I previously had, I acknowledge elucidating discussions with Prof. Frederic L. Canavan, S.J., and Mr. Marshall Lombardo on the philosophical aspects of natural philosophy.

This work was done under the auspices of the United States Atomic Energy Commission.

Appendix A. Chemical Procedures

Chemistry A

The method described below is due to Giles, Garrison, and Hamilton.[71] We described it here mainly to point out details that proved to be troublesome during the study. The procedure is as follows:

1. Dissolve the tantalum target in a conc. HF-conc. HNO_3 mixture in a platinum crucible.

   NOTE: High concentrations of HF, relative to HNO_3, proved to dissolve the foils most rapidly, but introduced excess fluoride that interfered later in the chemistry unless special effort was made to destroy the HF.

2. After the tantalum dissolves, continue heating the solution — with frequent addition of HNO_3 — to destroy the HF. After the HF is destroyed, Ta_2O_5 will begin to precipitate.

   NOTE: Heat only gently, as Re_2O_7 is volatile.

3. When the Ta_2O_5 begins to precipitate in the crucible, transfer the activity to a 50-cc centrifuge cone, and digest in a water bath until the Ta_2O_5 has completely precipitated.

   NOTE: Complete precipitation can be estimated from the volume of Ta_2O_5 formed. A blank foil can be used to determine the expected volume. It is very important to remove the Ta_2O_5 here.

4. After complete precipitation of Ta_2O_5 has occurred, centrifuge the Ta_2O_5 and discard the centrifugate. The volume should be about 5 cc.

5. Take up the 5 cc in about 15 cc of 36 N H_2SO_4 and transfer the solution to the distillation assembly.

6. CO_2 gas is passed through the distilling flask as the carrier gas. When the solution has been heated to 240°C, add conc. HBr dropwise. The rhenium volatilizes, probably as an oxybromide, and is collected in 10 cc of 16 N HNO_3 at 0°C.

NOTE: Ordinarily, if the distillation is carried out over a 15 to 20 min interval, about 1 cc of H_2SO_4 distills along with the activity. This introduces a volume problem later. To avoid this, heat the solution rapidly to 240°C and stabilize as quickly as possible. Then distill for about 5 min, during which time the major fraction of the rhenium activity distills. If this is done, very little H_2SO_4 is carried by the distillate, and very high specific activities can be obtained.

7. The collecting tube containing 10 cc of conc. HNO_3 is reduced to dryness (if no H_2SO_4 is present) on a water bath. If H_2SO_4 is present, the volume can only be reduced to that of the H_2SO_4.

NOTE: During the distillation process some of the HBr is carried by the CO_2 and oxidized to Br_2 in the HNO_3, collecting as a black, organic-looking substance on the bottom of the collecting tube. This is easily removed by heating during the evaporation of HNO_3, but a strong jet of air must be kept directly on the surface of the HNO_3, as otherwise the Br_2 evaporates in very large and explosive bubbles.

8. When the solution has been reduced to dryness, the activity is taken up in a minimum volume of NH_4HSO_4 solution (pH = 2).

NOTE: The volume is dependent on the number of sources that are needed. We assumed ~0.500 cc/ source.

8a. If H_2SO_4 distilled, reduce the volume to the volume of H_2SO_4 and cool to 0°C. Add 6 N NH_4OH dropwise with continuous agitation until the solution ceases to boil on addition of NH_4OH. Adjust to pH = 2, using thymol blue as an indicator (red-yellow change).

Chemistry B

The solution of rhenium activity in NH_4HSO_4 solution obtained in Chemistry A remaining after the sources had been prepared was allowed to stand until all the Re^{181} had decayed. Then 100 mg of tungsten, as $WO_4^{=}$, was added to about 5 cc of the solution in a 50-cc centrifuge cone. Ten cc of 6 N HNO_3 were added and the solution was digested for approximately 30-min. The WO_3 that precipitated was centrifuged, and the supernatant containing the rhenium activity was discarded. The WO_3 was dissolved in a minimum volume of 6 N NH_4OH, and reprecipitated by the addition of 6 N HNO_3. This purification was repeated several times, and WO_3 was finally precipitated free from rhenium activities. The WO_3 was slurried onto a counting plate and dried. Because it was to be used for gamma analysis, the sample was covered with "Scotch" tape to prevent the contamination of the gamma analyzer.

Chemistry C

Chemistry C is an adaption of the rhenium chemistry proposed by Meinke.[72]

A tantalum foil that had been bombarded with alpha particles was dissolved in a mixture of conc- HF and conc. HNO_3 in a platinum crucible. The solution was heated gently after the foil had dissolved completely to drive off the HF. After the HF was destroyed, the solution was transferred to a glass centrifuge cone and ~0.5 mg of rhenium carrier, as ReO_4^-, was added. Ten cc of 8 N HCl were then added, and ~1 cc of 10% $S_2O_3^{=}$ was added to precipitate Re_2S_7. The Re_2S_7 was washed twice with ~10 cc of 1 N HCl, then was slurried onto a counting plate and dried. The sample was covered with "Scotch" tape as above.

Chemistry D

The separation of carrier-free rhenium from the massive quantities of tungsten from the thick tungsten foils bombarded required a simple, but tedious, chemistry. This was necessary rather than Chemistry A because the efficiency of the rhenium distillation appears to be quite low (although an accurate study was not made to determine the efficiency). The foils, which had been bombarded with deuterons, were dissolved in a mixture of conc. HF and conc. HNO_3 in a platinum crucible. The solution was heated gently to destroy the HF and the massive amounts of tungsten were removed by repeated precipitations of WO_3 from the nitric acid solution. The rhenium activity stayed in solution, probably as the ReO_4^-, but some was carried down by the WO_3. To achieve greater yield, by freeing some of the ReO_4^- from the precipitated WO_3, the WO_3 was dissolved in 6 N NH_4OH, and reprecipitated in 6 N HNO_3. This was repeated twice, which roughly doubled the yield obtained. The ReO_4^- was eventually isolated in about 50 cc of solution containing milligram quantities of tungsten. Chemistry E was employed to complete the separation.

Chemistry E

To separate the rhenium activity from the tungsten remaining in solution, the chemistry proposed by Huffman *et al.*[73] was followed. This chemistry proved very successful, as specified, and so will not be discussed here.

Appendix B-1.

Electron lines observed in the decay of the short-lived rhenium isotopes in order of increasing energy.

Electron Energy (kev)	Magnetic Rigidity (gauss-cm)	Visual Intensity	Assignment Shell	Assignment Eγ (kev)	Isotope
15.15	418.11	m	K	84.67	182
15.22	419.30				
17.04	443.84	w	M_I	19.86	182
17.30	447.23	w	M_{II}	19.86	182
19.39	474.00	ew?	N_{II}	19.86	182
19.59	476.50	ew?	N_{III}	19.86	182
27.00	561.36	m	L_I	39.10	182
27.54	567.13	ew	L_{II}	39.10	182
30.58	598.43	s	K	100.09	182
34.39	635.77	s	L_I	46.48	183
34.96	641.19	mw	L_{II}	46.48	183
35.29	644.33	w	L_I	47.38	181
36.30	653.73	mw	L_{III}	46.48	183
36.54	655.97	ew(d)	M_I-M_{II}	39.10	182
37.62	665.99	m	K	107.13	182
38.48	673.78	m	K	107.93	183
39.05	679.20	m	K	108.57	182
40.32	690.35	m	K	109.73	183
40.49	691.86	m	L_I	52.59	183
40.82	694.78	ew	L_I	52.96	182
43.67	719.57	m	M_I	46.48	183
44.03	723.64	s	K	113.66	182
45.07	731.50	m	KL_IL_I	Auger	
45.63	736.22	m	KL_IL_{II}	Auger	
45.89	738.40	w	N_I	46.48	183
46.97	747.42	m	KL_IL_{III}	Auger	
47.54	752.18	m	$KL_{II}L_{III}$	Auger	
48.42	759.38	w	L_I	60.51	182
48.85	762.90	w	$KL_{III}L_{III}$	Auger	
49.71	769.94	ew	M_I	52.59	183
50.17	773.61	w	M_I	52.96	183
51.41	783.58	ew	K	120.94	182
51.96	787.95	ew	N_I	52.59	183
53.04	796.46	ew	K	122.55	181
53.63	801.16	s	L_I	65.71	182
54.19	805.48	w	L_{II}	65.71	182
54.49	807.85	ew	KL_IM_I	Auger	
54.99	811.64	ew	KLM	Auger	
55.64	816.80	m	L_I	67.74	182
56.20	821.08	w(d)?	L_{II}	67.74	182
56.64	824.45	ew	L_{II}	68.10	182
56.96	826.88	ew	KL_IN	Auger	
57.55	831.42	mw	L_{III}	67.74	182
58.86	841.32	ew?	$KL_{III}N$	Auger	
61.29	859.49	vs	K	130.76	182
61.78	863.13	ew	K	131.30	182
62.28	866.81	ew	L_I	74.41	182
62.88	871.80	m	M_I	65.71	182
63.14	873.10	ew	M_{II}	65.71	182
63.46	875.41	ew	M_{III}	65.71	182
64.25	881.21	s	K	133.78	182
64.93	886.10	w	M_I	67.74	182
65.14	887.63	w	M_{II}	67.74	182
65.47	890.06	ew	M_{III}	67.74	182
66.28	895.85	ew	KMN	Auger	
67.15	902.06	ew	N_I	67.74	182
72.59	940.25	s	L_I	84.67	182
73.14	944.04	m	L_{II}	84.67	182
74.47	953.18	m	L_{III}	84.67	182
74.86	955.82	ew	L_{II}	86.40	(182)?
76.16	964.65	ew(d)	L_{III}	86.40	(182)?
78.16	978.08	m	K	147.68	182
79.36	986.13	s	K	148.81	182
79.92	989.85	m	K	149.39	182
81.68	1001.5	vw	K	151.19	182
81.92	1003.1	m(d)	M_I	84.67	182
82.15	1004.6	ew	M_{II}	84.67	182
82.47	1006.7	ew	M_{III}	84.67	182
82.91	1009.6	m	K	152.41	182
84.14	1017.6	w(d)	N_I	84.67	182
84.58	1020.4	ew	O_I	84.67	182
86.86	1035.2	m	K	156.37	182
87.49	1039.2	m	L_{II}	99.07	183
88.00	1042.5	m	L_I	100.09	182
88.58	1046.2	vs	L_{II}	100.09	182
89.89	1054.5	vs	L_{III}	100.09	182
90.53	1058.6	w	K	160.09	182
91.10	1062.2	ew	L_I	103.13	(181)
91.59	1065.3	ew	L_{II}	103.13	(181)
92.69	1072.2	s	K	162.33	183

Appendix B-1 (cont.)

Electron Energy (kev)	Magnetic Rigidity (gauss-cm)	Visual Intensity	Assignment Shell	Eγ (kev)	Isotope
93.03	1074.3	ew	L_{III}	103.13	(181)
95.04	1086.8	wm	L_I	107.13	182
95.60	1090.3	wm	L_{II}	107.13	182
96.49	1095.8	wm	L_I	108.57	182
96.93	1098.5	wm	L_{III}	107.13	182
97.51	1102.1	s	M_{II}	100.09	182
97.82	1104.0	s	M_{III}	100.09	182
99.67	1115.3	vs	K	169.18	182
100.07	1117.7	vw	$O_{II}O_{III}$	100.09	182
101.56	1126.8	m	L_I	113.66	182
102.12	1130.1	w	L_{II}	113.66	182
103.39	1137.8	ms	K	172.78	182
104.39	1143.8	ew	M_I	107.13	182
104.86	1146.6	ew	M_{III}	107.13	182
105.80	1152.2	ew(d)	M_I	108.57	182
106.70	1157.6	ew(d)	N_{III}	107.13	182
107.44	1162.0	ew	M_{III}	109.73	183
108.01	1165.4	ew	N_I	108.57	182
108.99	1171.1	ew	L_I	120.94	182
109.85	1176.2	m	K	179.36	182
110.89	1182.3	vvw	M_I	113.66	182
111.52	1186.0	ew(d)	M_{III}	113.66	182
112.12	1189.4	ew	K	181.63	182
113.14	1195.4	vw	N_I	113.66	182
113.26	1196.1	ew(d)	N_{III}	113.66	182
118.63	1227.0	ms	L_I	130.76	182
119.21	1230.3	w	L_{II}	130.76	182
119.97	1234.6	w	K	189.48	182
120.61	1238.3	w	L_{III}	113.66	182
121.80	1245.0	s	K	191.31	182
127.99	1279.3	vvw	M_I	130.76	182
128.80	1284.2	wm	K	198.31	182
130.17	1291.8	vw	N_I	130.76	182
131.03	1296.5	vw	M_I	133.78	182
135.59	1321.5	ew	L_I	147.68	182
135.94	1323.5	ew	L_{II}	147.68	182
136.67	1327.4	w	L_I	148.81	182
137.27	1330.6	w	L_I	149.39	182
138.57	1338.2	w	K	208.18	182
139.19	1341.0	w	K	208.81	183
139.82	1344.4	vw	K	209.33	182
140.28	1346.5	ew	L_I	152.41	182
144.18	1367.8	vw	L_I	156.37	182
144.83	1371.2	w	K	214.41	182
146.18	1378.4	vw	K	215.69	182
148.09	1388.5	vw	L_I	160.09	182
150.25	1399.9	w	L_I	162.33	183
150.76	1402.6	vw	L_{II}	162.33	183
152.09	1409.5	w	K	221.60	182
152.54	1411.9	vw	K	222.05	182
156.57	1432.9	m	K	226.10	182
156.96	1435.2	m	L_I	169.18	182
157.50	1437.7	vvw	L_{II}	169.18	182
159.76	1449.4	ms	K	229.27	182
160.69	1454.2	vw	L_I	172.78	182
161.23	1456.95	vvw	L_{II}	172.78	182
166.36	1483.1	w	M_I	169.18	182
167.25	1487.7	vw	L_I	179.36	182
167.78	1490.3	ew	L_{II}	179.36	182
168.54	1494.2	ew	N_I	169.18	182
169.18	1497.4	vvw	L_{III}	179.36	182
170.07	1501.9	vvw	M_I	172.78	182
172.46	1513.9	ew(d)	N's	172.78	182
176.57	1534.5	vvw	M_I	179.36	182
177.92	1541.2	mw	K	247.43	182
179.31	1548.1	mw	L_I	191.31	182
182.59	1564.4	ew	?		181
183.89	1570.8	ew	K?	252.4	181
186.34	1582.8	ew	L_I	198.31	182
186.87	1585.4	ms	K	256.37	182
187.44	1588.2	ew	L_{II}?	198.31	182
187.98	1591.8	ew	L_{III}	198.31	182
188.59	1593.8	ew	M_I	191.31	182
190.93	1605.3	ew	?	?	?
194.58	1622.9	vw	K	264.09	182
195.77	1628.7	ew	M_{II}	198.31	182
195.95	1629.6	ew	M_{III}	198.31	182
196.05	1630.0	ew	L_I	208.18	182
197.56	1637.8	ew	L's	208.81	183
202.55	1661.3	ew(d)	L_I?	214.41	182

Appendix B-1 (cont.)

Electron Energy (kev)	Magnetic Rigidity (gauss-cm)	Visual Intensity	Assignment Shell	Eγ (kev)	Isotope
204.17	1669.0	ew	L_{II}	215.69	182
205.33	1674.5	ew	L_{III}	215.69	182
206.78	1681.4	mw	K	276.30	182
209.88	1696.1	ew	L_I	222.05	182
211.37	1703.1	ew(d)	M_I	214.41	182
211.96	1705.9	vw	K	281.42	182
214.0[illegible]	1715.8	vvw	L_I	226.10	182
217.02	1729.7	m	K	286.52	182
217.73	1733.0	m	L_{II}	229.27	182
219.07	1739.3	mw	L_{III}	229.27	182
223.27	1758.8	ew	M_I	226.10	182
226.70	1774.7	vw	M_{II}	229.27	182
227.00	1776.1	vw	M_{III}	229.27	182
228.85	1784.7	vvw	N's	229.27	182
230.37	1791.7	vvw	K	299.88	182
230.98	1794.4	vw	K	300.49	182
235.21	1813.9	vvw	L_I	247.43	182
235.90	1817.0	vvw	L_{II}	247.43	182
237.34	1823.6	vvw	L_{III}	247.43	182
240.85	1839.6	vvw(d)	L_{II}?	252.4	181
242.1	1845.4	ew(d)	L_{III}?	252.4	181
244.3	1855.3	w	L_I	256.37	182
244.9	1857.9	ew?	M_{II}	247.43	182
246.9	1867.1	ew	N's	247.43	182
249.3	1877.8	vvw(d)	K	318.8	181
252.55	1892.5	ew	L_{II}	264.09	182
253.43	1896.4	vvw	M_I	256.37	182
253.89	1898.5	vvw	L_{III}	264.09	182
262.7	1937.8	ew	K	332.2	181
263.96	1943.4	vvw	L_I	276.30	182
264.79	1947.1	vvw	L_{II}	276.30	182
266.15	1953.1	vvw	L_{III}	276.30	182
269.41	1967.5	w	K	338.98	182
269.93	1969.8	vvw	L_{II}	281.42	182
271.09	1974.9	vvw?	L_{III}	281.42	182
272.5	1981.1	vvw(d)	K?	342.0	181
273.9	1987.2	vvw?	M's	276.30	182
274.65	1990.6	vvw(d)	L_I	286.52	182
274.98	1992.0	vvw?	L_{II}	286.52	182
276.30	1997.8	vvw?	L_{III}	286.52	182
278.78	2008.7	ew	M_{II}	281.42	182
281.51	2020.6	w	K	351.02	182
283.90	2031.0	vvw(d)	M_{II}	286.52	182
288.56	2051.3	ew(d)	L_{II}	299.88	182
289.83	2056.8	ew	L_{III}	299.88	182
291.44	2063.7	w	K	360.95	181
296.14	2084.1	s	K	365.50	181
327.0	2215.4	ew	L_I	338.98	182
328.9	2223.5	vvw(d)	L's	338.98	182
339.3	2267.6	vvw(d)	L's	351.02	182
348.7	2306.2	vvw	L_I	360.95	181
350.3	2312.8	ew?	L's	360.95	181
353.4	2325.6	mw	L_I	365.50	181
353.6	2326.4	vvw	Line Questionable		
354.0	2328.0	ew	L_{II}	365.50	181
355.2	2333.0	ew	L_{III}	365.50	181
362.8	2364.5	vw	M_I	365.50	181
364.9	2372.8	vvw(d)	N_I	365.50	181
372.4	2403.6	vvw	K	441.9	181
400.4	2517.3	ew	K	469.9	181
417.3	2585.0	ew	K	486.8	181
419.5	2594.0	ew	K	489.0	181
429.7	2634.4	ew	L_I	441.9	181
487.8	2862.7	ew?	K	557.3	181
569.8	3176.7	ew	K	638.3	181
825.2	4118	ew?	K	894.7	181
884.3	4330.8	ew	K	953.8	181,2?
1007.2	4768.5	ew	K	1076.7	182
1052.3	4928.3	w	K	1121.3	182
1088.5	5055.9	ew	K	1158.0	182
1119.8	5165.7	ew	K	1189.3	182
1152.3	5279.7	ew	K	1221.8	182
1162	5313.2	ew	K	1231.3	182

Appendix B-2, a-1.
Electron lines observed in the decay of the short-lived rhenium isotopes according to transition energy.
60-hr Re^{182} electron lines of transitions seen by MBMD.

Transition Energy (kev)	Electron Energy (E_e) (kev)	Assignment Shell	Eγ (calc. from E_e)	Visual Intensity	Multi-polarity	Comments
33.36						Not observed in Re^{182} decay.[a]
42.71						Not observed in Re^{182} decay.
65.71					M1+E2	
	53.62	L_I	65.71	s		
	54.17	L_{II}	65.71	w		
	55.65	L_{III}	65.85	m		L_{III} 65.71, L_I 67.74 superimposed.
	62.89	M_I	65.70	m		
	63.14	M_{II}	65.71	ew		
	63.46	M_{III}	65.73	ew		
	65.14	N_I	65.73	w		N_I 65.71, M_{II} 67.74 superimposed.
67.74					E1	
	55.64	L_I	67.74	m		L_I 67.74, L_{III} 65.71 superimposed.
	56.20	L_{II}	67.74	w		
	57.55	L_{III}	67.75	mw		
	64.93	M_I	67.74	w		
	65.14	M_{II}	67.71	w		M_{II} 67.74, N_I 65.71 superimposed.
	65.47	M_{III}	67.74	ew		
	67.15	N_I	67.74	ew		
84.67					M1+E2	
	15.15	K	84.66	m		
	72.58	L_I	84.69	s		
	73.13	L_{II}	84.67	m		
	74.47	L_{III}	84.67	m		
	81.92	M_I	84.73	m(d)		
	82.15	M_{II}	84.72	ew		
	82.47	M_{III}	84.74	ew		
	84.14	N_I	84.73	w(d)		
	84.58	O_I	84.67	ew(d)		
100.09					E2	
	30.58	K	100.09	s		The K 100.09 would mask the M_I 33.36, if this transition were present.
	88.00	L_I	100.09	m		
	88.56	L_{II}	100.10	vs		
	89.89	L_{III}	100.09	vs		
	97.51	M_{II}	100.08	s		
	97.82	M_{III}	100.09	s		
	99.67	$N_{II}N_{III}$	100.09	vs		$N_{II}N_{III}$ 100.09, K 169.18 superimposed.
	100.07	$O_{II}O_{III}$	100.14	vw		
113.66					M1+E2	
	44.15	K	113.66	s		
	101.56	L_I	113.65	m		
	102.12	L_{II}	113.65	w		

a. In this Appendix, Re^{182} refers to 60-hr Re^{182}.

Appendix B-2, a-1 (cont.)

Transition Energy (kev)	Electron Energy (E_e) (kev)	Assignment Shell	Eγ (calc. from E_e)	Visual Intensity	Multi-polarity	Comments
113.66 (cont.)						
	103.39	L_{III}	113.59	ms		L_{III} 113.66, K 172.78 superimposed.
	110.84	M_I	113.65	w		
	111.52	M_{III}	113.79	ew(d)		
	113.14	N_I	113.73	vw		
	113.26	N_{III}	113.68	ew(d)		
116.40					(M1+E2)?[a]	
	46.97	K	116.48	m		K 116.40, KL_IL_{III} superimposed.
		L_I				Masked by M's 107.13.
		L_{II}				
152.41					E1	
	82.90	K	152.41	m		
	140.28	L_I	152.37	ew		
156.37					E1	
	86.87	K	156.38	m		
	144.18	L_I	156.27	vw		
179.36					M1+E2	
	109.85	K	179.36	ms		
	167.23	L_I	179.32	vw		
	167.82	L_{II}	179.35	ew		
	169.14	L_{III}	179.34	ew		
	176.55	M_I	179.36	ew		
198.31					E2	
	128.80	K	198.31	wm		
	186.34	L_I	198.43	ew		
	186.87	L_{II}	198.41	ms		L_{II} 198.31, K 256.37 superimposed.
	187.98	L_{III}	198.18	ew		
	195.77	M_{II}	198.34	ew		
	195.95	M_{III}	198.24	ew(d)		
222.05					E1	
	152.54	K	222.05	vw		
	209.88	L_I	221.97	ew		
229.27					E2	
	159.76	K	229.27	ms		
	217.02	L_I	229.11	m		L_I 229.27, K 286.52 superimposed.
	217.73	L_{II}	229.27	w		
	219.09	L_{III}	229.29	w		
	226.70	M_{II}	229.27	vw		
	227.00	M_{III}	229.27	vw		
	228.85	$N_{II}N_{III}$	229.27	vvw		

a. In Appendix B this type of multipolarity designation will refer to "Second Confidence" multipolarities.

Appendix B-2, a-1 (cont.)

Transition Energy (kev)	Electron Energy (E_e) (kev)	Shell	Assignment Eγ (calc. from E_e)	Visual Intensity	Multi-polarity	Comments
264.09					E2	
	194.58	K	264.09	mw		
	252.55	L_{II}	264.09	ew		
	253.89	L_{III}	264.19	ew		
927						Not observed in Re^{182} decay.
960						Not observed in Re^{182} decay.
1003						Not observed in Re^{182} decay.
1121.6						
	1052.3	K	1121.8	vw	M1+E2	
1155						Not observed in Re^{182} decay.
1189.3					E1+M2	
	1119.8	K	1189.3	ew		
1221.8					M1+E2	
	1152.3	K	1221.8	ew		
1231.3					M1+E2	
	1162	K	1231.5	ew		
1289						Not observed in Re^{182} decay.
1375						Not observed in Re^{182} decay.
1437						Not observed in Re^{182} decay.
1454						Not observed in Re^{182} decay.

Appendix B-2, a-2.
Electron lines observed in the decay of the short-lived rhenium isotopes according to transition energy.
60-hr Re^{182} electron lines of new transitions.

Transition Energy (kev)	Electron Energy (E_e) (kev)	Assignment Shell	Assignment E_γ (calc. from E_e)	Assignment Visual Intensity	Multi-polarity	Comments
19.86					(E1+M2)?	
	17.04	M_I	19.85	ew		These lines are weak and difficult to read.
	17.30	M_{II}	19.87	ew		
	19.39	N_{II}	19.86	ew?		
	19.59	N_{III}	20.01	ew?		
39.10					(M1)[a]	
	27.00	L_I	39.09	m		
	27.54	L_{II}	39.08	ew		
	36.54	$M_I M_{II}$	39.11	ew(d)		
52.96					(M2)?	
	40.82	L_I	52.91	ew		
	50.17	M_I	52.98	w		Apparent discrepancy in intensity between L_I and M_I might be due to rapid change in efficiency correction at these energies.
60.51					(M1)	
	48.42	L_I	60.51	w		
	57.55	M_I	60.36	mw		M_I 60.51, L_{III} 67.74 superimposed.
68.10					(E2)	
		L_I				L_I 68.10 masked by KLM-Auger electrons.
	56.64	L_{II}	68.18	ew		Assignment questionable.
		L_{III}				L_{II} is so weak L_{III} might not be observed.
74.41					(E1)?	
	62.28	L_I	74.37	ew		
107.13					(M1+E2)	
	37.62	K	107.13	m		
	95.02	L_I	107.11	wm		
	95.60	L_{II}	107.15	wm		
	96.93	L_{III}	107.13	wm		
	104.39	M_I	107.20	ew		
	104.86	M_{III}	107.13	ew		
	106.70	N_{III}	107.12	ew(d)		
108.57					(M1)	
	39.05	K	108.56	m		
	96.49	L_I	108.58	wm		
	105.80	M_I	108.61	ew(d)		
	108.01	N_I	108.60	ew		
120.94					(E1)	
	51.41	K	120.92	ew		
	108.99	L_I	121.08	ew		

a. In Appendix B this type of multipolarity designation will refer to "First Confidence" multipolarities.

Appendix B-2, a-2 (cont.)

Transition Energy (kev)	Electron Energy (E_e) (kev)	Shell	Assignment Eγ (calc. from E_e)	Visual Intensity	Multi-polarity	Comments
130.76					(M1+E2)	
	61.25	K	130.76	vs		
	118.63	L_I	130.72	ms		
	119..21	L_{II}	130.75	w		
	120.61	L_{III}	130.81	w		
	127.99	M_I	130.80	w		
	130.17	N_I	130.75	vw		
131.30					?	
	61.78	K	131.30	ew		
133.78					(M1)	
	64.25	K	133.76	s		
	121.80	L_I	133.89	s		L_I 133.78, K 191.31 superimposed.
	131.03	M_I	133.84	vw		
147.68					(M1+E2)	
	78.16	K	147.67	m		
	135.59	L_I	147.68	ew		
	135.94	L_{II}	147.48	ew		
	137.27	L_{III}	147.47	w		L_{III} 147.68, L_{II} 148.81, L_I 149.39 superimposed.
148.81					(E1+M2)?	
	79.36	K	148.87	s		
	136.67	L_I	148.76	w		
	137.27	L_{II}	148.80	w		L_{II} 148.81, L_I 149.39, L_{III} 147.68 superimposed.
	138.67	L_{III}	148.86	w		L_{III} 148.81, K 208.18 superimposed.
149.39					(E1)?	
	79.92	K	149.43	m		
	137.27	L_I	149.36	w		L_I 149.39, L_{II} 148.81, L_{III} 147.68 superimposed.
	139.19	L_{III}	149.39	w		L_{III} 149.39, K 208.81 (Re^{183}) superimposed.
151.19					?	
	81.68	K	151.19	vw		
160.09					(E1)	
	90.58	K	160.09	w		
	148.09	L_I	160.18	vw		
169.18					(M1)	
	99.67	K	169.18	vs		K 169.18, N's 100.09 superimposed.
	156.96	L_I	169.05	m		
	157.50	L_{II}	169.04	vvw		
	166.36	M_I	169.17	w		
	168.54	N_I	169.13	ew		

Appendix B-2, a-2 (cont.)

Transition Energy (kev)	Electron Energy (E_e) (kev)	Assignment Shell	Eγ (calc. from E_e)	Visual Intensity	Multi-polarity	Comments
172.78					(M1)	
	103.39	K	172.90	ms		K 172.78, L_{III} 113.66 superimposed.
	160.69	L_I	172.78	vw		
	161.23	L_{II}	172.77	vvw		
		L_{III}				L_{III} 172.78 not observed.
	170.07	M_I	172.88	vvw		
	172.46	N_I	172.88	ew(d)		
181.63					?	
	112.12	K	181.63	ew		
189.48					?	
	119.97	K	189.48	w		
191.31					(M1)	
	121.80	K	191.31	s		K 191.31, L_I 133.78 superimposed.
	179.31	L_I	191.40	mw		
	188.59	M_I	191.40	ew		
208.18					(M1)	
	138.67	K	208.18	w		
	196.05	L_I	208.14	ew		
	205.33	M_I	208.14	ew		M_I 208.18, L_{III} 215.69 superimposed.
209.33					(E1)?	
	139.82	K	209.33	vw		
	197.56	L_I or L_{II}		ew		
214.41					?	
	144.83	K	214.34	w		
	202.55	L_I	214.41	ew(d)		
	211.37	M_I	214.18	ew?		
215.69					(E2)	
	146.18	K	215.69	vw		
	204.17	L_{II}	215.71	ew		
	205.33	L_{III}	215.53	ew		
221.60					?	
	152.09	K	221.60	w		K 221.60, L_{III} 162.33 superimposed.
226.10					?	
	156.57	K	226.08	m		
	214.06	L_I	226.15	vvw		
	223.27	M_I	226.08	ew		
247.43					(E2)	
	177.92	K	247.43	mw		
	235.21	L_I	247.30	vvw		
	235.90	L_{II}	247.44	vvw		
	237.34	L_{III}	247.54	vvw		
	244.88	M_{II}	247.45	ew?		
	246.91	N_{II}	247.38	ew?		

Appendix B-2, a-2 (cont.)

Transition Energy (kev)	Electron Energy (E_e) (kev)	Assignment Shell	Eγ (calc. from E_e)	Visual Intensity	Multi-polarity	Comments
256.37					(M2)?	
	186.87	K	256.38	ms		
	244.30	L_I	256.39	w		
	253.43	M_I	256.24	vvw		
276.30					(E2)	
	206.78	K	276.29	mw		
	263.96	L_I	276.05	ew		
	264.79	L_{II}	276.33	ew		
	266.15	L_{III}	276.35	ew		
	273.88	M_{III}	276.15	ew?		
281.42					(E2)	
	211.96	K	281.47	vw		
	259.41	L_I	281.50	w		L_I 281.42, K 338.98 superimposed.
	269.93	L_{II}	281.47	vvw		
	271.09	L_{III}	281.29	vvw?		
	278.78	M_{II}	281.35	ew		
286.52					(E2)	
	217.02	K	286.53	m		K 286.52, L_I 229.27 superimposed.
	274.65	L_I	286.74	vvw(d)		
	274.98	L_{II}	286.52	vvw?		
	276.30	L_{III}	286.50	vvw?		
	283.90	M_{II}	286.47	vvw(d)		
299.83					(E2)	
	230.37	K	299.88	vvw		
	288.56	L_{II}	300.10	ew(d)		L_{II} 299.88, L_I 300.49 are perhaps superimposed.
	289.83	L_{III}	300.03	ew		
300.49					?	
	230.98	K	300.49	vw		
	288.56	L_I	300.65	ew(d)		L_I 300.49, L_{II} 299.88 are perhaps superimposed.
338.98					(E2)	
	259.41	K	338.92	w		
	327.00	L_I	339.09	ew(d)		
	328.92	L_{III}	339.12	vvw		
351.02					(E2)	
	281.51	K	351.02	w		
	339.30	L_I-L_{II}	350.84	vvw(d)		
1076.7					?	
	1007.2	K	1076.7	ew		
1158					?	
	1088.5	K	1158.0	ew		

Appendix B-2, b.

Electron lines observed in the decay of the short-lived rhenium isotopes according to transition energy.

20-hr Re^{181} electron lines.

Transition Energy (kev)	Electron Energy (E_e) (kev)	Assignment Shell	Assignment Eγ (calc. from E_e)	Assignment Visual Intensity	Multi-polarity	Comments
47.38						
	35.29	L_I	47.38	w		Might be K 117.89.
103.13					(M1+E2)	
	91.10	L_I	103.19	ew		These lines were assigned to Re^{181} because they were only observed on PM I in an exposure made shortly after bombardment. They, therefore, might belong to Re^{182}?
	91.59	L_{II}	103.13	ew		
	93.03	L_{III}	103.23	ew		
122.55						
	53.04	K	122.55	ew		Might be L_I 65.13.
252.4					(E2)	
	182.6	K	252.1	vw		Lines were observed only on the high-field magnets and hence E_e is not known better than 0.1%. The same is true for all the transitions below except the 360.95 and 365.50.
	240.8	L_I-L_{II}	252.4	vvw(d)		Might be K 310.4.
	242.1	L_{III}	252.3	ew		Might be K 318.8
	249.3	M's	252.1	vvw(d)		
332.2						
	262.7	K	332.2	vvw		
342.0						
	272.5	K	342.0	vvw(d)		
360.95						
	291.44	K	360.95	vw		
	348.72	L_I	360.81	ew(d)		
365.50					(M2)	
	296.14	K	365.65	vs		
	353.42	L_I	365.51	ms		
	353.99	L_{II}	365.53	vvw		
	355.20	L_{III}	365.40	vvw		
	362.84	M_I	365.65	vw		
	364.89	N_I	365.48	vvw(d)		
441.9						This transition, and the next three, were assigned to Re^{181} because they were seen on plates taken only very soon after bombardment. They therefore might belong to Re^{182}.
	372.4	K	441.9	vvw		
	429.7	L_I	441.8	ew		
469.9						
	400.4	K	469.9	vvw		
486.8						
	417.3	K	486.8	ew		
489.0						
	419.5	K	489.0	ew		
557.3						This transition, and the next three, were assigned to Re^{181} because photon peaks of similar energies were observed to decay with a 20-hour half life. The lines were also only observed on exposures taken soon after bombardment.
	487.8	K	557.3	ew?		
638.3						
	569.8	K	638.3	ew		
894.7						
	825.2	K	894.7	ew		
953.8						
	884.3	K	953.8	vvw		

Appendix B-2, c.
Electron lines observed in the decay of the short-lived rhenium isotopes according to transition energy.
71-day Re^{183} electron lines appearing in the short-lived spectrum.

Transition Energy (kev)	Electron Energy (E_e) (kev)	Assignment Shell	Assignment Eγ (calc. from E_e)	Assignment Visual Intensity	Assignment Multi-polarity	Comments
46.48					M1+E2	
	34.39	L_I	46.48	s		
	34.94	L_{II}	46.48	mw		
	36.33	L_{III}	46.53	mw		
	43.69	M_I	46.50	m		
	45.89	N_I	46.47	w		
52.59					M1+E2	
	40.50	L_I	52.59	m		
	49.93	M_I	52.74	w		
	51.96	N_I	52.55	ew?		
99.07					E2	
	87.52	L_{II}	99.06	m		
		L_{III}				L_{III} 99.07, L_{II} 100.09 (182) superimposed.
107.93					M1	
	38.43	K	107.94	m		
109.73					M1	
	40.32	K	109.83	m		
162.33					M1+E2	
	92.69	K	162.20	s		
	150.25	L_I	162.34	m		
	150.76	L_{II}	162.30	vw		
	152.09	L_{III}	162.29	w		L_{III} 162.33, K 221.60 (182) superimposed.
	159.76	M_{II}	162.33	ms		M's 162.33, K 229.27 (182) superimposed.
208.81					M1	
	139.19	K	208.70	w		

Appendix B-2, d.

Electron lines observed in the decay of the short-lived rhenium isotopes according to transition energy.

Electron lines not definitely assigned to an isotope.

Transition Energy (kev)	Electron Energy (E_e) (kev)	Assignment Shell	Eγ (calc. from E_e)	Visual Intensity	Multi-polarity	Comments
68.10						
	56.64	L_{II}	68.18	ew		This probably belongs to Re^{182} but it was only observed on one plate taken soon after bombardment.
	74.86			ew		Observed on only one early exposure.
	107.44			ew		Observed on only one exposure.
	183.9			ew??		Probably a film imperfection.
	272.5			ew		Observed on only one exposure.
	353.6			ew		Probably a film imperfection.

Appendix C-1.

Electron lines observed in the decay of the long-lived rhenium isotopes in order of increasing energy.

Electron Energy (kev)	Magnetic Rigidity (gauss-cm)	Visual Intensity	Assignment Shell	Assignment Eγ (kev)	Isotope
15.13	417.89	vw(d)	K	84.70	183
29.48	587.24	mw(d)	K	99.07	183
34.41	635.92	vvs	L_I	46.48	183
34.92	640.84	m	L_{II}	46.48	183
36.23	653.14	mw	L_{III}	46.48	183
38.38	672.93	ms	K	107.93	183
40.16	688.91	s	K	109.73	183
40.52	692.11	ms	L_I	52.59	183
41.03	696.64	w	L_{II}	52.59	183
41.57	702.26	ms	K	111.20	184
42.36	708.23	w	L_{III}	52.59	183
43.65	719.51	vs	M_I	46.48	183
43.89	721.47	vvw	M_{II}	46.48	183
44.13	723.48	vvw	M_{III}	46.48	183
45.09	731.66	vw	KL_IL_I	Auger	
45.91	738.52	mw(d)	N_I	46.48	183
46.34	742.16	vw	O_I	46.48	183
46.93	747.10	vw	KL_IL_{III}	Auger	
47.50	751.80	vw	$KL_{II}L_{III}$	Auger	
48.86	762.95	vw	$KL_{III}L_{III}$	Auger	
49.76	770.31	m	M_I	52.59	183
49.99	772.19	ew	M_{II}	52.59	183
50.30	774.69	ew	M_{III}	52.59	183
52.02	788.42	w	N_I	52.59	183
*54.51	808.01	vvw	KL_IM_I	Auger	
54.74	809.80	vvw(d)	KL_IM_{II}	Auger	
55.03	812.06	vvw(d)	$KL_{II}M_I$	Auger	
55.53	815.93	vvw(d)	$KL_{II}M_{III}$	Auger	
56.37	822.37	vvw(d)	$KL_{III}M_I$	Auger	
56.64	824.45	vvw(d)	$KL_{III}M_{II}$	Auger	
56.95	826.87	vvw(d)	$KL_{III}M_{III}$	Auger	
57.43	830.50	vvw(d)	KL_{II}N's	Auger	
58.82	841.05	vvw(d)	KL_{III}N's	Auger	
64.52	883.16	vvw(d)	KMM's	Auger	
67.21	902.50	ew	KNN's	Auger	
70.75	927.47	w	L_I	82.92	183
71.29	931.22	w	L_{II}	82.92	183
72.62	940.43	ms	L_I	84.70	183
73.14	944.03	ew	L_{II}	84.70	183
*52.51	792.27	vvw	O_I	52.59	183

Electron Energy (kev)	Magnetic Rigidity (gauss-cm)	Visual Intensity	Assignment Shell	Assignment Eγ (kev)	Isotope
74.59	953.93	vw(d)	K	144.12	183
80.07	990.88	vvw(d)	M_I	82.92	183
80.45	993.37	vvw(d)	M_{II}	82.92	183
80.80	995.71	vvw(d)	M_{III}	82.92	183
81.87	1002.75	vw(d)	M_I	84.70	183
82.31	1005.64	ew	N_I	82.92	183
82.73	1008.38	ew	O	82.92	183
84.21	1018.06	ew(d)	N_I	84.70	183
85.24	1024.71	ew	L_I	97.33	(184)
85.77	1028.18	ew	L_{II}	97.31	(184)
86.97	1035.85	ew	L_I	99.07	183
87.54	1039.54	s	L_{II}	99.07	183
88.88	1048.11	s	L_{III}	99.07	183
91.03	1061.72	vw	K	160.53	183
91.78	1066.43	vw	K	161.36	183
92.95	1073.78	vvs	K	162.33	183
95.85	1091.82	mw	L_I	107.93	183
96.51	1095.89	mw	M_{II}	99.07	183
96.84	1097.91	w	M_{III}	99.07	183
97.53	1102.10	vvw	L_{III}	107.93	183
97.64	1102.86	m	L_I	109.73	183
98.13	1104.94	ew	L_{II}	109.73	183
98.56	1108.50	vw	N_{II}	99.07	183
99.08	1111.65	vw	L_I	111.20	184
99.73	1115.67	vs	L_{II}	111.20	184
101.04	1123.58	vs	L_{III}	111.20	184
105.13	1148.23	vvw	M_I	107.93	183
106.98	1159.19	vvw	M_I	109.73	183
108.66	1169.12	ms	M_{II}	111.20	184
108.94	1170.79	m	M_{III}	111.20	184
110.76	1181.46	mw	$N_{II}N_{III}$	111.20	184
111.16	1183.83	ew	$O_{II}O_{III}$	111.20	184
123.15	1252.60	vvw	K	192.64	183
135.72	1322.18	ew(d)	K	205.06	183
139.38	1342.02	m	K	208.81	183
140.47	1347.90	ew?	K	209.87	183
149.23	1394.48	vvw	L_I	161.29	183
150.35	1400.41	ms	L_I	162.33	183
150.83	1402.95	vw	L_{II}	162.33	183
*152.30	1410.60	vvw	L_{III}	162.33	183

Appendix C-1 (cont.)

Electron Energy (kev)	Magnetic Rigidity (gauss-cm)	Visual Intensity	Assignment Shell	Eγ (kev)	Isotope
157.93	1439.95	ew	M_{II}	160.53	183
158.47	1442.67	ew	M_{I}	161.36	183
159.65	1448.75	w	M_{I}	162.33	183
161.93	1460.47	vw	N_{I}	162.33	183
162.44	1463.10	ew?	O_{I}	162.33	183
171.49	1509.09	ew?	K	241.1	184
174.88	1526.04	ew	K	244.26	183
175.81	1530.70	ew	K	245.32	183
176.75	1535.35	vvw	K	246.05	183
183.35	1568.09	ew	K	252.84	184
196.88	1633.97	ew	L_{I}	208.81	183
198.19	1640.33	ew?	$L_{II}L_{III}$	208.81	183
206.17	1678.48	ew?	M_{I}	208.81	183
222.30	1754.30	ew?	K	291.71	183
234.00	1808.33	ew	L_{I}	246.05	183
235.73	1816.22	ew?	?	?	?
240.71	1838.95	ew	L_{I}	252.84	184
241.30	1841.64	ew	L_{II}	252.84	184
242.56	1847.36	ew?	L_{II}	252.84	184
243.45	1851.41	ew	K	313.03	183
281.9	2020.6[a]	m	$L_{II}L_{III}$	291.71	183
284.5	2033.8	m	K	354.04	183
290.7	2060.5	w(d)	$M_{II}M_{III}$	291.71	183
296.0	2083.4	vvw?	K	365.50	183
337.1	2257.6	vvw?	K	406.58	183
344.3	2287.7	vvw?	L_{I}	354.04	183
347.7	2302.1	ew?	?	?	?
572.2	3185.8	w	K	641.7	184
718.2	3729.0	ew?	K	787.7	184
722.6	3745.2	w	K	792.1	184
780.0	3954.6	ew?	L_{I}	792.1	184
825.0	4117.4	vvw	K	894.5	184
834.0	4149.9	vw	K	903.5	184
891.4	4356.3	ew	L_{I}	903.5	184

a. These transitions seen only on the 350-gauss magnet.

Appendix C-2, a.
Electron lines observed in the decay of the long-lived rhenium isotopes according to transition energy.
71-day Re^{183} electron lines.

Transition Energy (kev)	Electron Energy (E_e) (kev)	Assignment Shell	Eγ (calc. from E_e)	Visual Intensity	Multi-polarity	Comments
40.97						Not observed in Re^{183} decay.
46.48					M1+E2	
	34.41	L_I	46.50	vvs		
	34.92	L_{II}	46.46	m		
	36.23	L_{III}	46.43	mw		
	43.66	M_I	46.47	vs		
	43.89	M_{II}	46.46	vvw		
	44.13	M_{III}	46.40	vvw		
	45.91	N_I	46.50	mw(d)		
	46.34	O_I	46.43	vw		
52.59					M1+E2	
	40.52	L_I	52.61	ms		
	41.03	L_{II}	52.57	w		
	42.36	L_{III}	52.56	w		
	49.76	M_I	52.57	m		
	49.99	M_{II}	52.56	vw		
	50.30	M_{III}	52.57	ew		
	52.02	N_I	52.61	w		
	52.51	O_I	52.60	vvw		
82.92					M1+E2	
	70.75	L_I	82.84	ew		
	71.29	L_{II}	82.83	w		
	72.62	L_{III}	82.82	w		L_{III} 82.92, L_I 84.70 superimposed.
	80.07	M_I	82.88	vvw(d)		
	80.45	M_{II}	83.02	vvw(d)		
	80.80	M_{III}	83.07	vvw(d)		
	82.31	N_I	82.90	ew		
	82.73	O_I	82.82	ew		
84.70					M1	
	15.13	K	84.64	vw(d)		
	72.62	L_I	84.71	ms		
	73.14	L_{II}	84.68	w		L_{II} 84.70, K 142.25 superimposed.
	74.59	L_{III}	84.79	vw(d)		L_{III} 84.70, K 144.12 superimposed.
	81.87	M_I	84.68	vw(d)		
	84.21	N_I	84.80	ew(d)		
99.07					E2	
	29.48	K	98.99	mw(d)		
	86.97	L_I	99.06	ew		
	87.54	L_{II}	99.08	s		
	88.88	L_{III}	99.08	s		
	96.51	M_{II}	99.08	mw		
	96.84	M_{III}	99.11	w		
	98.56	N_{II}	99.03	vw		

Appendix C-2, a (cont.)

Transition Energy (kev)	Electron Energy (E_e) (kev)	Assignment Shell	Er (calc. from E_e)	Visual Intensity	Multi-polarity	Comments
101.94						Not observed in Re^{183} decay.
102.49						Not observed in Re^{183} decay.
103.14						Not observed in Re^{183} decay.
107.93					M1	
	38.38	K	107.89	ms		
	95.85	L_I	107.94	mw		
	96.51	L_{II}	108.05	mw		L_{II} 107.93, M_{II} 99.07 superimposed.
	97.53	L_{III}	107.73	ew		This line might possibly be misassigned, but the energy discrepancy is probably due to the difficulty in reading the line.
	105.13	M_I	107.94	vvw		
109.73					M1	
	40.16	K	109.67	s		
	97.64	L_I	109.73	m		
	98.13	L_{II}	109.67	vw		
	99.73	L_{III}	109.93	vs		L_{III} 109.73, L_{II} 111.20 (Re^{184}) superimposed.
	106.98	M_I	109.79	vvw		
120.38						Not observed in Re^{183} decay.
142.25					M1	
	72.62	K	142.13	ms		K 142.25, L_I 84.70 superimposed.
144.12					M1	
	74.59	K	144.10	vw(d)		K 144.12, L_{III} 84.70 superimposed.
160.53					E2	
	91.03	K	160.54	vw		
	149.23	L_{II}	160.77	vvw		L_{II} 160.53, L_I 161.36 superimposed.
	150.35	L_{III}	160.55	ms		L_{III} 160.53, L_I 162.33 superimposed.
	157.94	M_{II}	160.51	ew		
	158.47	M_{III}	160.74	ew		M_{III} 160.53, M_I 161.36 superimposed.
161.36					M1	
	91.78	K	161.29	vw		
	149.23	L_I	161.32	vvw		L_I 161.36, L_{II} 160.53 superimposed.
	158.47	M_I	161.28	ew		M_I 161.36, M_{III} 160.53 superimposed.
162.33					M1+E2	
	92.95	K	162.46	es		
	150.35	L_I	162.44	ms		L_I 162.33, L_{III} 160.53 superimposed.
	150.83	L_{II}	162.37	vw		
	152.30	L_{III}	162.50	vvw		
	159.65	M_I-M_{III}	162.46	w		
	161.93	N_I	162.52	vw		
	162.44	O_I	162.53	ew?		
192.64					M1	
	123.15	K	192.66	vvw		
203.27						Not observed in Re^{183} decay.

Appendix C-2, a (cont.)

Transition Energy (kev)	Electron Energy (E_e) (kev)	Assignment Shell	Eγ (calc. from E_e)	Visual Intensity	Multi-polarity	Comments
205.06					M1	
	135.72	K	205.23	ew(d)		
208.81					M1	
	139.38	K	208.89	m		
	196.88	L_I	208.97	ew		
	206.17	M_I	208.98	ew?		
209.87					E2	
	140.47	K	209.98	ew?		
	198.19	L_{II}	209.73	ew?		
244.26					E2	
	174.88	K	244.39	ew		
245.3					(M1)	Not observed in Ta^{183} decay.
	175.81	K	245.32	ew		
246.05					M1	
	176.75	K	246.26	vvw		
	234.00	L_I	246.09	ew		
291.71					E2	
	222.30	K	291.81	vw		
	282.0	L_{II}-L_{III}	292.2	m		Seen on the 350-gauss magnet.
	290.7	M_{II}-M_{III}	293.0	w(d)		
313.03					M1	
	243.37	K	312.88	ew		
354.04					M1	
	284.5	K	354.0	m		Seen on the 350-gauss magnet.
	344.3	L_I	356.4	vvw?		Seen on the 350-gauss magnet.
365.50					(M1)	
	296.0	K	365.5	vvw?		Seen on the 350-gauss magnet.
406.58					(E2)	
	337.1	K	406.6	vvw?		Seen on the 350-gauss magnet.

Appendix C-2, b.
Electron lines observed in the decay of the long-lived rhenium isotopes according to transition energy.
50-day Re^{184} electron lines.

Transition Energy (kev)	Electron Energy (E_e) (kev)	Assignment Shell	Eγ (calc. from E_e)	Visual Intensity	Multi-polarity	Comments
97.33					(M1+E2)	
	85.24	L_I	97.33	ew		
	85.77	L_{II}	97.31	ew		
		L_{III}				L_{III} masked by L_{II} and L_{III} of 99.07.
111.20					E2	
	41.67	K	111.18	ms		
	99.08	L_I	111.17	vw		
	99.73	L_{II}	111.27	vs		
	101.04	L_{III}	111.24	vs		
	108.66	M_{II}	111.23	ms		
	108.94	M_{III}	111.21	m		
	110.76	$N_{II}N_{III}$	111.18	mw		
	111.16	$O_{II}O_{III}$	111.18	ew		
241.1					E1	
	171.49	K	241.1	ew?		
252.84					E2	
	183.35	K	252.84	w		
	240.71	L_I	252.83	ew		
	241.30	L_{II}	252.88	ew		
	242.56	L_{III}	252.82	ew?		
641.7					(M1+E2)	From this transition on the electron lines were seen on the 350-gauss magnet.
	572.2	K	641.7	w		
787.7					?	
	718.2	K	787.7	ew?		
792.1					(M1+E2)	
	722.6	K	792.1	w		
	780.0	L_I	792.1	ew?		
894.5					(M1+E2)	
	825.0	K	894.5	vvw		
903.5					(E2)	
	834.0	K	903.5	vw		
	891.4	L_I	903.5	ew		

c. Electron lines not definitely assigned to an isotope.

	235.7		ew?	
	345.1		ew?	

Appendix D

Electron lines of 12.7-hr Re^{182} observed in the decay of Os^{182}, according to transition energy. All the lines observed in the decay of this isomer have been reported previously by MBMD.

Transition Energy (kev)	Electron Energy (E_e) (kev)	Assignment Shell	Assignment E_γ (calc. from E_e)	Assignment Visual Intensity	Multi-polarity	Comments
33.36						Not observed in Re^{182} decay.[a]
42.71						Not observed in Re^{182} decay.
65.71					M1+E2	
	53.64	L_I	65.73	mw		
	62.80	M_I	65.61	vw(d)		
67.74					E1	
	55.64	L_I	67.73	ms		
	56.17	L_{II}	67.71	m		
	57.59	L_{III}	67.79	m		
	64.97	M_I	67.78	mw		
	65.17	M_{II}	67.74	vvw?		
	65.54	M_{III}	67.81	w		M_{III} 67.74, unidentified Os line superimposed.
	67.24	N_I	67.83	w		
84.67					M1+E2	
	15.11	K	84.62	m		
	72.58	L_I	84.67	ms		L_I 84.67, L_I 84.70 (Re^{183}) superimposed.
	73.07	L_{II}	84.61	mw		
	74.42	L_{III}	84.62	mw		
	81.80	M_I	84.61	mw		M_I 84.67, M_I 84.70 (Re^{183}) superimposed.
100.09					E2	
	30.54	K	100.09	ms		It should be noticed that the K 100.09 and M_I 33.36 have the same energy.
	88.47	L_{II}	100.01	vs		
	89.87	L_{III}	100.07	vs		
	97.51	M_{II}	100.08	s		
	97.80	M_{III}	100.07	s		
	99.60	$N_{II}N_{III}$	100.02	m		
	100.00	$O_{II}O_{III}$	100.09	vw		
113.66					M1+E2	
	44.18	K	113.69	mw		
116.40					(M1+E2)	
	47.00	K	116.51	m		K 116.40, KL_IL_{III}-Auger electron superimposed.
152.41					E1	
	82.85	K	152.36	mw		
	140.40	L_I	152.49	vvw		This might be an Os line (unassigned).
156.37						Not observed in Re^{182} decay.
179.36						Not observed in Re^{182} decay.
198.31						Not observed in Re^{182} decay.
222.05						Not observed in Re^{182} decay.
264.09						Not observed in Re^{182} decay.

a. Re^{182} in this table refers only to 12.7-hr Re^{182}.

Appendix D (cont.)

Transition Energy (kev)	Electron Energy (E_e) (kev)	Shell	Assignment $E\gamma$ (calc. from E_e)	Visual Intensity	Multi-polarity	Comments
927						Not observed in Re^{182} decay.
960						Not observed in Re^{182} decay.
1003						Not observed in Re^{182} decay.
1121.6					M1+E2	
	1052.3	K	1121.8	ew		
1155						Not observed in Re^{182} decay.
1189.3					M1+E2	
	1119.8	K	1189.3	ew		
1221.8					E2	
	1152.3	K	1221.8	ew		
1231.3					M1+E2	
	1162.0	K	1231.5	ew		
1289						Not observed in Re^{182} decay.
1375						Not observed in Re^{182} decay.
1437						Not observed in Re^{182} decay.
1454						Not observed in Re^{182} decay.

REFERENCES

1. Charles Henry Dodgson, Through The Looking Glass (1872) Ch. IV.
2. M. G. Mayer, Phys. Rev. 78, 16 (1950).
3. Haxel, Jensen, and Suess, Ergeb. Exakt. Naturw. 26, 244 (1952).
4. A. Bohr, Kgl. Danske Videnskab. Selskab, Mat.-fys. Medd. 26, No. 14 (1952).
5. A. Bohr and B. R. Mottelson, Kgl. Danske Videnskab. Selskab, Mat.-fys. Medd. 27, No. 16 (1953).
6. Alder, Bohr, Huus, Mottelson, and Winther, Revs. Modern Phys. 28, 432 (1956).
7. F. S. Stephens, Jr., Decay Schemes and Nuclear Spectroscopic States in the Heavy-Element Region (thesis), UCRL-2970, June 1955.
8. Stephens, Asaro, and Perlman, Phys. Rev. 96, 1568 (1954).
9. R. Sheline, Institute for Theoretical Physics, Copenhagen, Denmark, talk given at the Conference on Nuclear Structure, Pittsburgh, Pennsylvania, June 1957.
10. G. D. O'Kelley and J. L. Olsen, A Ring-Focused, Long Magnetic Lens Beta-Ray Spectrometer, California Research and Development Company Report MTA-38, May 1954.
11. G. D. O'Kelley, The Spectrometric Determination of Some Beta-Particle and Conversion-Electron Energies (thesis), UCRL-1243, (1951).
12. W. G. Smith, I. Neutron-Deficient Isotopes in the Noble Metal Region. II. Conversion-Electron Spectra of Some Heavy Elements, (thesis), UCRL-2974, June 1955.
13. A. Ghiorso and A. E. Larsh, in Chemistry Division Quarterly Report, UCRL-2647, July 1954.
14. This 100-channel gamma analyzer is a commercially available model manufactured by the Pacific Electro-Nuclear Company, Culver City, California.

15. D. Strominger, I. Experimental Study of Nuclear Isomers in the Millimicrosecond Lifetime Range. II. Applications of Nilsson's Wave Functions for Deformed Nuclei (thesis), UCRL-3374, June 1956.

16. Manufactured by the Harry W. Dietart Co., Detroit 4, Michigan.

17. M. Mladjenović and H. Slätis, Arkiv Fysik 8, 65 (1954).

18. M. I. Kalkstein and J. M. Hollander, A Survey of Counting Efficiencies for a 1-1/2-Inch Diameter by 1-Inch High Sodium Iodide (Thallium-Activated) Crystal, UCRL-2764, October 1954.

19. W. G. Smith and J. M. Hollander, Phys. Rev. 101, 746 (1956).

20. M. Sweeney and J. O. Rasmussen, in Chemistry Division Quarterly Report, UCRL-2932, March 1955.

21. G. Wilkinson, Nature 160, 864 (1947).

22. Cork, Nester, Le Blanc, and Brice, Phys. Rev. 92, 119 (1953).

23. Bisi, Ferrani, and Zappa, Nuovo Cim. 1, 651 (1951).

24. Bisi, Ferrani, and Zappa, Nuovo Cim. 3, 661 (1956).

25. Derbrunner, Heer, Kundig, and Ruetschi, Helv. Phys. Acta 29, 235 (1956).

26. Hollander, Perlman, and Seaborg, Revs. Modern Phys. 25, 469 (1953).

27. Strominger, unpublished data, (1955).

28. Murray, Boehm, Marmier, and DuMond, Phys. Rev. 97, 1007 (1955).

29. S. H. Vegors, Jr., and P. Axel, Phys. Rev. 101, 1067 (1956).

30. A. J. Bureau and C. L. Hammer, Phys. Rev. 105, 1006 (1957).

31. M. E. Rose, privately circulated tables. Also, with G. H. Goertzel, in Beta- and Gamma-Ray Spectroscopy, K. Siegbahn, Ed., (Interscience, New York, 1955) App. IV, p. 905.

32. L. A. Sliv and I. M. Band, Publication of the Leningrad Physico-Technical Institute (1956); Translated into English by P. Axel and published as University of Illinois Report 57 ICC K1 (1957).

33. Muller, Hoyt, Klein, and DuMond, Phys. Rev. 88, 775 (1952).

34. H. Brysk and M. E. Rose, Theoretical Results on Orbital Capture, ORNL-1830, January 1950.

35. P. Gray, Electron Capture and the Auger Effect in the Heaviest Elements (thesis), UCRL-3104, August 1955.

36. C. D. Coryell, in Annual Review of Nuclear Science, (Annual Reviews, Inc., Stanford, 1953) Vol. 2, p. 305.

37. S. G. Nilsson, Kgl. Danske Videnskab. Selskab, Mat.-fys. Medd. 29, No. 16 (1955).

38. S. A. Moszkowski, in Beta- and Gamma-Ray Spectroscopy, K. Siegbahn, Ed., (Interscience, New York, 1955) Ch. XIII, p. 391.

39. D. Strominger and J. O. Rasmussen, Nuclear Phys. 3, 197 (1957).

40. G. Alaga, Phys. Rev. 100, 432 (1955).

41. Thulin, Rasmussen, Gallagher, Smith, and Hollander, Phys. Rev. 104, 471 (1956).

42. B. R. Mottelson and S. G. Nilsson, Phys. Rev. 99, 1615 (1955).

43. G. Wilkinson and H. G. Hicks, Phys. Rev. 77, 314 (1950).

44. J. O. Newton and V. S. Shirley, unpublished data (1957).

45. V. S. Shirley, unpublished data (1956).

46. Alaga, Alder, Bohr, and Mottelson, Kgl. Danske Videnskab. Selskab, Mat.-fys. Medd. 29, No. 9 (1955).

47. H. Margenau and G. M. Murphy, The Mathematics of Physics and Chemistry (Van Nostrand, New York, 1951) p. 498.

48. A. H. Wapstra and G. J. Nijgh, Nuclear Phys. 1, 245 (1956).

49. E. L. Church and J. Weneser, Phys. Rev. 104, 1382 (1956).

50. S. G. Nilsson, Nuclear Structure Dependence of Conversion Coefficients in Electric Multipole Transitions, UCRL-3803, June 1957.

51. T. Huus and J. H. Bjerregaard, Phys. Rev. 52, 1579 (1953).

52. McClelland, Mark, and Goodman, Phys. Rev. 93, 904 (1954).

53. P. H. Stelson and F. K. McGowan, Phys. Rev. 99, 112 (1955).

54. E. M. Bernstein and H. W. Lewis, Phys. Rev. 99, 617 (A) (1955).

55. Clark, DuMond, Gordan, and Marsh, Bull. Amer. Phys. Soc. Ser. II, 2, 69 (1957).

56. J. W. Mihelich, Phys. Rev. 95, 626 (1954).

57. R. C. Williams and R. I. Roulston, Can. J. Phys. 34, 1087 (1956).

58. G. Bäckstrom, Arkiv Fysik, 10, 387 (1956).

59. F. Asaro, Phys. Rev. (to be published).

60. B. J. Sears and M. G. Radtke, Algebraic Tables of Clebsch-Gordan Coefficients, Chalk River, (Canada) Report TPI-75, August 1954.

61. A. K. Kerman, Kgl. Danske Videnskab. Selskab, Mat.-fys. Medd. 30, No. 15 (1956).

62. D. Strominger, unpublished data (1956).

63. Birdsall, Clark, Jopson, Livdahl, Smith, and Van Atta, Bull. Amer. Phys. Soc. 2, 187 (1957).

64. K. Fajans and F. Voigt, Phys. Rev. 58, 177 (1940).

65. Gallagher, Strominger, Unik, and Rasmussen, Phys. Rev. (to be published).

66. F. D. S. Butement and A. J. Poë, Phil. Mag. 46, 482 (1955).

67. F. R. Metzger and R. D. Hill, Phys. Rev. 82, 646 (1951).

68. R. M. Steffen, Phys. Rev. 82, 827 (1951).

69. I. Bergström and R. D. Hill, Arkiv Fysik 8, 21 (1954).

70. R. W. Hoff and J. O. Rasmussen, Phys. Rev. 101, 280 (1956).

71. Giles, Garrison, and Hamilton, J. Chem. Phys. 18, 995 (1950).

72. W. W. Meinke, Chemical Procedures Used in Bombardment Work at Berkeley, UCRL-432, August 1949.

73. Huffman, Oswalt, and Williams, Anion Exchange Separation of Molybdenum and Technetium and of Tungsten and Rhenium, UCRL-3324, February 1956.